5-2019

THE CHARACTERIZATION OF T-CELL MANUFACTURING FOR ADOPTIVE T-CELL THERAPIES

amir ALPERT

THE CHARACTERIZATION OF T-CELL MANUFACTURING FOR ADOPTIVE T-CELL THERAPIES

by

Amir Isaac Alpert, B.S.

APPROVED:

____
Greg Lizee, Ph.D
Advisory Professor

____
Michael Curran, Ph.D

____
Michelle Barton, Ph.D

____
Vidya Gopalakrishnan, Ph.D

____
Chantale Bernatchez, Ph.D

APPROVED:

____
Dean, The University of Texas

MD Anderson Cancer Center UTHealth Graduate School of Biomedical Sciences

THE CHARACTERIZATION OF T-CELL MANUFACTURING FOR ADOPTIVE T-CELL THERAPIES

A

DISSERTATION

Presented to the Faculty of

The University of Texas

MD Anderson Cancer Center UTHealth

Graduate School of Biomedical Sciences

in Partial Fulfillment

of the Requirements

for the Degree of

DOCTOR OF PHILOSOPHY

by

Amir Isaac Alpert, B.S.

Houston, Texas

May, 2019

Dedication

This work is dedicated to Momotaz Rahman, whose eternal love and support helped me through the toughest period of my life.

Acknowledgments

Immatics US Inc, who gave a PhD student a chance, it’s been an experience beyond my wildest imagination.

Deans Barton and Blackburn, who allowed me to take the position at Immatics while continuing my PhD in a first of its kind arrangement for the university. I truly thank you for your trust and commitment to my progress inside and outside the walls of this university.

Chase Light, whose calm head and hands made life manageable in my industry-academic life balance, words cannot fully express my gratitude to you throughout this process.

Abstract

THE CHARACTERIZATION OF T-CELL MANUFACTURING FOR ADOPTIVE T-CELL THERAPIES

Amir Alpert, B.S.

Advisory Professor: Gregory Lizee, Ph.D.

Adoptive T-cell therapy using genetically modified T cells has emerged as a potential therapeutic option for several malignancies. Central to the production of the cellular therapy is the manufacturing using a stimulation, genetic engineering, and expansion methodology. Within this framework, there is a delicate balance between expansion of the cells to a therapeutically relevant dosage and the need to retain the proliferative potential of the ‘living drug’. I show that as T-cells are expanded for elongated periods of time, they lose their proliferative potential and become functionally senescent despite the presence of multiple proliferative cytokines. In addition, I show that expression of CD28 correlates with multiple manufacturing metrics, including final T-cell fold expansion. I propose that the loss of CD28 expression creates a T-cell expansion bottleneck in which certain T-cell clones are heavily favored compared to others during manufacturing. Compounding the multiple correlations, I performed a meta-analysis of available clinical trial data to show that younger patients appear to respond better to T-cell manufacturing involving CD28 costimulation, while older patients appear to respond better to T-cell manufacturing lacking CD28 costimulation.

Table of Contents

List of Illustrations

List of Tables

Introduction

Structure Human Immune System and Antigen Presentation

The human immune system functions to differentiate the ‘self’ from the ‘non-self’ in a selective efficient manner to not induce autoimmunity (‘self’ attack ‘self’), yet it must mount a potent defense in the context of a foreign pathogen. The system is dissected into the innate and adaptive immune systems. The primary function of the innate system is to respond rapidly to an acute infection. While the adaptive system takes longer to response, it can form complex memory formation aimed at responding to future infections.

The innate system is composed of several different levels, starting with the skins ability to serve as a physical barrier from the outside world. The digestive enzymes of the stomach and the saliva form another high order level aimed at destroying pathogens before they have a chance to establish themselves. Additionally, the complement system is composed of more than 30 macromolecules which assist in eliminating foreign pathogens by complementing other arms of the immune system. The innate system is also composed of an active cellular arm such as granule containing neutrophils, basophils, eosinophils, mast cells, natural killer (NK) cells, and monocytes (Spiering 2015).

Within the innate system, monocytes differentiate into dendritic cells (DCs) and macrophages, functioning as highly endocytic professional antigen presenting cells (APCs). These cells are bone marrow derived and particularly adept at endocytosis by which they monitor the blood and surrounding tissues for signs of pathogenic infections. Endocytosed particulates may be recognized as pathogen-associated molecular patterns (PAMPs) via toll-like receptors (TLRs) at the cell surface or endosomal compartments.

The interactions between PAMPs and TLRs are extremely diverse, with examples including the recognition of bacterial lipopolysaccharide by TLR4, bacterial flagellin protein by TLR5, and CpG DNA by TLR9 (Akira 2006). Following their respective PAMP binding, TLRs primarily signal via a MyD88 or TRIF dependent pathway, resulting in NF-κβ signaling and the secretion of IL-12, IL-6, tumor necrosis factor (TNF), and other inflammatory cytokines (Kawai and Akira 2010). PAMPs recognition in the cytosol is mediated via NOD-LRR and CARD helicase proteins as in the recognition of peptidoglycan peptides γ-D-glutamyl-meso-diaminopimelic acid (iE-DAP) and muramyl dipeptide (MDP) by NOD1 and NOD2 (Chamaillard 2003) or the double-stranded RNA (dsRNA) detector RIG-1(Yoneyama et al. 2004), both of which activate the NF-κβ pathway as well.

While primarily associated with recognition of foreign pathogens, PAMP-like signals may also be endogenous in nature. The injection of live or dead tumor cells has also been shown to be immunogenic, as in the injection of UV treated or untreated tumor cytosol (Shi 2000). As necrotic, and in certain contexts apoptotic, cells release cytosolic contents due to loss of plasma membrane integrity, it was theorized that there existed a class of endogenous sterile immunogenic compounds (Rock, Lai, and Kono 2011). Since this work, these compounds have been elucidated via cytosolic fractionation coupled immunogenic assays and have become known as damage-associated molecular patterns (DAMPs) underscoring their similarity in function to PAMPs. The molecular DAMPs signature is as complex as those of PAMPs, with examples including the recognition of nuclear HMGB1 protein by TLR4/2, ATP by $P2X_7$, double-stranded DNA by AIM2, and a plethora of other examples (Zelenay and Reis e Sousa 2013).

Following APC activation by PAMPs or DAMPs, the APC primary function shifts from monitoring to antigen processing and presentation. As such, the activated APC will show increased expression of major histocompatibility complex class I (MHC-I) and class II (MHC-II). Every nucleated cell expresses MHC-I on the cell surface loaded with 8-11 long amino acid peptides derived from proteasomal degradation. Intracellular proteins are degraded either at the end of their functionality based on the respective protein half-life, or from a source of translationally defective ribosomal products (DRiPs). DRiPs are created from defective protein synthesis originating from defective mRNA transcription, incorrect reading frame usage, aborted protein complex formation, faulty amino acid insertion, or augmented ubiquitylation (Berglund et al. 2007; Dolan et al. 2011). The proteasomal cleaved short peptide sequences are transferred into the endoplasmic reticulum (ER) via the transporter associated with antigen presentation (TAP) protein complex. Once in the ER, the peptides are assembled with the heavy (HLA-A, B, or C) and light chain (B2-microglobin) of MHC-I and transferred to the cell surface via the Golgi transfer process (Vyas, Van der Veen, and Ploegh 2008).

In contrast to MHC-I expression, major histocompatibility complex class II (MHC-II) expression is mostly restricted to the professional antigen presenting cells of the immune system, as in DCs, macrophages, and B cells. The alpha and beta chains of MHC-II (HLA-DR, HLA-DQ, and HLA-DP) are assembled with the invariant chain in the ER and transported to late endosomal compartments. Once in the endocytic compartment, the invariant chain is cleaved and replaced with an endocytosed protease cleaved peptide which are usually 15-24 amino acids in length (Neefjes et al. 2011). It should be noted that while MHC-II expression is primarily restricted to professional antigen presenting cells, its expression can be regulated by IFN-γ and TGF-β in mesenchymal stem cells (Romieu-Mourez 2007), lung epithelium (Cunningham 1997), and melanoma tumor cells lines (Johnson et al. 2016)

Cross Presentation and Activation of T-cells

While MHC-I is classically considered to present intracellular degraded peptides, the process of cross-presentation enables MHC-I to be loaded with extracellular endocytosed peptides. This is particularly relevant in the context of DCs, especially the conventional DCs 1 subtype (cDC1) (Embgenbroich and Burgdorf 2018). There are two pathways for cross-presentation, a TAP-dependent (cytosolic) or TAP-independent (vacuolar) pathway. In the cytosolic pathway, endocytosed antigens are transported from the endosomal compartments into the cytosol, where they are processed by the proteasome, and loaded onto MHC-I via the previously described TAP-ER pathway (Ackerman 2003). In the vacuolar pathway, antigens are directly processed by lysosomal proteases (e.g. cathepsin S) and loaded onto MHC-I independent of proteasomal degradation (Shen et al. 2004). As will be discussed in greater detail, a central feature of APC antigen presentation is to activate the CD8 T cell compartment of the adaptive immune system. In order to, presumably, maximize the chance of proper T-cell activation, DCs have a unique ability to alkalize their endosomal compartments and slow the process of antigen proteolytic degradation via the activity of NOX2 (Mantegazza et al. 2008), a lower expression of lysosomal cathepsins (Lennon-Duménil et al. 2002), and the ability to utilize endocytic receptors which show augmented lysosomal fusion kinetics (Chatterjee et al. 2012). These attributes, in theory, maximize the chance of cross-presentation and priming of the CD8 T-cell compartment.

Following DC activation by PAMPs, and to a lesser extent specific DAMPs, their chemoattractant phenotype changes from one of preferential inflammatory signal homing, characterized by the expression of CCR5 and CCR1, to that of lymphoid organ homing, characterized by the expression of CCR7 (Sallusto 1998). Additionally, there is a marked upregulation of costimulatory molecules CD80 and CD86 (Banchereau and Steinman 1998). As the activated mature DCs enter the lymphoid regions they are in a state which enables T cell activation in the classical 1, 2, 3 signaling model. They express MHC bound peptide antigens (signal 1), costimulatory molecules (signal 2), and pro-inflammatory cytokines (signal 3) enabling them to prime T cells (figure 1).

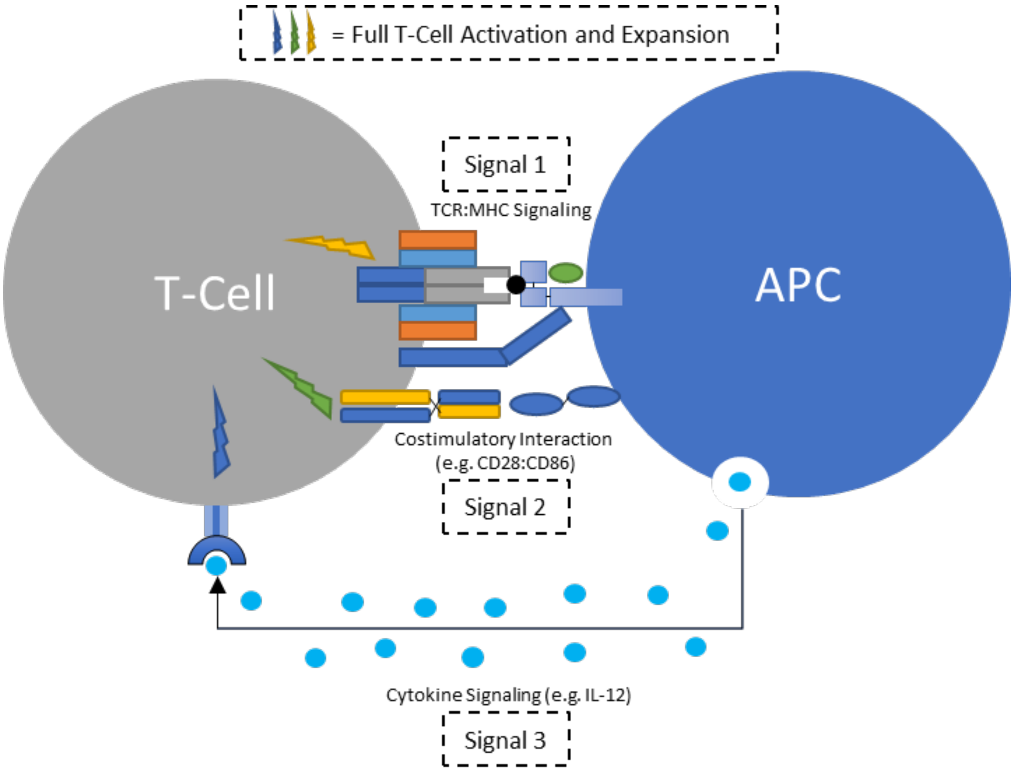

Figure 1: 1,2,3 Model of T-cell activation. Full T-cell activation requires multiple excitatory signals with signal 1 delivered by the stimulatory T-cell receptor (TCR): MHC interaction in which the peptide presenting MHC complex on the APC presents a peptide fragment (black circle) to the TCR. Signal 2 is composed of a costimulatory receptor interaction, such as the one between CD28 of the T cell and CD86 expressed by mature APCs. Finally, a pro-inflammatory growth cytokine signal is delivered from the APC to the T-cell such as the cytokine signaling of IL-12. When these three signals are integrated in the T cell, full T-cell activation and expansion is likely to occur.

The T-cell lineage of the adaptive immune system is divided into αβ and γδ based on their somatically rearranged T-cell receptor (TCR). αβ cells make up the highest percentage of the T-cell compartment and are deemed as 'conventional' T cells based on their recognition of MHC-peptide complexes (Curtin 1974). Within the αβ T cells, there also exists so called 'non-conventional' T cells that recognize antigens in an MHC independent manner, such as mucosal-associated invariant T (MAIT) cells involved in bacterial immunity, invariant natural killer (iNK T) cells, and germline-encoded mycolyl-reactive (GEM) T cells (Van Rhijn et al. 2013; Beckman 1994; Le Bourhis et al. 2010). In contrast, γδ cells represent a small fraction of the blood T cells, but they can account for nearly half of the gut resident T cells in line with their role in recognizing CD1 bound pyrophosate intermediates derived from bacterial lipid synthesis (Russano et al. 2007). By far, the conventional αβ T cells are the most well studied and understood with respect to T-cell activation, differentiation, receptor diversity, and antigen recognition (Attaf et al. 2015).

The αβ TCR is a heterodimer composed of an alpha and beta strand linked by a disulfide bond which non-covalently associates with three different CD3 complexes (εγ, εδ, ζζ) (Wang and Reinherz 2012). The α and β strands are composed of a constant membrane proximal region and a variable membrane distal region composed of three hypervariable complimentary determining regions (CDR1,2, and 3) generated via somatic V(D)J recombination. The process of V(D)J TCR recombination ensures that an extremely diverse set of TCRs exist to cover the equally diverse range of potential MHC bound peptides. Theoretically, as many as 1×10^{15} unique TCR recombinations are possible (Davis and Bjorkman 1988), though this number is likely an overestimation of the true number of unique TCRs in any one individual (Nikolich-Zugich, Slifka, and Messaoudi 2004).

Structural investigations depict a diagonal binding model in which a relatively flat interaction occurs between the variable regions of the αβ strands and the MHC peptide binding groove (Garboczi et al. 2000). Upon binding to the MHC complex, structural rearrangements occur by which the cytosolic portions of the CD3ε subunit releases from the inner leaflet of the plasma membrane, exposing the immunoreceptor tyrosine-based activation motifs (ITAMs) of the CD3 cytoplasmic tails (Deford-Watts et al. 2009). In addition to the TCR-MHC interaction, a CD8 or CD4 coreceptor interacts with the conserved non-peptide bound regions of either MHC-I or MHC-II, respectively (Wang et al. 2001; Gao et al. 1997). It is this, primarily, bimodal coreceptor expression which dictates whether a T cell will be a CD8 T cell and interact with MHC-I-peptide complexes or whether it will be a CD4 T cell and interact with MHC-II peptide complexes.

T-cell Differentiation

Regardless of coreceptor expression, T cells are thought to differentiate in a linear model starting with their exit from the thymus as naive T cells (Tn), classically characterized by the expression of CD62L, CCR7, CD45RA, CD28, and CD27 (Rosa et al. 2001). As with the expression of CCR7 in mature DCs, these naive T cells are well suited to migrate to the lymphoid regions via the expression of CCR7 and CD62L (Weninger et al. 2001). For the naive T cell to become fully activated, it requires signaling via 1) the MHC-TCR interaction, 2) costimulatory signaling (e.g. CD28), and 3) stimulatory cytokines (e.g. IL-2) and it is within the lymphoid regions that such signals are prominent.

For example, in the classical TCR-MHC ligation + CD28 costimulation, the IL-2 receptor high-affinity receptor CD25 is expressed along with autocrine signaling IL-2 via NFAT, PI3K/Akt, and PKC-θ signaling pathways (Shaw et al. 1988; Kane et al. 2001; Pfeifhofer-Obermair, Thuille, and Baier 2012).
Upon receiving signals 1, 2, and 3, naive T cells enter a rapid proliferative state via the activation of the PI3K/AKT-mTOR pathway. However, in the absence of costimulation, naive T cells enter a state of anergy in which they fail to respond to TCR or IL-2 signaling (Xing and Hogquist 2012).

Following activation, naive cells are thought to upregulate the apoptotic FAS receptor, CD95, and the shared IL-2 and IL-15β receptor, CD122 to form a compartment of highly proliferative stem cell memory T cells (Tscm) (Gattinoni et al. 2011). It remains to be elucidated as to what extent naive T cells remain in this state or whether all naive cells enter this state. It appears that reducing the activating signal can prevent further differentiation of Tscm as suggested by recent developments of T-cell activation in the presence of Akt inhibitors (Klebanoff et al. 2017) and WNT signaling agonists (Sabatino et al. 2016). Tscm cells continue to differentiate, in part, through the upregulation of the master splicing regulator RNA-binding protein heterogeneous nuclear ribonucleoprotein L-like (HNRPLL) (Wu et al. 2008) and the formation of the central memory T cell compartment (Tcm), characterized by the shift from CD45RA expression to CD45RO. Tcm differentiation is continued into the formation of the effector memory (Tem) compartment with the accompanied loss of CCR7 and CD62L expression, enabling them to exit the lymphoid regions and enter the peripheral tissues (Sallusto et al. 1999). The Tem compartment is phenotypically diverse in costimulation, with a mixture of cells expressing CD27 and/or CD28 or no costimulation at all (Romero et al. 2007).

In the absence of additional survival signals, Tem cells are destined to end up as short-lived proliferatively senescent effector memory RA (Teff or Temra) cells, characterized by the expression of inhibitory proteins such as killer-cell lectin like receptor G1 (KLRG1) (Voehringer, Koschella, and Pircher 2002). This linear model of T-cell differentiation (figure 2) is further supported by transcriptomic analysis of the different compartments as a majority of differentially expressed genes showed a continual increase or decrease going from Tn to Tscm, Tcm and Tem (Gattinoni et al. 2011).

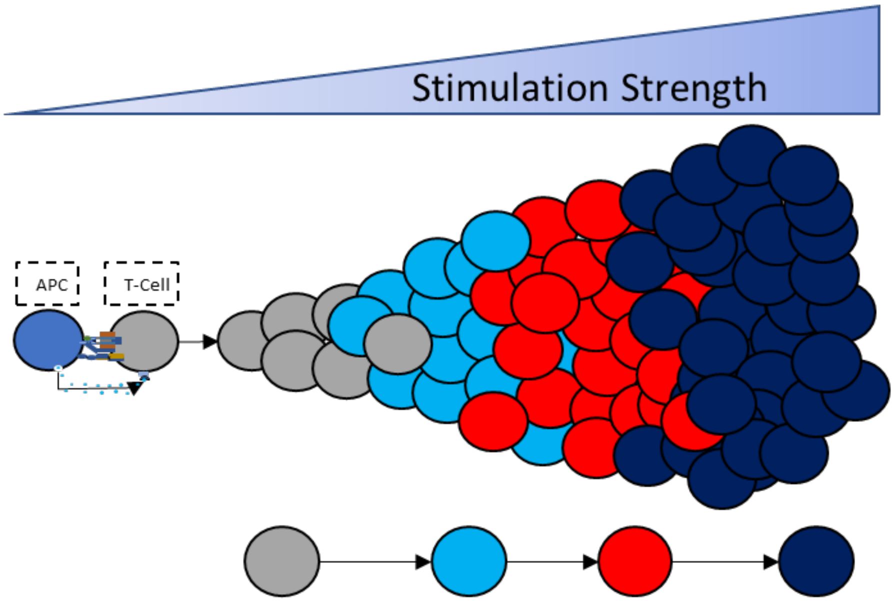

	Tnaive/scm	Tcm	Tem	Teff/emra
CCR7	+++	++	-	-
CD62L	+++	++	-	-
CD27	+++	++	+/-	-
CD28	++/+++	+++	+/-	-
CD45RA	+	-	-	+
CD45RO	-	+	+	-
CD122	-/+	+++	+++	+/-
CD95	-/+	+++	+++	+++
KLRG1	-	+/-	++	+++

Figure 2. Linear T-cell differentiation model. Upon T-cell stimulation, shown via APC ligation, Tnaive/scm cells undergo a rapid proliferation and expansion based on the cumulative strength of the signals received. The linear model suggests a progression from Tnaive/scm to Tcm, Tem, and finally to short lived Teff/emra cells. During this expansion, T-cells undergo phenotypic changes as described in the table below the diagram. Figure is adapted from Gattinoni2012, Nature Cancer Reviews.

The cytokine milieu (signal 3) which a T cell encounters has profound effects on their differentiation and acquisition of effector functions. CD4 T-cell effector function differentiation has been extensively studied, with the classifications of CD4 cells as Th1, Th2, Th17, Treg, or Tfh. Th1 cells are strong producers of cytokines related to anti-viral/tumor immunity such as IFN-γ and TNF-α along with T-cell growth cytokines such as IL-2 and their differentiation is supported in the absence of IL-4 and the presence of IL-12 (Hsieh et al. 1993). On the other hand, Th2 cells support humoral immunity via the production of IL-4, IL-5, and IL-6 and are preferentially differentiated in environments rich in IL-2 and IL-4 (Le Gros et al. 1990). Th17 cells are primed for production of IL-17, IL-22, and IL-21 via differentiation in environments rich in TGF-β, IL-6, and IL-21 (Zhou et al. 2007). Tregs act as immunosuppressive regulatory T cells via secretion of inhibitory cytokines such as TGF-β, IL-10, and IL-35 (Read, Malmström, and Powrie 2000; Asseman et al. 1999; Collison et al. 2007) and expression of inhibitor receptors such as cytotoxic T-lymphocyte-associated protein 4 (CTLA-4) (Oderup et al. 2006). Natural Treg (nTreg) form within the thymus, taking place in the context of strong TCR-MHC interactions, while induced Tregs (iTregs) form in the periphery when CD4 T cells are stimulated in the presence of TGF-β and IL-2 (Blueston and Abbas 2003).

Like CD4 cells, following CD8 T-cell activation, a rapid expansion and gain of effector function occurs which is context dependent based on the encountered cytokine milieu and strength of TCR signaling. In example, IL-12 has been shown to increase the differentiation of naive CD8 T cells into Tem cells compared to IFN-α, which preferentially supported the development of Tcm cells. It was further shown that the degree to which cells proliferated was dependent on the strength of TCR, costimulation, and the type of cytokines used, with IL-12 and strong TCR/costimulation yielding the most proliferation (Ramos et al. 2009). Understanding the effects of cytokine induced differentiation enables the use of IL-21 in the generation of clinically relevant antigen specific CD8 T cells, with increased expression of the CD28 costimulatory receptor and increased production of IL-2 in effector responding T cells (Li, Bleakley, and Yee 2005). Similarly, the expansion of human T cells in the presence of IL-7 and IL-15 preserved the less differentiated CD62L+CD45RA+ population in comparison to expansion with IL-7,IL-15, and IL-2 (Cieri et al. 2013).

Cancer Immunotherapy – Antibody

The detailed understanding of the immune processes described have enabled immunotherapy to emerge as a leading cancer treatment (Couzin-Frankel 2013). The most developed and commercially implemented form of immunotherapy comes in the form of antibody-based therapy, segregated based on whether they work independently or in combination with the patient's immune system. In the immune independent form, the antibodies work to block or inhibit pathways that are essential for cancer cell survival as in the administration of Bevacizumab blockage of VEGF-A growth factor signaling and the inhibition of angiogenesis in colorectal, lung, breast, renal, brain, eye, and ovarian cancer (Viallard and Larrivee 2017). Alternatively, Rituxamab has been approved for the treatment of non-Hodgkin's lymphoma where it serves as a depleting antibody by mediating tumor cell destruction via immune dependent antibody-dependent cellular toxicity and complement-dependent cytotoxicity (Shaw, Quan, and Totoritis 2003).

Antibody based therapy has also been used to boost the effector function of T-cells by blocking inhibitory pathways, so called checkpoint blockade therapies (CBT). The first CBT developed was against the cytotoxic T-lymphocyte antigen 4 (CTLA-4) receptor which blocks T-cell costimulation by interfering with the CD28:CD80/86 signaling axis (Krummel 1995). Following its initial identification, the CTLA-4 antagonist Ipilimumab was approved for the treatment of metastatic melanoma (Schadendorf et al. 2015). Programmed cell death protein 1 (PD-1) expressed by T cells interacts with its tumor expressed ligand PD-L1 to lower TCR proximal signaling (Yokosuka et al. 2012), with the αPD-1 antibody Nivolumab recently approved in multiple solid tumor indications (Prasad and Kaestner 2017). Additionally, agonists are being developed to stimulate T cells as in the targeting of tumor necrosis factor receptor family member 4-1BB, a known T-cell costimulatory receptor (Chester, Ambulkar, and Kohrt 2016).

Antibody based therapies have yielded impressive results, with a considerable percentage of patients achieving long-term durable responses. These approaches have the benefit that they can potentially activate a widespread indiscriminate pool of T cells against a wide variety of tumor antigens. However, there are indications that a lack of CD8 T-cell infiltrate predicts a failure to respond to CBT (Chen et al. 2016). Theoretically, a lack of CD8 infiltrate could be overcome by increasing the number of activated tumor specific T cells in the patient. Adoptive cell transfer (ACT) therapy aims to achieve such a scenario via the *ex vivo* propagation of cancer specific T cells, followed by eventual patient infusion. ACT has been practiced in multiple forms as in 1) Tumor infiltrating lymphocyte (TIL), 2) expansion of *ex vivo* antigen specific T cells , and 3) T-cell gene transfer (GT) cellular therapies (Tumeh et al. 2010).

Cancer Immunotherapy – TILs

TIL therapy relies on the *ex vivo* expansion of tumor reactive T cells extracted from patient biopsies, with a majority of trials using similar expansion protocols with only minor differences (Radvanyi 2015). The general process begins with the processing of tumor biopsies into single cell suspensions followed by culturing of in T-cell growth cytokines, such as IL-2. Once the T cells have grown to a certain threshold, they are processed via a rapid expansion protocol (REP) in which time they are given a TCR stimulation, high doses of growth cytokine, and irradiated feeder cells for costimulatory support. By the end of this process, therapeutic dosages in tens of billions of cells are achieved for infusion (Besser et al. 2010). While there is much work to do in elucidating the biomarkers that predict therapeutic response, several groups have found that response rates correlate with product phenotype and manufacturing characteristics, such as final telomere length, CD8 to CD4 ratio, fold expansion during manufacturing, and T cell persistence *in vivo* (Besser et al. 2010; Robbins et al. 2004; Zhou et al. 2005).

With regards to the targeting of tumors by TILs, gene mutation represents a rich source for cancer associated antigens as a hallmark of cancer formation is the accumulation of unrepaired genetic mutations. Gene mutations create changes in the final protein sequence via single amino acid insertions/deletions, shifting the phase of the open-reading frame, or by the removal of a stop-codon leading to an extended translational sequence, leading to the production of potential neoantigens. It is estimated that as many as half of the cancer associated antigens recognized by T cells are derived from mutated genes (Coulie et al. 2014). The Rosenberg group at the National Cancer Institute, as well as many other labs, are currently pioneering the identification of these neoantigens from resected tumor samples in an effort to develop personalized cancer therapies (Yossef et al. 2018). Additionally, multiple groups have identified neoantigen reactive T cells in infused TIL products, with examples of products that contain up to 12%of T cells recognizing a single mutation (Lu et al. 2014; Cohen et al. 2015). Though there are examples of TILs against shared neoantigens, such as KRAS "hotspot" mutation G12D (Tran et al. 2016), the majority of TILs target unidentified or unique neoantigens, making it a truly personalized medicine.

In addition to neoantigens, tumors express more categories of MHC expressed cancer associated antigens, such as cancer associated viral antigens and cancer-germline antigens. The viral antigens are of high interest as it is estimated that nearly one-sixth of new cancer diagnosis world-wide are due to infectious agents (~ two million) in which nearly two-thirds are associated with a viral infection (de Martel et al. 2012). Cancer-germline antigens, also referred to as cancer-testis antigens, are characterized by their expression in male germinal cells and cancerous lesions. The expression is nearly absent in normal healthy tissue and the expression in the male testis is of little concern due to the presence of a blood-testis barrier and an absence of HLA class I expression on germ cells (Ghafouri-Fard 2014). More than 60 cancer-germline genes have been identified, with a majority of them being located on the X chromosome, with the two largest gene sets belonging to the melanoma antigen gene family (MAGE) (MAGEA n=12, MAGEB n=9, MAGEC n=4) and cancer and testis antigen family (GAGE) (GAGE n=9, XAGE n=10) gene families (Coulie et al. 2014). Both antigen classes have been explored using *ex vivo* T cell cloning and T-cell GT cellular therapy approaches.

As with TIL protocols, there are several clinically applied protocols for the *ex vivo* cloning of cancer associated antigen specific T cells. In general, they share the common features in which a patient's T cells are first stimulated with an APC to selectively activate and expand the low frequency T cells of interest. Nasopharyngeal carcinoma is nearly universally infected with Epsein-Barr virus (EBV) and the viral antigens expressed are potential targets for ACT (Niedobitek 2000). As such, protocols have been devised by which autologous EBV-transformed lymphoblastoid B-cell lines serve as antigen presenting cells in the generation of EBV specific cytotoxic T cells through two rounds of *ex vivo* stimulation (Straathof et al. 2005). Melanoma antigen recognized by T cells 1 (MART-1) reactive T cells have been generated through the use a more laborious procedure in which MART-1 pulsed autologous DCs serve as APCs for IL-21 primed T cell cloning, cell-sorting, and REP (similar to TIL process) (Chapuis et al. 2012). While MART-1 does not belong to the cancer-germline class of antigens, it is exclusively expressed by non-vital melanocytes, making it a suitable candidate for immunotherapy. Additionally, other investigators have adapted this same DC based *ex vivo* cloning strategy with the use of cancer-germline antigens (Immatics US Inc, data not published).

While TIL and *ex vivo* cloning protocols aim to expand a preexisting pool of cancer associated antigen specific T cells, GT cellular therapy overcomes this limitation by delivering a molecule with defined antigen specificity directly to a starting polyclonal population of T cells. For sake of simplicity, we can consider these approaches generally equivalent in their manufacturing process, though they do differ in the type of gene transferred (Harris and Kranz 2016). The GT approaches can be divided in to chimeric antigen receptor (CAR) and TCR transfer based on the molecule delivered.

Cancer Immunotherapy – Gene Therapy

CARs are synthetic cell surface receptors, composed of an antibody derived single chain variable fragment (scFv) fused to a linker transmembrane domain, attached to an activating signaling intracellular domain (June and Sadelain 2018). The scFv enables the recognition of extracellular antigens with high affinity in an MHC independent manner, which enables CARs to target tumors which have down-regulated their antigen processing machinery (Lichtman and Dotti 2017). First generation CAR technology utilized a singular CD3ζ intracellular tyrosine activation motif (ITAM), which proved ineffective in boosting T cell activation and persistence *in vivo.* Later, second generation CAR constructs combined the CD3ζ ITAM combined with costimulatory domains from CD28 or 4-1BB (Sadelain, Brentjens, and Riviere 2009). These advanced constructs showed superior functionality and formed the basis for the clinical success in target CD19+ B-cell malignancies and the FDA approval of the novel cellular immunotherapies Kymriah and Yescarta (Baybutt et al. 2018). While αCD19 CARs have had the most clinical success, CARs targeting other hematological antigens, such as B-cell maturation antigen have shown early signs of clinical success (Ali et al. 2016). It remains to be seen whether CAR technology can translate its success to solid tumors (Newick et al. 2017), where TCR based immunotherapies have shown more success.

While CAR technology is a synthetic biology approach, TCR GT starts by first isolating a TCR of interest from a pre-existing pool of naturally occurring

TCRs. Clinically validated TCRs have been isolated from previously treated clinically responding TIL patients in the treatment of melanoma and synovial sarcoma (Morgan et al. 2006; Robbins et al. 2008). This approach has the benefit that the TCRs have shown a safety and efficacy profile *in vivo*. In contrast, clinical TCRs have been isolated via the vaccination of human HLA transgenic mice followed by the cloning of the TCRs from reactive T-cell populations (Johnson et al. 2009). This approach has the benefit that it may yield high avidity TCRs that have bypassed human thymic selection, though it is hindered by potential immunogenicity against the transferred TCRs *in vivo*. Additionally, clinical TCRs have been created via *ex vivo* T-cell stimulation cloning approaches in which healthy donor T cells are stimulated with MHC-peptide loaded artificial APCs (Walter et al. 2003). This strategy ensures that the TCR has gone through human thymic selection, increasing the safety profile, though these TCRs are likely of lower TCR avidity and untested *in vivo*. Following identification, TCR affinity may be artificially increased by directed mutagenesis, though it should be noted that this approach has proven quite controversial following the death of patients in two separate clinical trials using affinity enhanced TCRs targeting MAGE-A3 (Morgan et al. 2013; Linette et al. 2013).

Regardless of whether it be a CAR or a TCR, the process of making the T-cell product can be divided into five critical steps: the leukapheresis to isolate the patients peripheral blood mononuclear cells (PBMCs), activation and genetic modification of the T cells from the PBMCs with a non-viral or virally encoded TCR/CAR vector, expansion of the T cells to create a clinically relevant dose, optional lymphodepletion of the patient before T-cell infusion, and infusion of the modified T cells into the patient (Maus and June 2016).

The activation of the T-cell compartment is primarily achieved via the use of agonistic αCD3 with or without costimulatory stimulation via αCD28, followed by the expansion in, usually, IL2 (Kohl et al. 2018), though IL7 + IL15 has recently gained interest as it yields a more naive T-cell final product (Xu et al. 2014).

Specific Aims and PhD Outline

During the expansion, T cells begin clonal expansion and acquisition of T-cell effector functions while losing their proliferative potential and ability to persist *in vivo* (Gattinoni, Klebanoff, and Restifo 2012). Compounding this problem is the fact that many industry standard assays (e.g IFN-γ release and chromium release) are effector centric and can be anti-correlative with *in vivo* T-cell efficacy (Gattinoni, Klebanoff, et al. 2005). As effector functions are gained with longer T-cell manufacturing, it is perhaps the nature of these assays that has prevented the shortening of T-cell manufacturing protocols. The work described in this dissertation is directed as addressing these critical problems. My specific aims are to:

1) Develop an *in vitro* assay aimed at predicting long-term tumor control rather than short-term effector function

2) Compare the effect of *ex vivo* expansion durations on the quality of gene therapy transfer T-cells using the newly-developed assay and perform mechanism of action (MOA) studies

3) Determine the clinical relevance of the MOA studies using correlative studies aimed at testing the pre-clinical determined mechanism

In terms of the assay, I aimed to develop it to be functional based, guided by pre/clinical correlatives, robust with minimal manipulation, and validated with clinical efficacy or clinical data analysis. Towards this goal, I developed the "cytokine sensitivity assay" (CSA, figure 3). This assay involves the thawing of a T-cell final product, which is then quickly exposed to growth cytokines of interest, followed by the tracking of the T cell response in an environment devoid of T-cell receptor (TCR) stimulation. This assay shares many similarities to other assays with the notable exception that the cells used 1) were frozen and thawed to mimic the way in which the T cells will be infused into patients and 2) the cytokines were added in every 7 days compared to the usual 2-4 day regimen (Berger et al. 2008). Importantly, the cytokines used were either homeostatic cytokines (IL7 or IL15), known to be important for T-cell persistence at a steady state (Fry and Mackall 2005; Gattinoni, Finkelstein, et al. 2005) or IL2 which is usually given following T-cell infusion to increase T-cell engraftment and expansion (Andersen et al. 2016).

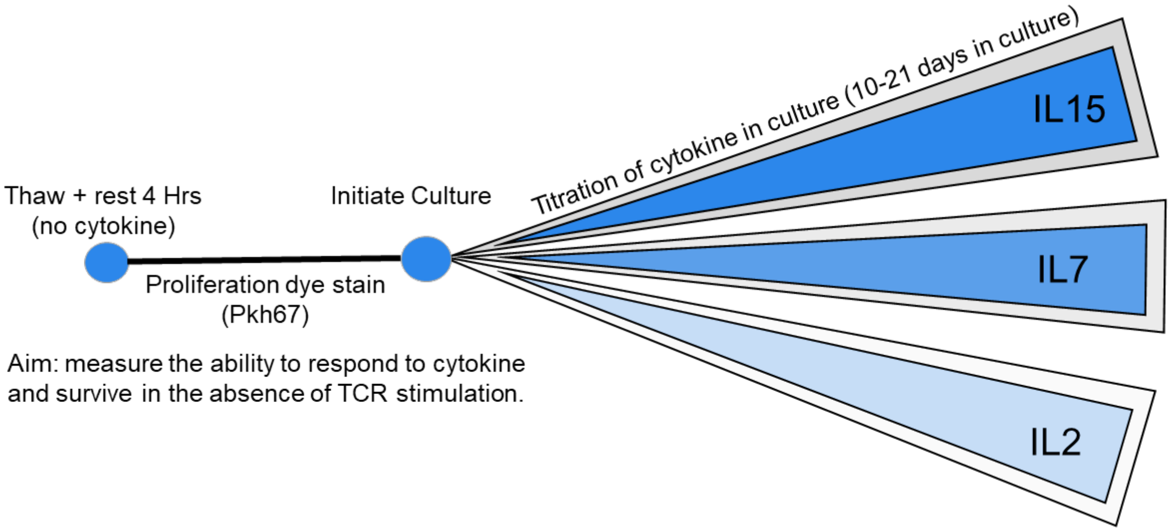

Figure 3: The cytokine sensitivity assay. The process is initiated by thawing a frozen T-cell product, resting the cells in the absence of any growth cytokines, and labelling with a proliferation dye. The cells are then exposed to a titration of various cytokines and the cell behavior (e.g. proliferation, apoptosis, division, etc.) is tracked over a 21-day period, depending on the experimental details.

Following the development of the CSA, mechanistic studies were performed to measure the following attributes during T-cell *ex vivo* expansion:

1) Multi-parameter phenotypic flow cytometry
2) Relative Telomere Length
3) Whole RNA sequencing
4) Single molecule DNA sequencing

From the CSA results, I observed that T cells expanded for a shorter period of time performed significantly better than the T cells expanded for a longer duration .Further, it was noted that the T cells from younger healthy donors performed perceptively better than T cells derived from older, healthy donors. Therefore, I sought to understand this mechanistically.

During the phenotypic mechanism of action studies, it was noted that there was an age correlated loss of the costimulatory molecule CD28. This was a critical observation as CD28 stimulation is often used in the manufacturing of T cells. This observation has been made by many other investigators (Weng, Akbar, and Goronzy 2009), though to my knowledge, it has not been applied to the field of gene transfer therapy T-cell manufacturing. In addition, many manufacturing metrics (e.g. total T cell fold expansion and the final CD8 to CD4 ratio) are correlated with the starting percentage of CD28 expression. Further investigations showed that the telomere length, a critical aspect of cellular proliferation potential (Qian, Yang, and Cao 2014), decreased during T-cell expansion and that this loss correlated with donor age (expected) and CD28 expression (unexpected). The loss of telomere length was further supported by an increased loss of telomerase activity as T-cell expansion was prolonged.

From these mechanistic studies, I propose a mechanism of T-cell expansion in which intrinsic (e.g. donor age or CD28 expression) or extrinsic (type of manufacturing performed) factors can create *ex vivo* bottlenecks to T-cell clonal survival. This model would suggest that the estimated number of cellular divisions that a T cell would undergo during expansion is vastly misrepresented by commonly used methods of estimated population doublings (Ghassemi et al. 2018). For example, if we have a final T-cell product which achieved a total T-cell fold expansion of 64-fold, then a predicted estimate would be that each T-cell underwent eight population doublings according to the following equations:

$$\text{Fold expansion} = (\text{Final Cell \#} / \text{Starting Cell \#})$$

$$\text{Estimated Divisions Per Cell} = \text{Log}_2(\text{Fold Expansion})$$

However, if there is a significant amount of cellular death, due to the proposed bottlenecks, then the estimated divisions per cell would be underestimated by this logic. To my knowledge, no one has proposed a system for accurately estimating the number of cell divisions per T-cell when starting from a polyclonal T-cell population, such as the one found in clinical T-cell expansion protocols. I propose that this number can be accurately quantified for a certain percentage of T-cells by using single molecule DNA sequencing of CDR3 regions (unique to each T-cell clone) by the following equations:

$$\text{Clonal Fold Expansion} = (\text{Final Clone \#} / \text{Starting Clone \#})$$

$$\text{Estimated Divisions Per Clone} = \text{Log}_2(\text{Clonal Fold Expansion})$$

Using the proposed formula, the proposed bottleneck model was supported by showing that CD28 expression correlated with the loss of T-cell clones during manufacturing, with the most elderly of the donors containing fewer unique T-cell clones by day 10 of the expansion protocol compared to an early post-activation time-point. Additionally, the percentage of clones which changed significantly relative to the total clone number correlated with the starting percentage of CD28 in the T-cell population.

The clinical relevance of these findings was ultimately supported by a meta-analysis of current CD19 comparable CAR clinical trials (n=47 patients). It was determined that patients younger than 45 would likely benefit from a CD3 + CD28 method of T-cell manufacturing, while patients older than 45 would likely benefit from a CD3 only method of T-cell manufacturing. It is an aim of my post-doctoral work to follow up with this finding among others discussed in the results section.

Methods

T-Cell Manufacturing

Healthy donor whole blood was purchased from Hemacare and PBMCs were isolated by Ficoll gradient. PBMCs were activated for 16-24 hours in TexMACS (Milltenyi 130-097-196) supplemented with 5% Human AB serum (Gemini 100-318) media by plating at 1e6 live PBMC/mL on tissue culture flasks coated overnight with 1 ug/mL anti-CD3 (eBioscience 16-0037-85) and 1 ug/mL anti-CD28 (eBioscience 16-0289-85) antibody in PBS (Lonza 17-516F) at 4 degrees Celsius. The next day, total cells were isolated and resuspended to 1e6 live-cell/mL and 5 mLs were plated into a well of a Grex24 well plate (Wilson Wolf 80192M). Cells were either mock transduced or transduced with a TCR lentiviral construct (produced by Lentigen) in the presence of 10 ng/mL IL7 (peprotech 200-07), 100 ng/mL IL15 (peprotech 200-15), and 10 μg/mL protamine sulfate. The next day, cells were fed with 35 mL of complete TexMACS supplemented with IL7 and IL15 at above mentioned concentrations. Cells were grown for an additional 2, 5, or 8 days depending on the desired manufacturing time (4, 7, or 10 total days). After manufacturing, cells were counted and frozen down at $5e^6$/mL in Cyrostore10, placed at -80 degrees Celsius for 16-24 hours and then stored long-term at LN2 vapor phase until needed.

PkH67 stain

PkH67 (Sigma PKH67GL) stain was performed per manufacturer's protocol with the exception that the day 4 manufactured cells were stained at a 2X concentration to account for the larger cell size compared to day 7 or day

10 manufactured cells. PkH staining was performed before the flow cytometry viability dye stain.

Cytokine Sensitivity Assay (CSA)

T-cell products were thawed and rested for approximately four hours in TexMACS supplemented with 5% Human AB serum and 100 U/mL Benzonase (Sigma E10114) at 1-2e6/mL. Following resting period, cells were labeled with PkH and 2e5 lymphocytes were cultured in a Grex24 well flask with a titration of IL7, IL15, or IL2 (R&D Systems 202-IL) for a total of 21 days. During this time, cells were counted by volumetric flow cytometry every three to four days and phenotyped with memory T-cell panel every seven days. Cytokines were replenished every seven days to the starting concentration.

Flow Cytometry Stain and Acquisition

Live cells were quantified and resuspended to 1-2e^{6} live-cell/mL in PBS then stained with Live-Dead stain according to manufacturer’s protocol. Cells were then washed with Flow buffer and then resuspended at desired antibody concentrations as indicated in the tables below and stained for 15-30 minutes in the dark at 4 degrees Celsius, with the exception that the CCR7 stain was done at 37 degrees Celsius in RPMI (Gibco 11835-030) without serum. Cells were then washed in Flow buffer and resuspended in fixation buffer and stored at 4 degrees Celsius until acquired on the BD Fortessa or Miltenyi MACSQuant analyzer. The following tables contain the reagents used for all flow cytometry staining.

Memory T - Cell Panel for Cytokine Sensitivity Assay					
Fluorochrome	Antigen	Clone	Dilution	Provider	Catalog Number
AX488	PkH	N/A	N/A	Sigma	PKH67GL-1KT
PerCP-Cy5.5	CD3	HIT3a	80	BioLegend	300328
PE	Vb8	JR2	80	BioLegend	348104
PE-Cy7	CD45Ro	UCHL1	80	BioLegend	304230
APC-fire750	CD95	DX2	80	BioLegend	305638
BV421	CCR7	G043H7	80	BioLegend	353208
Aqua	Live/dead	NA	400	Thermo fischer	L34957
BV605	CD8	SK1	80	BD Horizon	564116
BV650	CD27	O323	80	BioLegend	302827
BV785	CD62L	DREG56	80	BioLegend	304830

Cytokine Receptor T - Cell Panel for Cytokine Sensitivity Assay					
Fluorochrome	Antigen	Clone	Dilution	Provider	Catalog Number
AX488	Vb8	JR2	80	BD BioScience	555606
PE	CD127	A019D5	80	BioLegend	351304
APC	CD122	TU27	80	BioLegend	339008
BV421	CD25	G043H7	80	BD Horizon	562442
BV605	CD8	SK1	80	BD Horizon	564116

Costimulation Phenotyping Panel					
Fluorochrome	Antigen	Clone	Dilution	Provider	Catalog Number
PerCP-Cy5.5	CD3	HIT3a	80	BioLegend	300328
PE	CD127	A019D5	80	BioLegend	351304
PE-Cy7	CD57	HNK-1	80	BioLegend	359623
APC	CD122	TU27	80	BioLegend	339008
APC-fire750	CD8	Sk1	80	BD Pharmingen	560179
BV421	CCR7	G043H7	80	BioLegend	353208
Aqua	Live/dead		400	Thermo Fisher	L34957
Bright 600	KLRG1	13F12F2	80	BioLegend	138419
BV650	CD27	O323	80	BioLegend	302827
BV785	CD28	CD28.2	80	BioLegend	302949

Telomere length determination

Relative telomere length was determined according to manufacturers instructions (Dako/Agilent K5327). Briefly, T-cells were mixed at a 1:1 ratio with control 1301 tumor cells (4N genome). Cells were then permeabilized and a Telomere PNA FITC probe was hybridized overnight. The next day, a counter propidium iodide stain was performed to discriminate intact cells and the cells were acquired by flow cytometry. The telomere length of the test cells was calculated as a ratio to that of the control 1301 tumor cell line.

Telomerase Activity Assay

Relative telomere length was determined according to manufacturers instructions (Sigma 11854666910). Briefly, T cell lysate was isolated and telomeric DNA was amplified using biotinylated primers. Following the PCR, a colorimetric ELISA is performed to detect these biotinylated fragments and absorption spectrums are fit to a standard curve.

CDR3 sequencing (Adaptive Biotech) and Analysis of T-cell receptor variable beta chain sequencing

Immunosequencing of the CDR3 regions of human TCRβ chains was performed using the immunoSEQ® Assay (Adaptive Biotechnologies, Seattle, WA). Extracted genomic DNA was amplified in a bias-controlled multiplex PCR, followed by high-throughput sequencing. Sequences were collapsed and filtered in order to identify and quantitate the absolute abundance of each unique TCRβ CDR3 region for further analysis as previously described (Robins et al. 2009; Carlson et al. 2013; Robins et al. 2012).

Statistical Analyses of TCR-β sequencing results

Clonality was defined as 1- Peilou's eveness (Kirsch, Vignali, and Robins 2015) and was calculated on productive rearrangements by: $1+\frac{\sum_{i}^{N} p_i \log_2(p_i)}{\log_2(N)}$ where P_i is the proportional abundance of rearrangement i and N is the total number of rearrangements. Clonality values range from 0 to 1 and describe the shape of the frequency distribution: clonality values approaching 0 indicate a very even distribution of frequencies, whereas values approaching 1 indicate an increasingly asymmetric distribution in which a few clones are present at high frequencies. Statistical analysis was performed in R version 3.2.

RNAseq (Novogene) Data Analysis

Downstream analysis was performed using a combination of programs including STAR, HTseq, Cufflink and our wrapped scripts. Alignments were parsed using Tophat program and differential expressions were determined through DESeq2/edgeR. GO and KEGG enrichment were implemented by the ClusterProfiler. Gene fusion and difference of alternative splicing event were detected by Star-fusion and rMATS software

RNAseq (Novogene) Reads mapping to the reference genome

Reference genome and gene model annotation files were downloaded from genome website browser (NCBI/UCSC/Ensembl) directly. Indexes of the reference genome was built using STAR and paired-end clean reads were aligned to the reference genome using STAR (v2.5). STAR used the method of Maximal Mappable Prefix(MMP) which can generate a precise mapping result for junction reads.

RNAseq (Novogene) Quantification of gene expression level.

HTSeq v0.6.1 was used to count the read numbers mapped of each gene. And then FPKM of each gene was calculated based on the length of the gene and reads count mapped to this gene. FPKM, Reads Per Kilobase of exon model per Million mapped reads, considers the effect of sequencing depth and gene length for the reads count at the same time, and is currently the most commonly used method for estimating gene expression levels (Mortazavi et al., 2008).

RNAseq (Novogene) Differential expression analysis

(For DESeq2 with biological replicates) Differential expression analysis between two conditions/groups (two biological replicates per condition) was performed using the DESeq2 R package (2_1.6.3). DESeq2 provide statistical routines for determining differential expression in digital gene expression data using a model based on the negative binomial distribution. The resulting P-values were adjusted using the Benjamini and Hochberg's approach for controlling the False Discovery Rate(FDR). Genes with an adjusted P-value <0.05 found by DESeq2 were assigned as differentially expressed. (For edgeR without biological replicates) Prior to differential gene expression analysis, for each sequenced library, the read counts were adjusted by edgeR program package through one scaling normalized factor. Differential expression analysis of two conditions was performed using the edgeR R package (3.16.5). The P values were adjusted using the Benjamini & Hochberg method. Corrected P-value of 0.05 and absolute foldchange of 1 were set as the threshold for significantly differential expression.

RNAseq (Novogene) Correlations

To allow for log adjustment, genes with 0 FPKM are assigned a value of 0.001. Correlation were determined using the cor.test function in R with options set alternative =”greater” and method = “Spearman”.

RNAseq (Novogene) Clustering

To identify the correlation between difference, we clustered different samples using expression level FPKM to see the correlation using hierarchical clustering distance method with the function of heatmap, SOM(Self-organization mapping) and kmeans using silhouette coefficient to adapt the optimal classification with default parameter in R.

RNAseq (Novogene) GO and KEGG enrichment analysis of differentially expressed genes

Gene Ontology (GO) enrichment analysis of differentially expressed genes was implemented by the cluster Profiler R package, in which gene length bias was corrected. GO terms with a corrected p-value less than 0.05 were considered significantly enriched by differential expressed genes. KEGG is a database resource for understanding high-level functions and utilities of the biological system, such as the cell, the organism and the ecosystem, from molecular level information, especially large-scale molecular datasets generated by genome sequencing and other high-through put experimental technologies (http://www.genome.jp/kegg/). We used cluster Profiler R package to test the statistical enrichment of differential expression genes in KEGG pathways.

Chapter 1: Cytokine Sensitivity Assay (CSA)

To investigate the role of *ex vivo* T-cell expansion length on T-cell fitness, T-cells were manufactured for 4, 7, or 10 days (see methods section for details). After this manufacturing, the T-cells were analyzed via the CSA and the following metrics were analyzed:

1) Cell survival as measured by fold growth of T-cells
2) Apoptosis as measured by propidium iodide and Annexin-V stain
3) Division as measured by the dilution of proliferation dye PkH67
4) Cytokine receptor expression as measured by flow cytometry
5) T-cell memory phenotype as measured by flow cytometry

As shown in the following CSA related figures, the longer expansions led to a dramatic reduction in the fitness of the T-cells when assessed within the CSA as exemplified by:

1) Decreased T-cell survival
2) Increased Apoptosis
3) Decreased division rate
4) Decreased survival of the T-naïve_scm compartment

Of importance, as the CSA presented was performed for 21 days, each sample was analyzed at 7 time points and this necessitated the definition of a single metric to describe the temporal behavior. For this purpose, the area under the curve (integration) of the temporal data was calculated and is used as a single defining metric to represent the behavior of the sample over the 21 days in the following results.

Reduced T-cell proliferation with longer duration of CD3/CD28 expansions.

Thawed, expanded T-cells were assessed for their ability to survive in the presence of IL7, IL15, or IL2 in the absence of additional antigen or CD3 stimulation. Day 4 expanded T-cells were able to substantially outgrow the Day 7 or Day 10 expanded T-cells in all three cytokine conditions with an approximately 10-, 30-, and 15-fold peak fold growth in IL7, IL15, and IL2 (figure 4). Conversely, day 7 and day 10 expanded T cells were unable to sustain substantial growth in any of the cytokine conditions. Importantly, in the absence of all cytokines, each T-cell population died at a similar rate regardless of expansion protocol length.

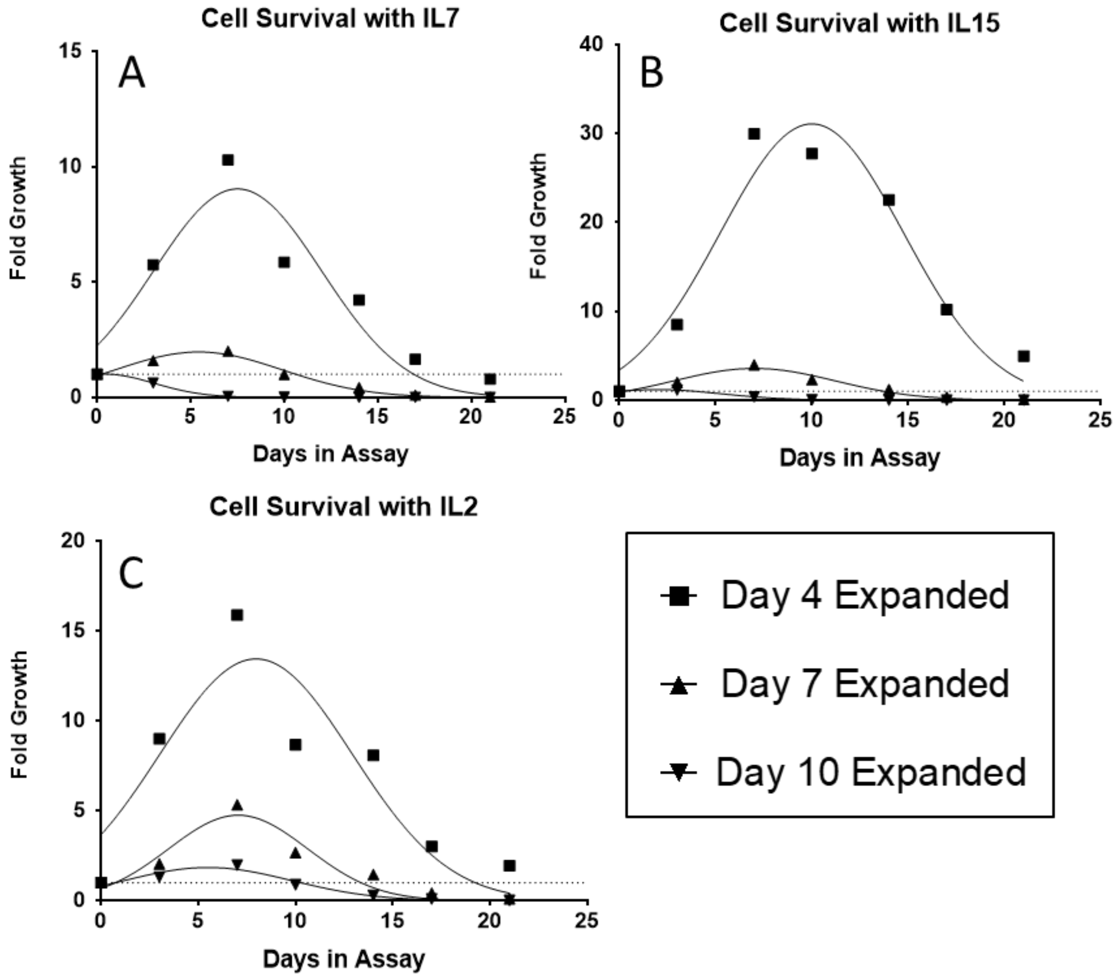

Figure 4: Lymphocyte fold growth plots from CSA with multiple cytokines. T-cells expanded for 4, 7, or 10 days were assessed in the presence of 10 ng/mL IL7 (A), 10 ng/mL IL15 (B), or 300 U/mL IL2 (C) over a period of 21 days with sampling every 2-3 days. Fold growth is calculated as the ratio of the starting T-cell number to the T-cell number at the designated time point. Note that each plot has a different scale on the Y-axis to facilitate data visualization. Best fit lines are derived by linear quadratic equations of cell survival.

Summary of cytokine sensitivity assay T-cell survival.

The integrated survival of each fold growth curve shown in figure 4 was determined by calculating the area under the curve. From an analysis of three biological donors, there was a trend in which the day 4 expanded T cells outperformed the day 7 or day 10 expanded cells (figure 5). For IL2, there was an approximately 5-fold drop in survival between day 4 and day 7 expanded cells, with an approximately 2-fold drop in survival between day 7 and day 10 expanded cells. For IL7, there was an approximately 6-fold drop in integrated survival between day 4 and day 7 expanded cells, with an approximately 4-fold drop between day 7 and day 10 expanded cells. For IL15, there was an approximately 8-fold drop in integrated survival between day 4 and day 7 expanded cells, with an approximately 6-fold drop between day 7 and day 10 expanded cells. Importantly, while there was no statistical significance due to the large degree of donor to donor variation, there was a consistent trend in which the earlier expanded cells out survived the later expanded cells.

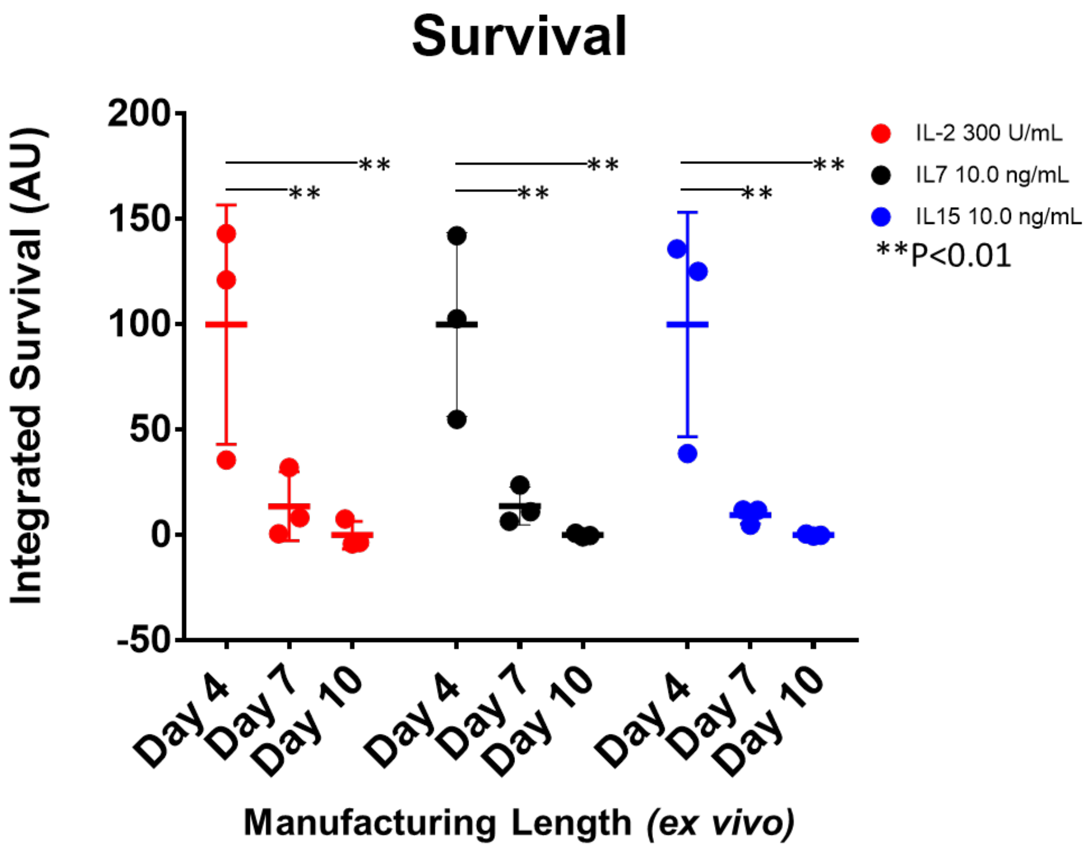

Figure 5: Lymphocyte fold growth plots from CSA with multiple cytokines. T-cells expanded for 4, 7, or 10 days were assessed in the presence of 10 ng/mL IL7 (black), 10 ng/mL IL15 (blue), or 300 U/mL IL2 (red) over a period of 21 days with sampling every 2-3 days. Integrated survival is the area under the curve of the fold growth plots as shown in figure 2. Each point represents three technical replicates of each donor with a total of 3 donors shown. **P<0.01 by Anova.

Summary of cytokine sensitivity assay T-cell division.

From the fold growth survival data, I asked whether the earlier expanded T-cells were able to undergo a more rapid entry into cell division compared to the later expanded cells. The earlier expanded cells underwent division as calculated by the percentage of cells which diluted the proliferation dye at each time point across 10 days in the CSA (figure 6). The analysis was done up to 10 days as the later expanded cells did not have enough cells for accurate analysis past day 10. For the IL2 conditions, there was an approximately 30% drop in the integrated division between day 4 and day 7 expanded cells and an approximately 50% drop between day 4 and day 10 expanded cells which was statistically significant ($p=0.0307$). For IL7, the same trend was seen with an approximately 40% drop between day 4 and day 7 expanded cells with an approximately 80% drop between day 4 and day 10 expanded cells which was statistically significant ($p=0.0006$) by ANOVA. For IL15, the same trend was seen with an approximately 20% drop between day 4 and day 7 expanded cells with an approximately 40% drop between day 4 and day 10 expanded cells which was statistically significant ($p=0.0025$).

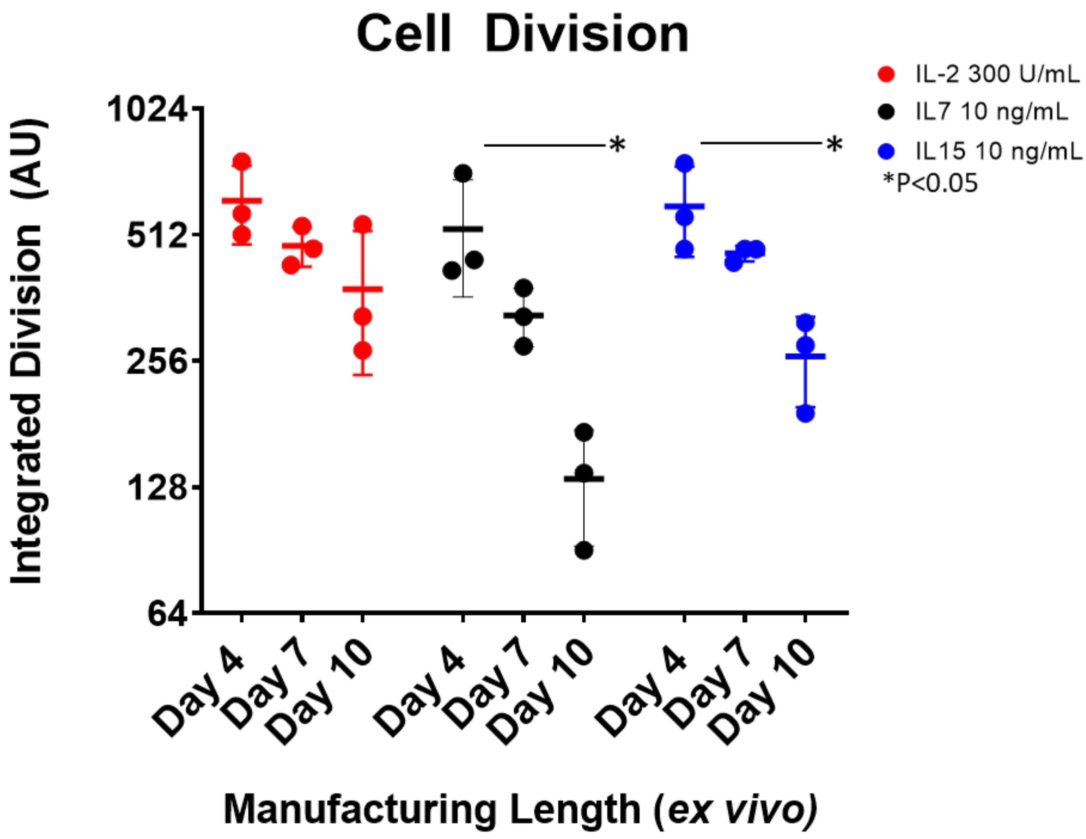

Figure 6: Summary of division from CSA with multiple cytokines. T-cells expanded for 4, 7, or 10 days were assessed via in the presence of 10 ng/mL IL7 (black), 10 ng/mL IL15 (blue), or 300 U/mL IL2 (red) over a period of 21 days with sampling every 2-3 days. Integrated division is calculated based on the percentage of lymphocytes in which at detectable dilution of PkH67 was detected by day 10 in the assay. Each point represents three technical replicates of each donor with a total of 3 donors shown. *P<0.05 by Anova.

Summary of cytokine sensitivity assay T-cell apoptosis

Since there was an increased fold growth of the earlier expanded cells and an increased division, I then asked whether there was a corresponding decrease in apoptosis as assessed via the staining by propidium iodide (PI) and Annexin-V (figure 7).

For the IL2 conditions, there was a statistically insignificant increase (approximately 1.8-fold) in apoptosis between day 4 and day 7 cells, while there was a statistically significant ($p=0.0092$) increase (approximately 3-fold) between day 4 and day 10 cells. For the IL7 conditions, there was a statistically insignificant increase (approximately 2-fold) in apoptosis between day 4 and day 7 cells, while there was a statistically significant ($P<0.0001$) increase (approximately 7-fold) between day 4 and day 10 cells. For the IL15 conditions, there was a statistically insignificant increase (approximately 1.6-fold) in apoptosis between day 4 and day 7 cells, while there was a statistically significant ($P=0.0010$) increase (approximately 5.5-fold) between day 4 and day 10 cells.

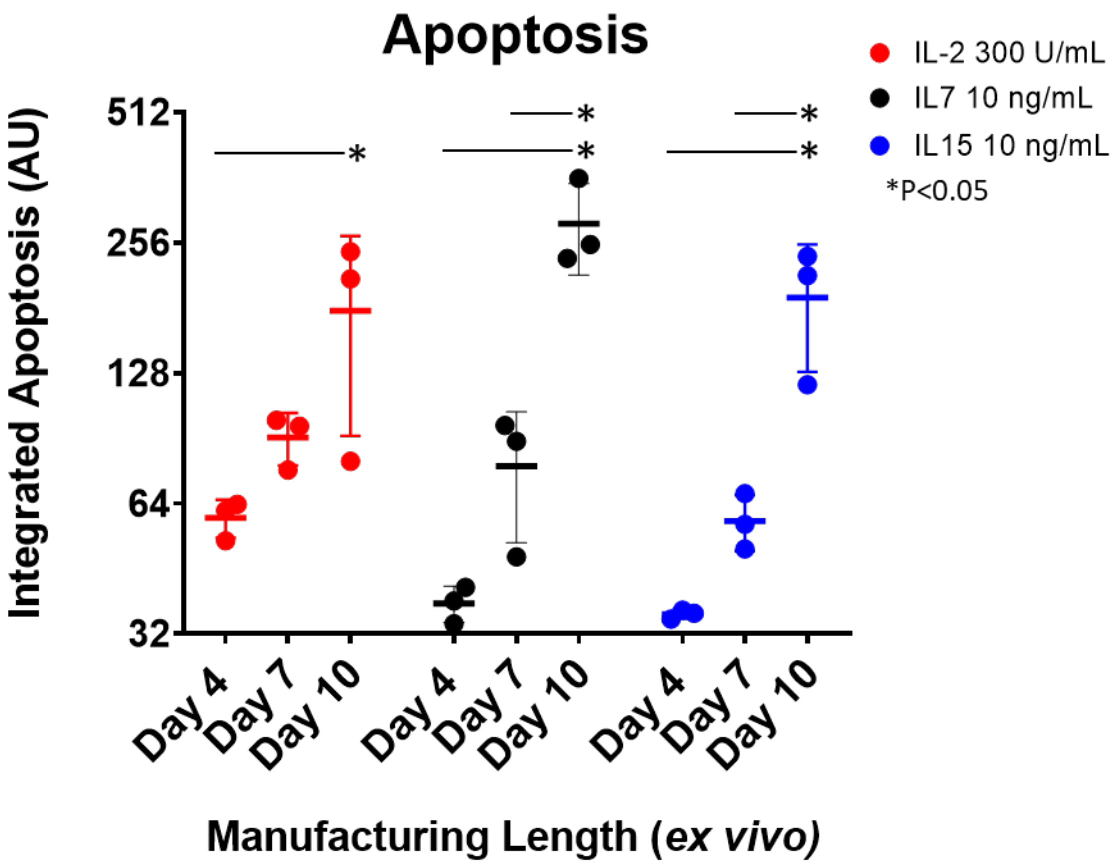

Figure 7: Summary of apoptosis induction in CSA with multiple cytokines. T-cells expanded for 4, 7, or 10 days were assessed via in the presence of 10 ng/mL IL7 (black), 10 ng/mL IL15 (blue), or 300 U/mL IL2 (red) over a period of 21 days with sampling every 2-3 days. Integrated apoptosis is calculated based on the percentage of lymphocytes staining positive for propidium iodide and annexin-V by day 10 in the assay. Each point represents three technical replicates of each donor with a total of 3 donors shown. *P<0.05 by Anova.

Correlations between cytokine receptor expression and cytokine induced survival

The CSA is an assay that measures the response to cytokine induced survival, proliferation, and apoptosis. I postulated that these changes would correlate with the expression of the respective cytokine receptors within each T-cell population at the beginning of the assay. I measured the expression of the defining subunit of the IL2, IL7, and IL15 cytokine receptors respectively as IL2α receptor (CD25), IL7α receptor (CD127), and IL15β receptor (CD122) (figure 8 – 10). Of note, IL15β receptor is a shared subunit between the IL2 and IL15 receptors, though it is commonly assigned to be the reactive subunit of the IL15 receptor. There was a strong correlation between the IL2α receptor expression based on percentage of lymphocytes (R^2=0.82) or as the mean fluorescence intensity (MFI) of CD25 expression (R^2=0.89) and the response to IL2 induced survival of in the CSA. There was no correlation between the IL7α receptor expression based on percentage of lymphocytes (R^2=0.04) the response to IL7 induced survival of in the CSA. Of interest, there was a moderate correlation between the MFI of IL7α receptor expression (R^2=0.76) and IL7 induced survival. There was a weak correlation between the IL15β receptor expression based on percentage of lymphocytes (R^2=0.42) or a moderate correlation as the MFI of IL15β receptor expression (R^2=0.67) and the response to IL15 induced survival of in the CSA.

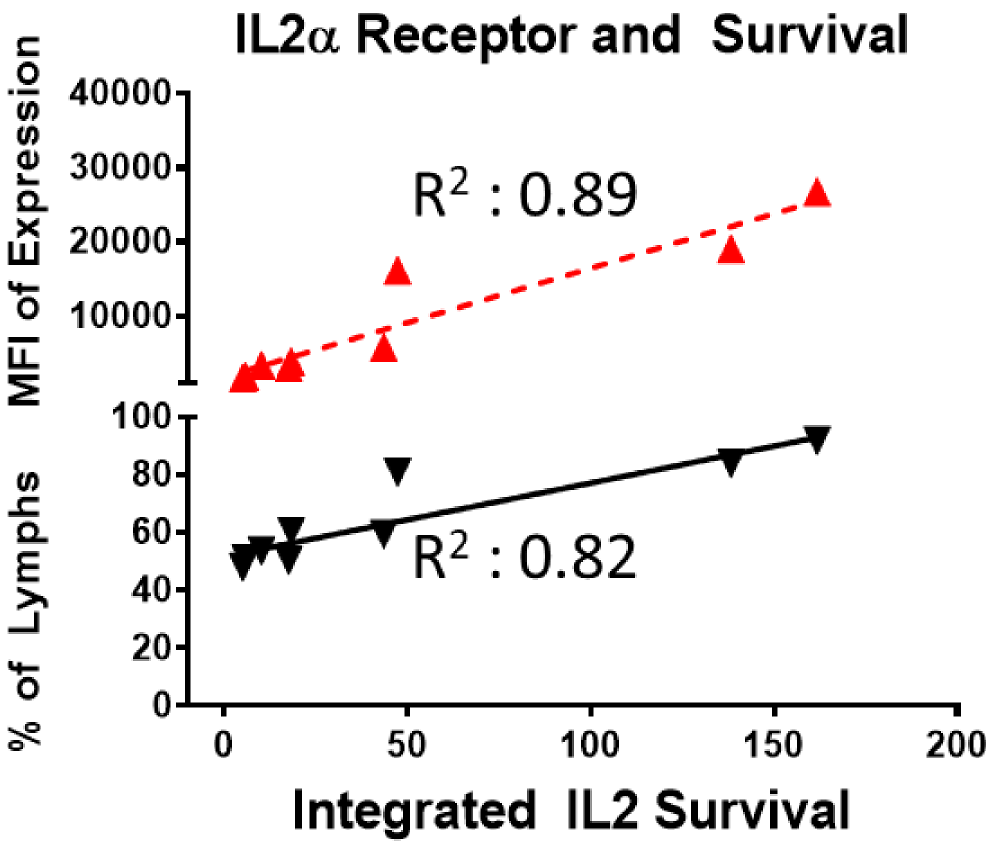

Figure 8: IL2α receptor expression correlates with area under the curve (AUC) fold growth in CSA response with IL2. IL2α receptor expression was calculated at day 0 before initiation of the CSA with IL2 by mean fluorescence intensity (MFI) of IL2α receptor (red) or by the percentage of lymphocytes expressing IL2α receptor (black). R^2 correlations are shown for each respective line. Each sample point is the mean of a technical replicate (n=3) for 3 total biological replicates. IL2α receptor expression was monitored with a BV421 conjugated antibody. AUC represents the integration of the fold growth of the cells over the 21-day period CSA as shown in figure 2.

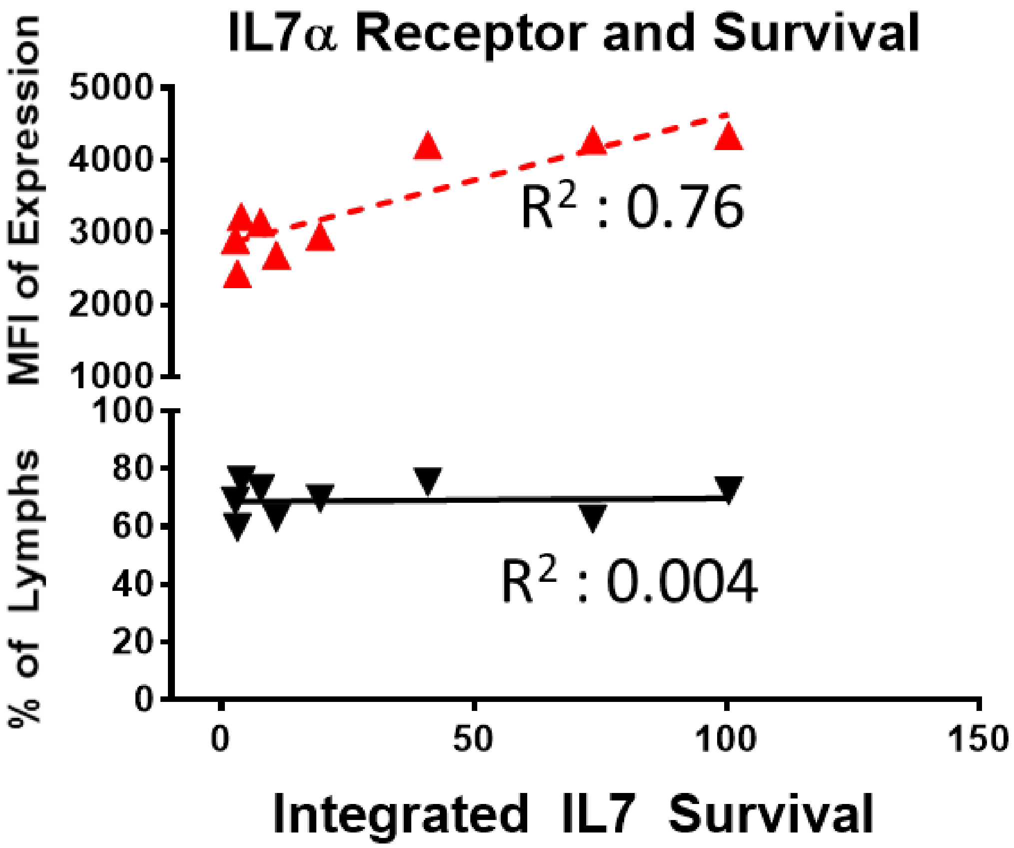

Figure 9: CD127 expression correlates with percentage dividing cells in CSA response with IL7. IL7α receptor (CD127) expression was calculated at day 0 before initiation of the CSA with IL7 by mean fluorescence intensity of IL7α receptor expression (MFI)(red) or by the percentage of lymphocytes expressing IL7α receptor (black). R^2 correlations are shown above each respective line. Each sample point is the mean of a technical replicate (n=3) for 3 total biological replicates. IL7α receptor expression was monitored with a PE conjugated antibody. AUC represents the integration of the percentage of dividing cells by day 3 as shown in figure 2.

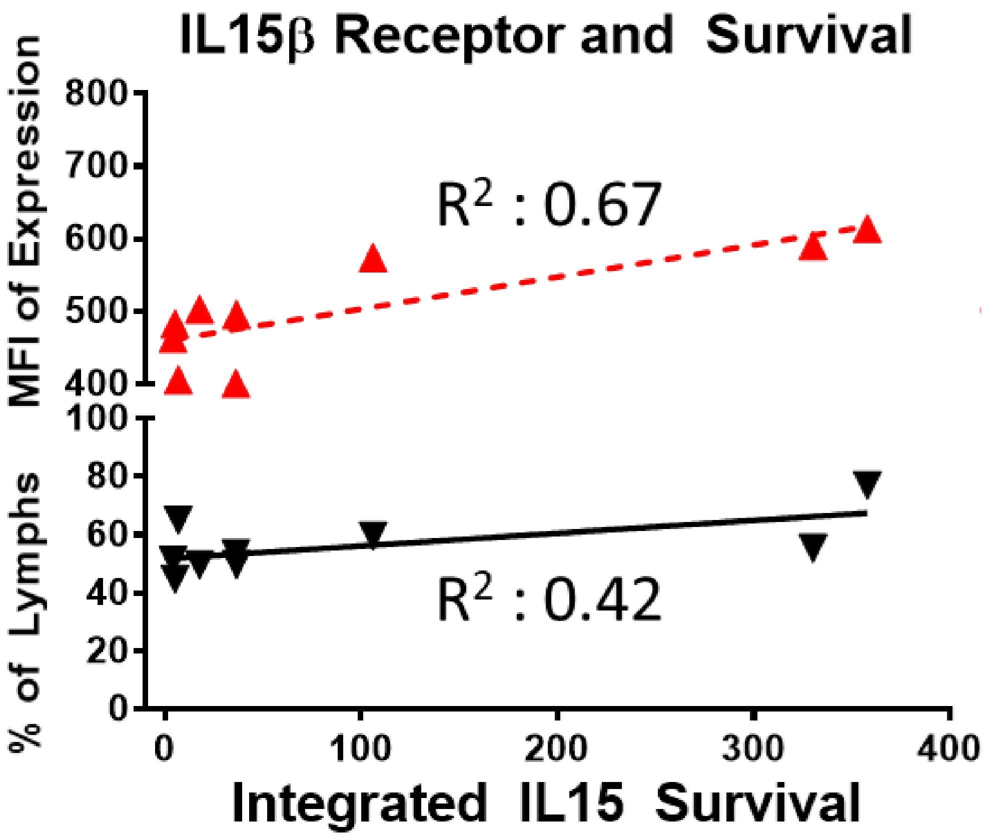

Figure 10: CD122 expression correlates with percentage dividing cells in CSA response with IL15. IL15β receptor (CD122) expression was calculated at day 0 before initiation of the CSA with IL15 by mean fluorescence intensity of IL15β receptor expression (MFI)(red) or by the percentage of lymphocytes expressing IL15β receptor (black). R^2 correlations are shown above each respective line. Each sample point is the mean of a technical replicate (n=3) for 3 total biological replicates. CD122 expression was monitored with an APC conjugated antibody. AUC represents the integration of the fold growth of the cells over the 21-day period CSA as shown in figure 2.

CSA shows preferential survival of distinct T-cell memory populations

Based on the previous results, I investigated whether the survival and proliferation in CSA was restricted to distinct memory compartments or whether each T-cell memory compartment was affected equally across all cytokine conditions. Additionally, I wanted to determine whether the cells continued to differentiate during the CSA or whether the starting memory compartment ratios were maintained. As shown in the following three representative figures (figures 11 – 13), IL2 CSA induced a preferential loss of the earlier differentiated Tnaive_scm and Tcm phenotypes while preserving the later differentiated Tem and Temra phenotypes. Conversely, IL15 and IL7 CSA maintained a nearly equal ratio between the early and later differentiated compartments for the day 4 expanded cells across a 21 day CSA. Only the day 4 expanded cells readily maintained the earlier differentiated phenotypes in all conditions tested, while the day 7 and day 10 expanded cells readily lost the earlier phenotypes and showed a marked differentiation towards later differentiated Tem and Temra cells. In fact, for the day 4 expanded cells in the IL15 and IL7 CSA at day 21 in the assay, there was still greater than 50% of cells restricted to the Tnaive_scm and Tcm compartments, while these compartments were completely lost in the later expanded cells.

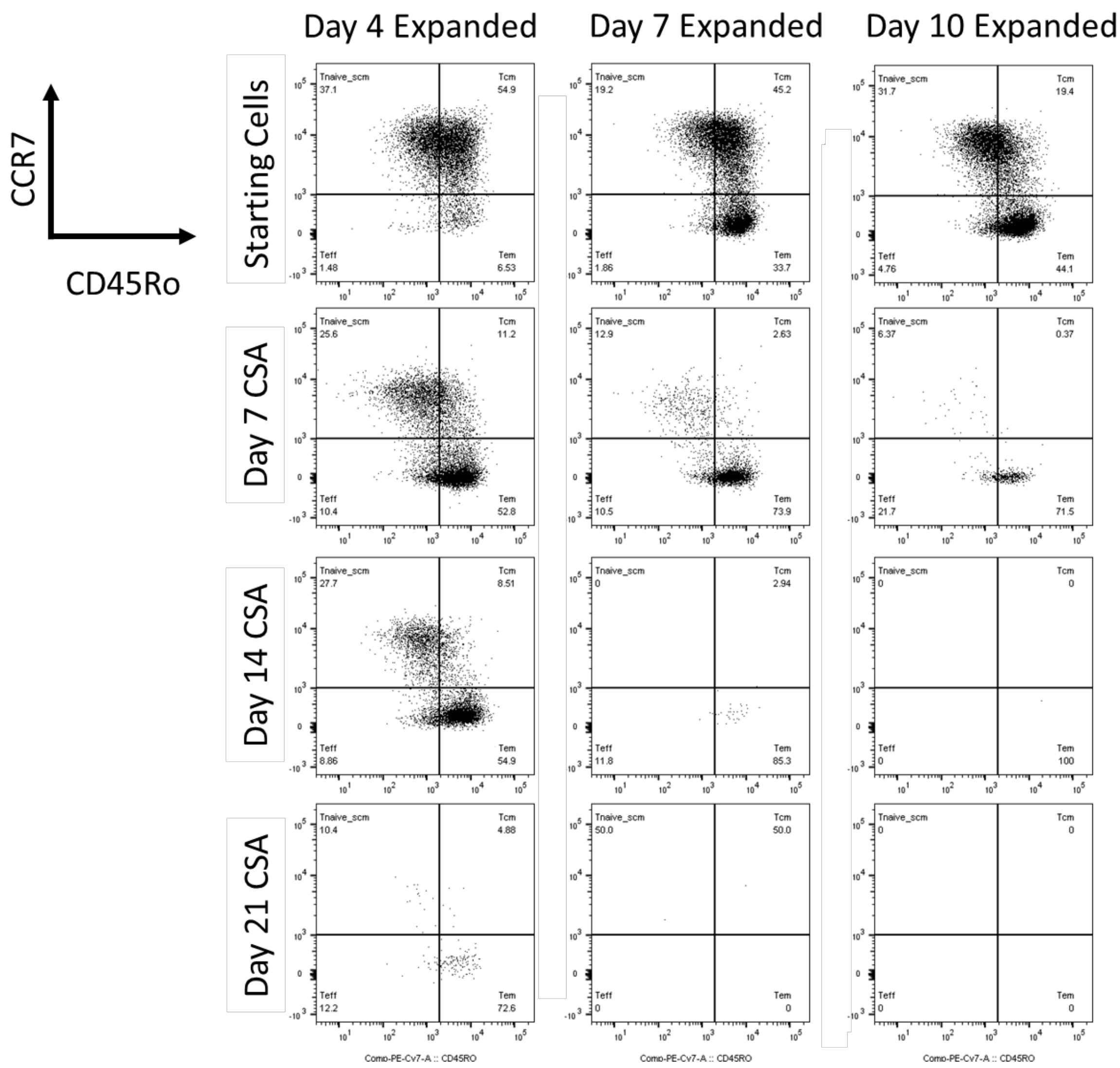

Figure 11: T-cell memory compartments in IL2 CSA. T-cell memory phenotype was assessed on the starting cells and then every 7 days for the length of the 21-day IL2 CSA as shown in figure 3. T-cell memory phenotype was analyzed via CCR7 and CD45Ro expression and compartments are annotated in each quadrant. Data is representative of three biological replicates performed.

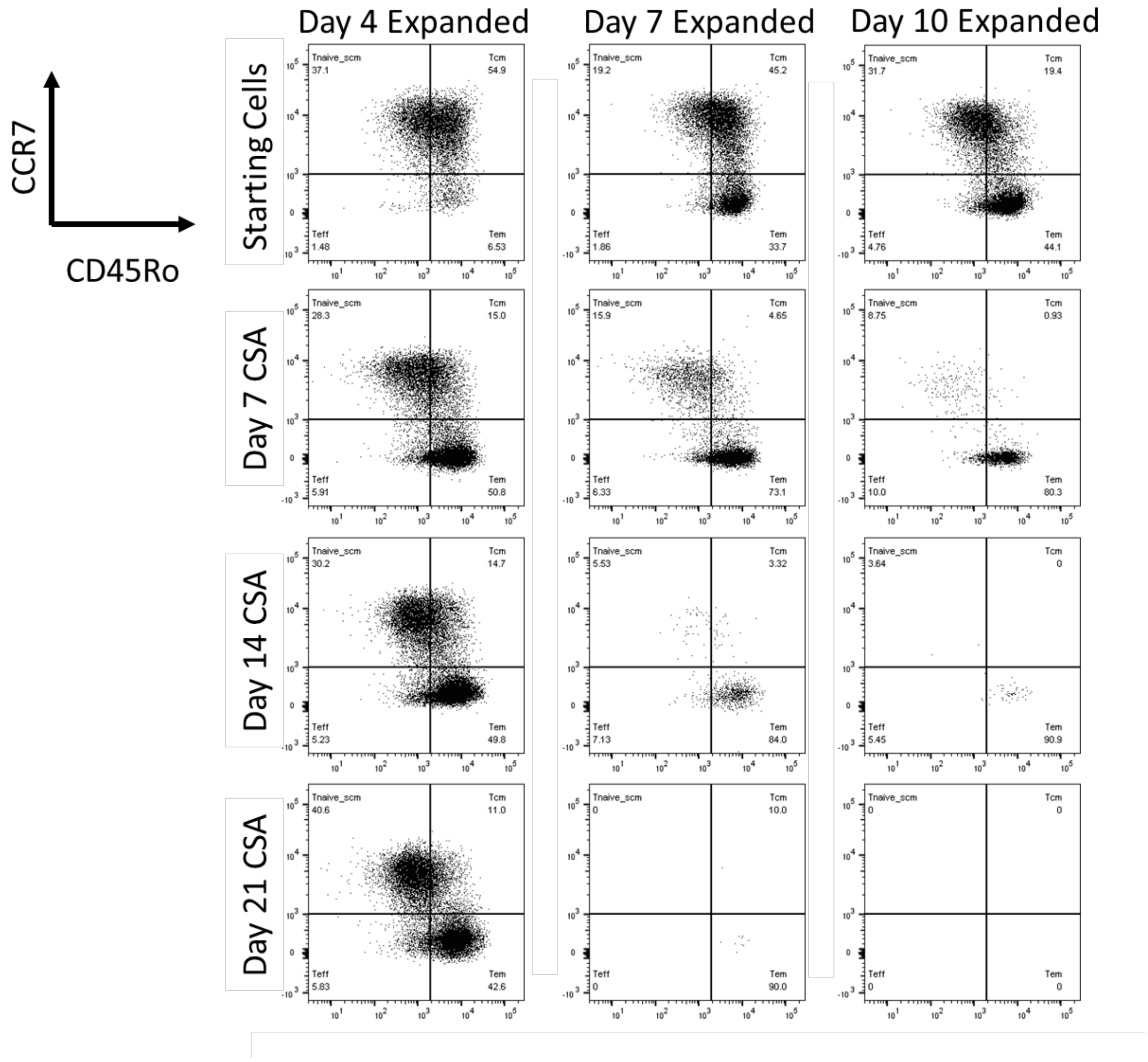

Figure 12: T-cell memory compartments in IL15 CSA. T-cell memory phenotype was assessed on the starting cells and then every 7 days for the length of the 21-day IL15 CSA as shown in figure 3. T-cell memory phenotype was analyzed via CCR7 and CD45Ro expression and compartments are annotated in each quadrant. Data is representative of three biological replicates performed.

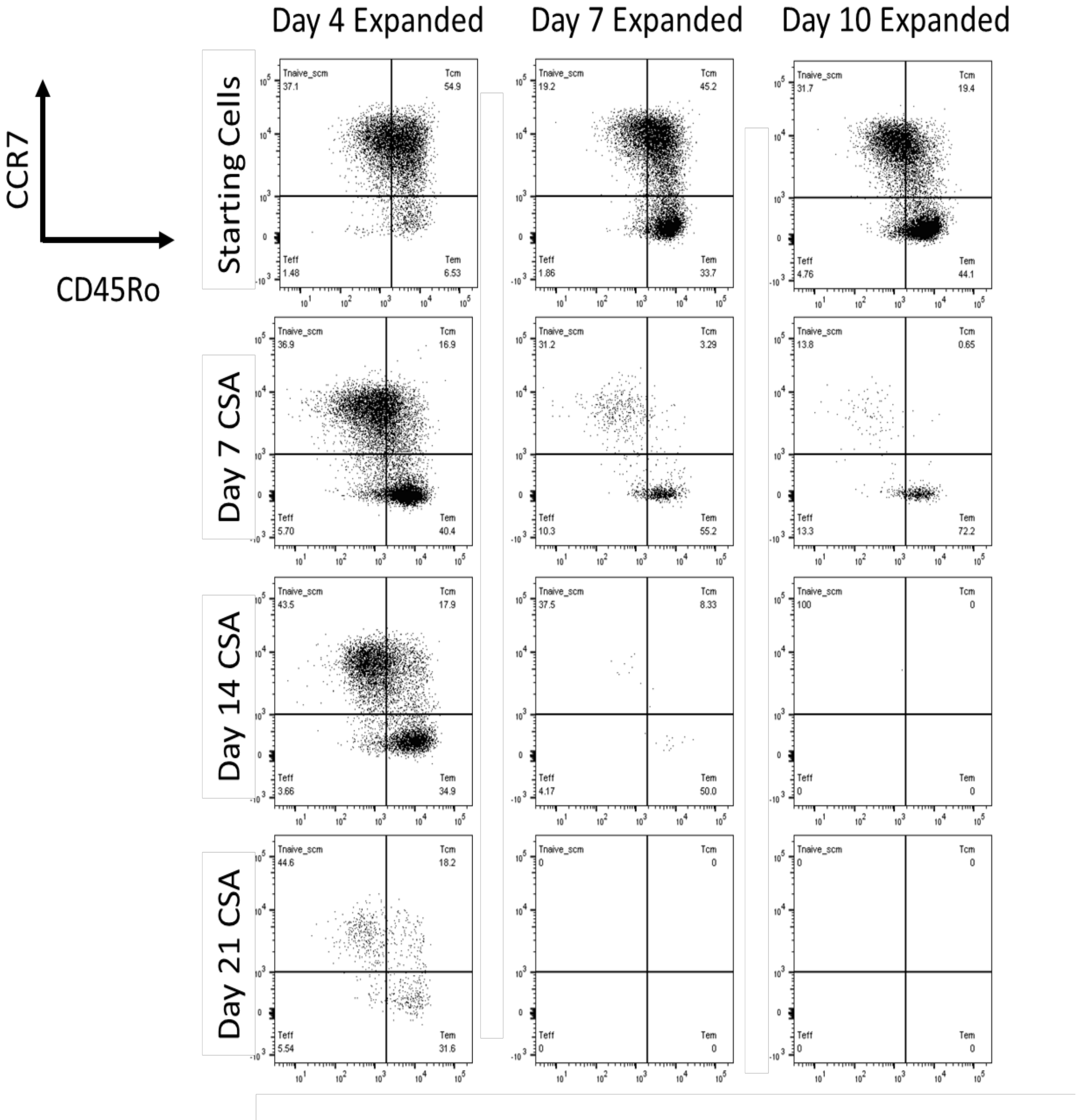

Figure 13: T-cell memory compartments in IL7 CSA. T-cell memory phenotype was assessed on the starting cells and then every 7 days for the length of the 21-day IL7 CSA as shown in figure 3. T-cell memory phenotype was analyzed via CCR7 and CD45Ro expression and compartments are annotated in each quadrant. Data is representative of three biological replicates performed.

Chapter 2: Mechanism of Action (MOA) Phenotyping of Cells During CD3/CD28 Manufacturing

From the CSA, the T cells appeared to be less functional in their ability to respond to proliferative cytokines, with context dependent correlations to starting cytokine receptor expression. In addition, the increased differentiation in day 7 and day 10 cells is in line with the reduced proliferative capacity in the CSA. The data suggested that a small fraction of the day 10 expanded T-cells retained the ability to respond to cytokines. This observation suggested that T-cell population heterogeneity was at play in the observed behavior. To further investigate this diversity and the loss of proliferative potential, I focused on analyzing the effect of T-cell expansion on proliferative ability by measuring:

1) Final relative telomere length (figure 14)
2) Telomerase activity (figure 15)
3) Costimulatory molecule expression (figures 17 and 18)
4) Whole RNA expression (figure 19 - 21)

Telomere length reduction with elongated CD3/CD28 manufacturing

The loss of telomere length is a hallmark of dysfunctional cells as they become highly differentiated and eventually senescent (Nan-Ping Weng 1995). To investigate whether this effect was taking place in our differentially expanded T-cells, I used a fluorescence *in situ* hybridization assay to assess the relative telomere length (RTL) of the T-cells against an internal cell line control (see methods for details). For all four donors analyzed, there was a loss in RTL throughout the expansion protocol, with the day 4 expansion cells always having the highest RTL (figure 14). There was an approximate 20% loss in RTL between day 4 and day 7 expanded cells and an additional 10% loss in RTL between day 7 and day 10 expanded cells when all donors were grouped together. There were signs of an age bias in the data as well, with the younger donors, on average, having longer RTL compared to the older donors when compared at the day 10 expanded time-point.

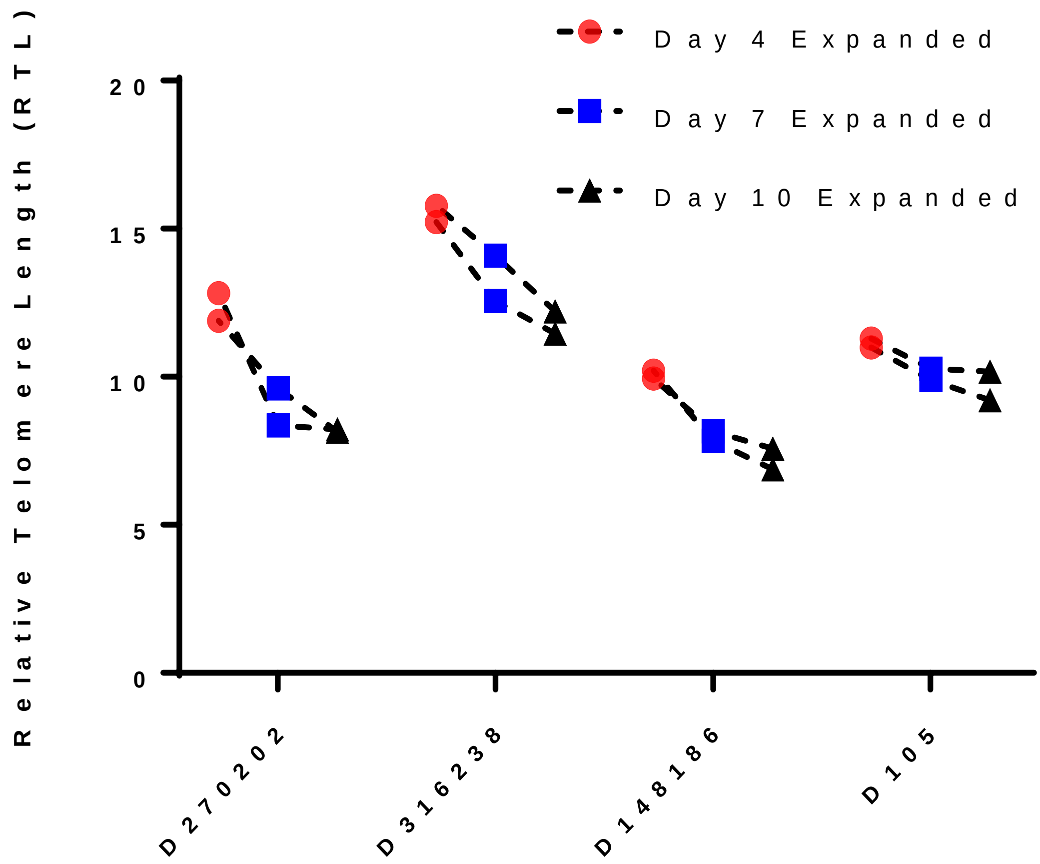

Figure 14: Continual loss of telomere length during CD3/CD28 T-cell expansion. The relative telomere length was assessed by fluorescence *in situ* hybridization relative to a tumor cell line control in 4 healthy donors. Each sample point represents a replicate of a technical duplicate. Donor ages: D270202: 50, D316238: 31, D148186: 49, D105: 45.

Reduced telomerase activity during elongated CD3/CD28 manufacturing

Based on the reduction in telomere length and recent publications showing heterogeneity in telomerase induction following CD3 + CD28 stimulation (Huang et al. 2017), I decided to check the levels of active telomerase via an enzyme linked immunosorbent assay (ELISA). There was a statistically insignificant reduction (approximately 10%) between day 4 and day 7 expanded cultures (figure 15). In contrast, there was a 40% reduction in activity between day 4 and day 10 expanded cells which was statistically significant (p=0.0004) and an approximately 25% reduction between day 7 and day 10 which was also statistically significant (p=0.0165). Taken together, there is an expansion correlated loss in both the RTL and the final levels of active telomerase with the elongated expansions producing cells which are less fit for additional expansions.

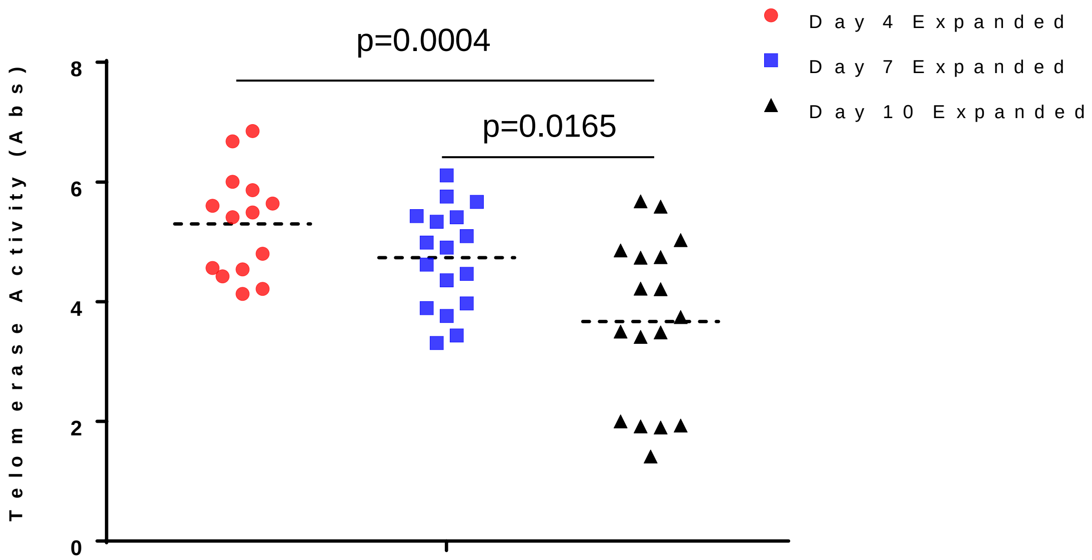

Figure 15: Reduced Telomerase Activity with Elongated CD3/CD28 T-cell Expansion. Telomerase activity was measured via an ELISA based colorimetric assay from whole cell lysate of cells taken from day 4, 7, or 10 in T-cell expansion. Each point represents a technical triplicate sample from a total of 5 biological replicates.

Telomere length reduction correlates with the starting CD28 expression

In recent publications, the expression of telomerase was restricted to the CD28 expressing cells of either the CD4 or CD8 compartment following CD3 + CD28 stimulation (Huang et al. 2017). Given the data from figures 14 and 15, I reasoned that the final relative telomere length may also correspond with this CD28 expressing fraction of cells. There was an R^2 correlation of 0.5636 between the starting CD28 percentage of cells in the PBMCs and the final relative telomere length (figure 16). This analysis was carried out from multiple healthy donors and multiple non-small cell lung cancer derived PBMCs.

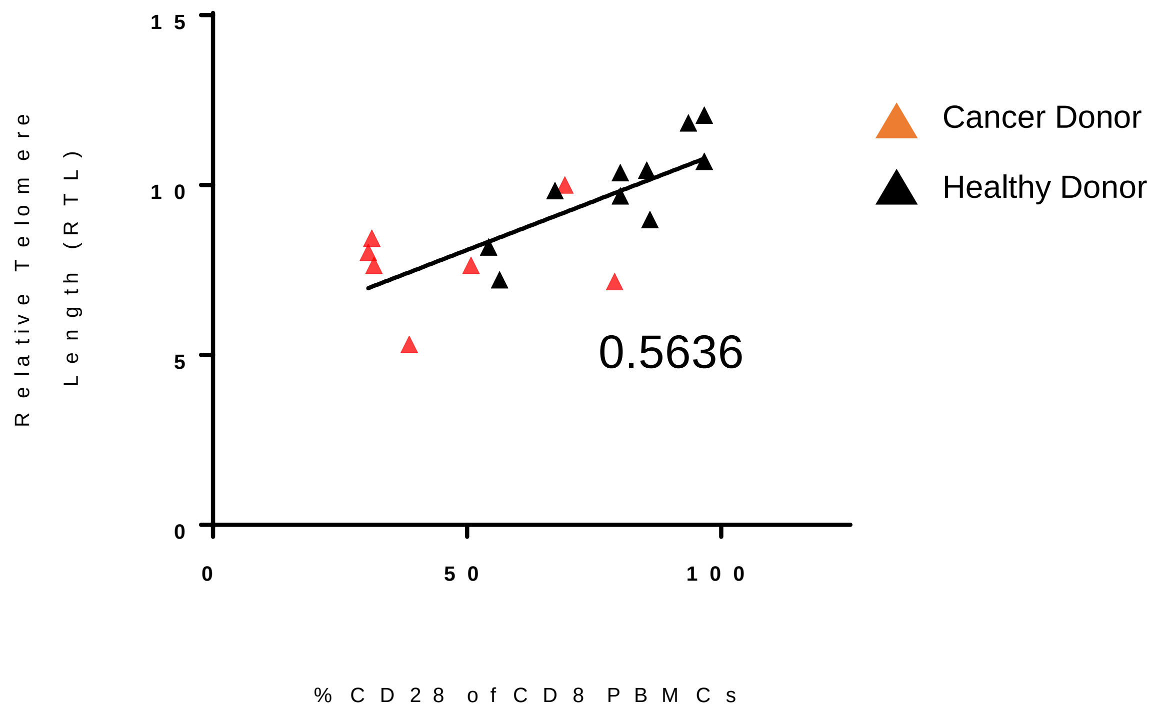

Figure 16: Final relative telomere length correlates with starting CD28 expression. Relative telomere length (RTL) was calculated as described above for both healthy donor and cancer patient derived PBMCs. RTL is shown for day 10 expanded T-cells. Percentage of CD28 expressing cells were calculated from the starting donor PBMCs. R^2 correlations are shown on the graph.

Loss of T-cell early memory phenotypes during CD3/CD28 manufacturing.

There was a distinct difference in the starting memory compartments between the differentially expanded cells from the CSA studies with regards to CCR7 and CD45Ro expression. From this observation, I decided to do a higher resolution analysis of the starting memory compartment differences between the differentially expanded samples. There was a small statistically insignificant difference in the Tnaive_scm compartment between day 4, 7, and 10 (mean values of 20.03%, 11.1%, 17.47 % of CD8 cells) (figure 17). There was a statistically significant difference ($P<0.05$) within the Tcm compartment between day 4, 7, and 10 expanded cells (mean values 58.27, 37.73, 16.8 % of CD8 cells). There was a statistically significant difference ($P<0.05$) within the Tem compartment between day 4, 7, and 10 expanded cells (mean values of 18.9, 48.13, and 58.9 % of CD8 cells). There was a small statistically insignificant difference within the Temra compartment between day 4, 7, and 10 expanded cells (mean values of 2.70, 3.06, and 6.80 % of CD8 cells). From this analysis, the major memory compartment differences were found in the Tcm to Tem transition, with later expanded cells containing fewer Tcm and more Tem T cells.

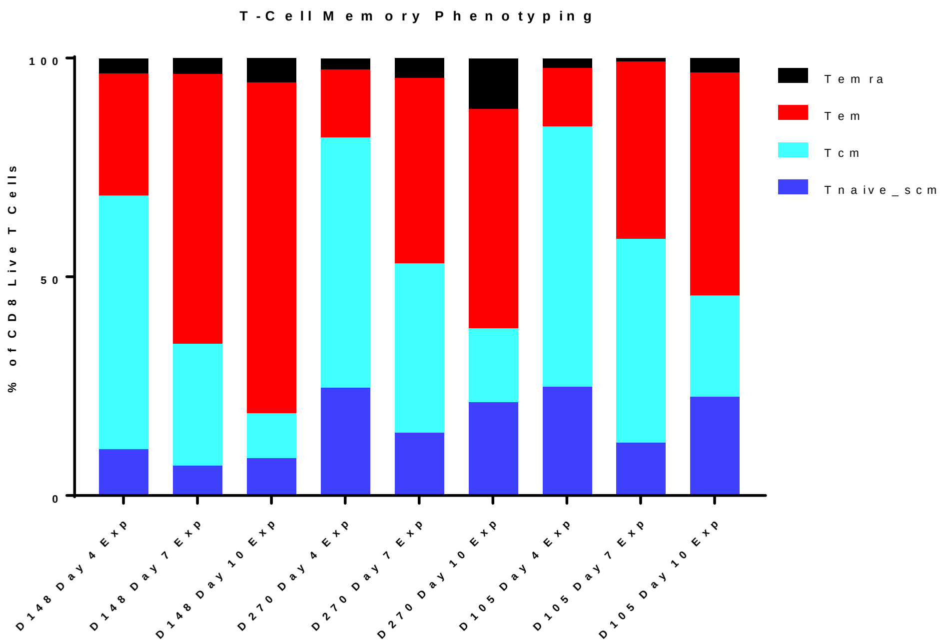

Figure 17: T-Cell Differentiation During CD3/CD28 Manufacturing.

Representative PBMCs were cultured as described previously and then phenotyped by flow cytometry at the indicated expansion day. Memory phenotypes are defined based on CD45Ro and CCR7 expression, Tnaive_scm = CD45Ro-CCR7+, Tcm=CD45Ro+CCR7+, Tem=CD45Ro+CCR7-, and Temra= CD45Ro-CCR7-. Three biological donors are shown.

Loss of CD28 and CD27 expression during CD3/CD28 manufacturing.

In addition to the conventional memory compartments, I also phenotyped the cells for expression of costimulatory markers CD28 and CD27, both of which are known to be associated with increased T-cell persistence *in vivo* (Huang et al. 2006; Powell et al. 2005). During CD3 + CD28 expansion, there was a stepwise loss of both CD28 and CD27, with the most drastic loss by day 10 in the manufacturing period (figure 18). While none of the comparisons between day 4, 7, and 10 expanded cultures yielded statistical significance ($P<0.05$), there were trends towards significance ($P=0.0520$) within the CD27+CD28+ compartment between the day 4 and day 10 expanded cultures (mean values of 58.47 and 21.43% of CD8 cells). Additionally, there was a nearly significant enrichment ($P=0.1581$) in the double negative CD27-CD28- compartment between day 4 and day 10 expanded cells (mean values 10.24% and 29.77% of CD8 cells).

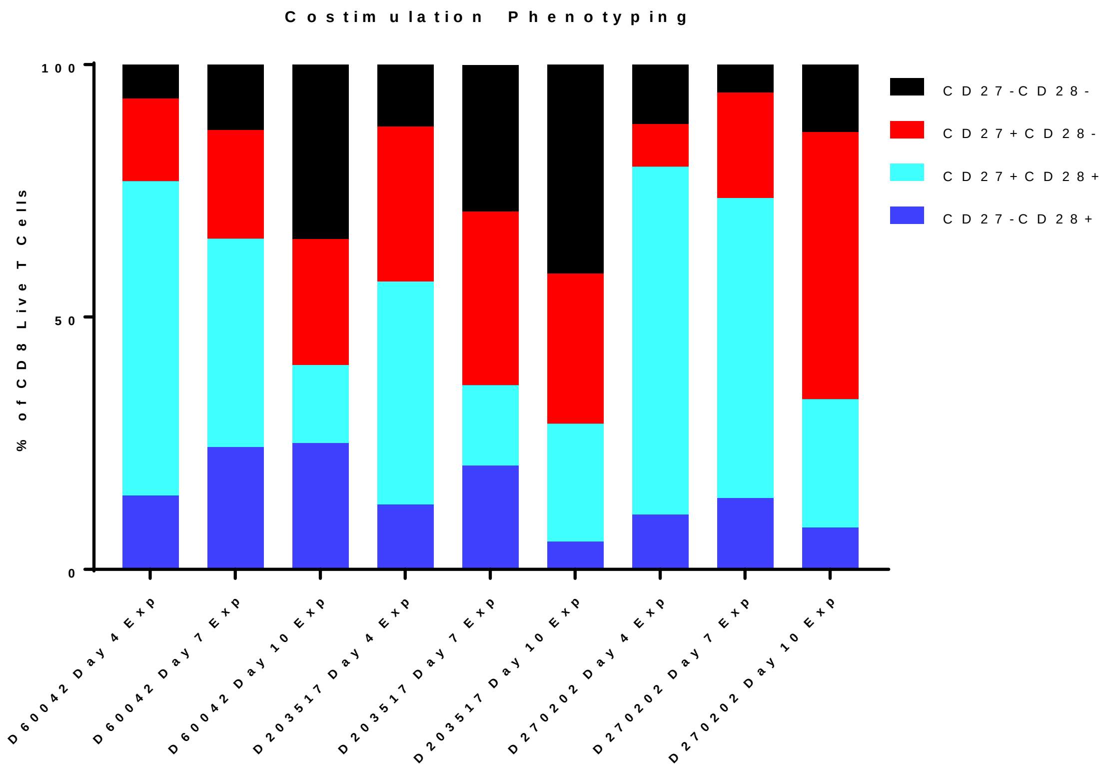

Figure 18: Loss of costimulation during CD3/CD28 manufacturing. CD27 and CD28 expression was assessed via flow cytometry on day 4, 7, and 10 during the T-cell expansion period. Three biological donors are shown.

Differential gene expression analysis identifies clusters the earlier expanded cells as a unique cluster compared to later expanded cells.

While the previous data suggested a phenotypic difference between the differentially expanded T cells, the explorations were limited to the number of designated targets investigated (e.g. CD28 or T-cell memory compartments). To widen the scope of the phenotyping studies, RNAseq was performed from three biological donors expanded for 4, 7, or 10 days (figure 19). From this sequencing, cluster analysis was performed (see methods for details), which revealed distinct grouping of the day 4 expanded cells compared to the day 7, which appeared in an intermediary cluster, while the day 10 cells appeared in a unique cluster of their own. This data supports a linear differentiation model of T-cell expansion in which gradual changes at the RNA level take place throughout the expansion protocols.

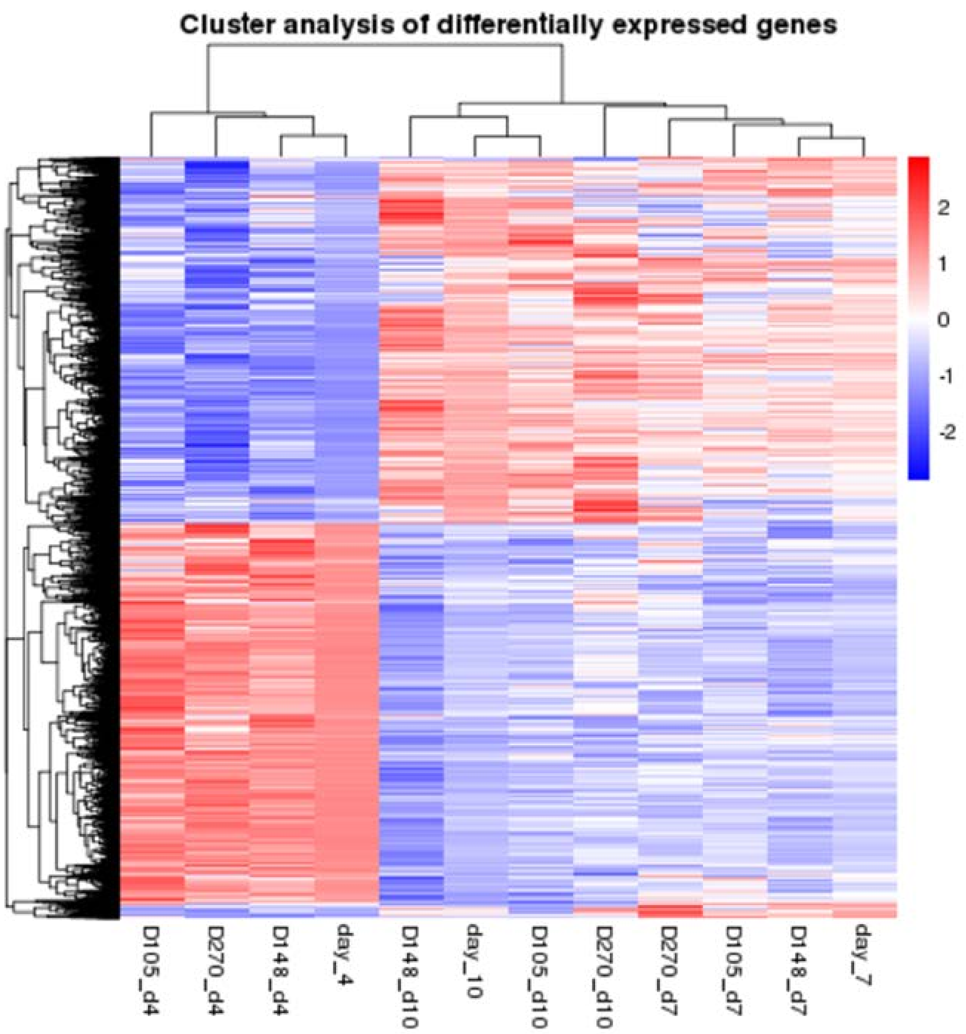

Figure 19: Differential gene expression seen in early manufactured cells by RNAseq. Three biological donors were expanded for 4, 7, or 10 days and then whole RNA was isolated and sent to Novogene for RNA sequencing analysis and bioinformatics. From this analysis, we see that there is a distinctly different clustering pattern of the day 4 expanded cells compared to the day 7 and day 10 expanded cells. The DXXX_dX nomenclature denotes individual donor samples followed by the day in the expansion (e.g D148_d4 is donor D148 expanded for 4 total days). The day_x represents a grouping of the individual similarly expanded cells (e.g. day_4 is grouping of all day 4 expanded donors).

Earlier expanded cells show an increased number of differentially expressed genes compared to the later expanded samples.

The whole RNA sequencing was analyzed for differentially expressed genes (DEGs, figure 20) between the day 4, 7, and 10 expanded cells across three biological donors. From this analysis, the gene expression profiles appear to change the most early in the manufacturing process as evident by the 5,078 DEGs in the day 4 vs day 7 comparison and the 5,643 DEGs in the day 4 vs day 10 comparison. With respect to both sets, there was a roughly equal distribution of up and down regulated genes. In contrast, there was relatively few DEGs when comparing the day 7 vs day 10 manufactured cells, with 90 genes identified, with a equal split between up and down regulated as well.

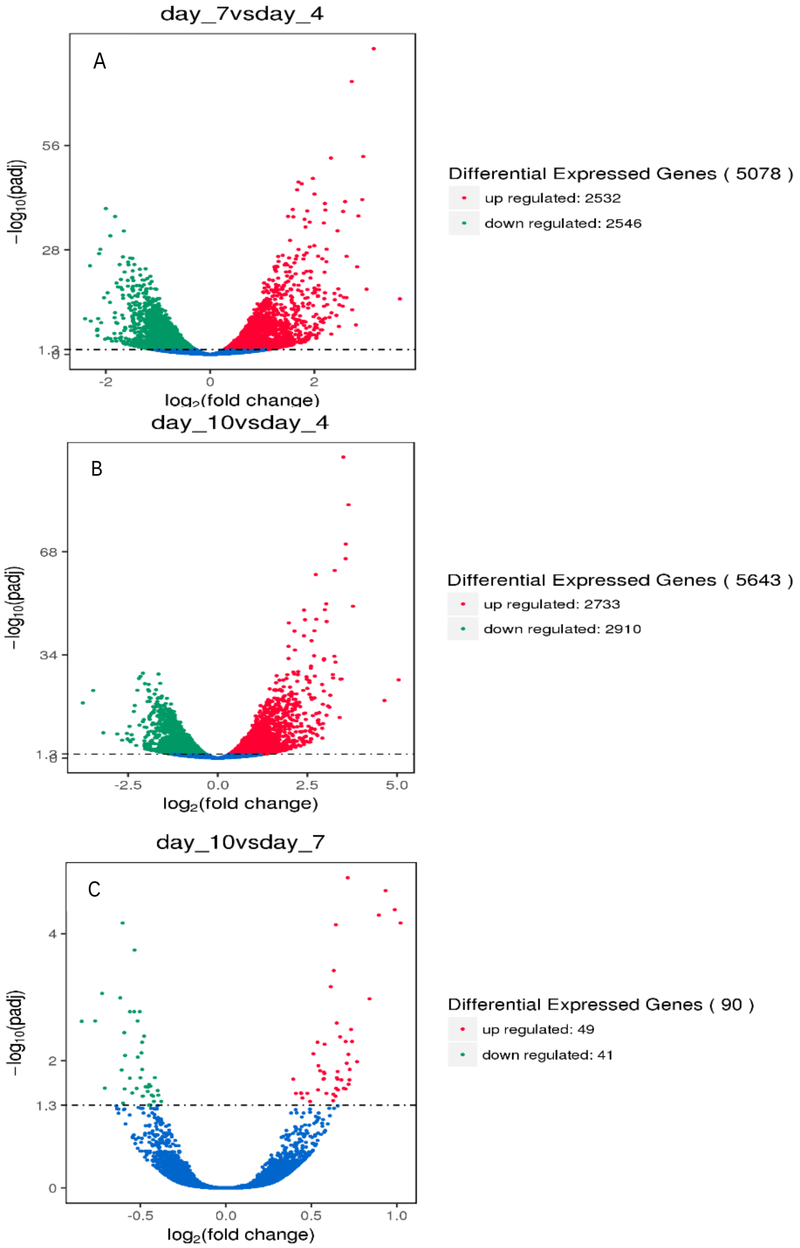

Figure 20: RNAseq analysis during T-cell manufacturing.

Volcano plot representation of RNAseq data during T-cell manufacturing comparing (A) day 4 vs day 7**,** (B) day 4 vs day 10, and (C) day 7 vs day 10. DEGs cut-off was set to 1 fold up or down with a padj-value of less than 0.05. Number of DEGs is shown in the key for each plot.

KEGG analysis highlights loss of cell cycle associated genes and an upregulation of apoptosis associated genes throughout manufacturing

In order to better understand the dramatic gene expression changes occurring during manufacturing, KEGG pathway analysis was performed to identify gene pathways that were over-represented in the differing gene sets. I focused on pathways that were likely related to T-cell proliferation and persistence based on the functionality results seen in the CSA (figures 1-5). In comparing the later time points to day 4 in manufacturing, there is a significant down regulation in DNA replication and cell cycle gene pathways. Compounding this effect, there was a significant up regulation in apoptosis, p53 signalling gene pathways during the same period in manufacturing. In agreement with the gene expression results in figure 18, there were very few significantly enriched pathways between day 7 and day 10 in manufacturing (figure 19). A thorough description and analysis of the respective pathways is reserved for the discussion section. Additionally, a manual search of the differentially expressed genes identified multiple highly differentially expressed genes belonging to apoptotic, cell cycle, and T-cell growth pathways (table 1).

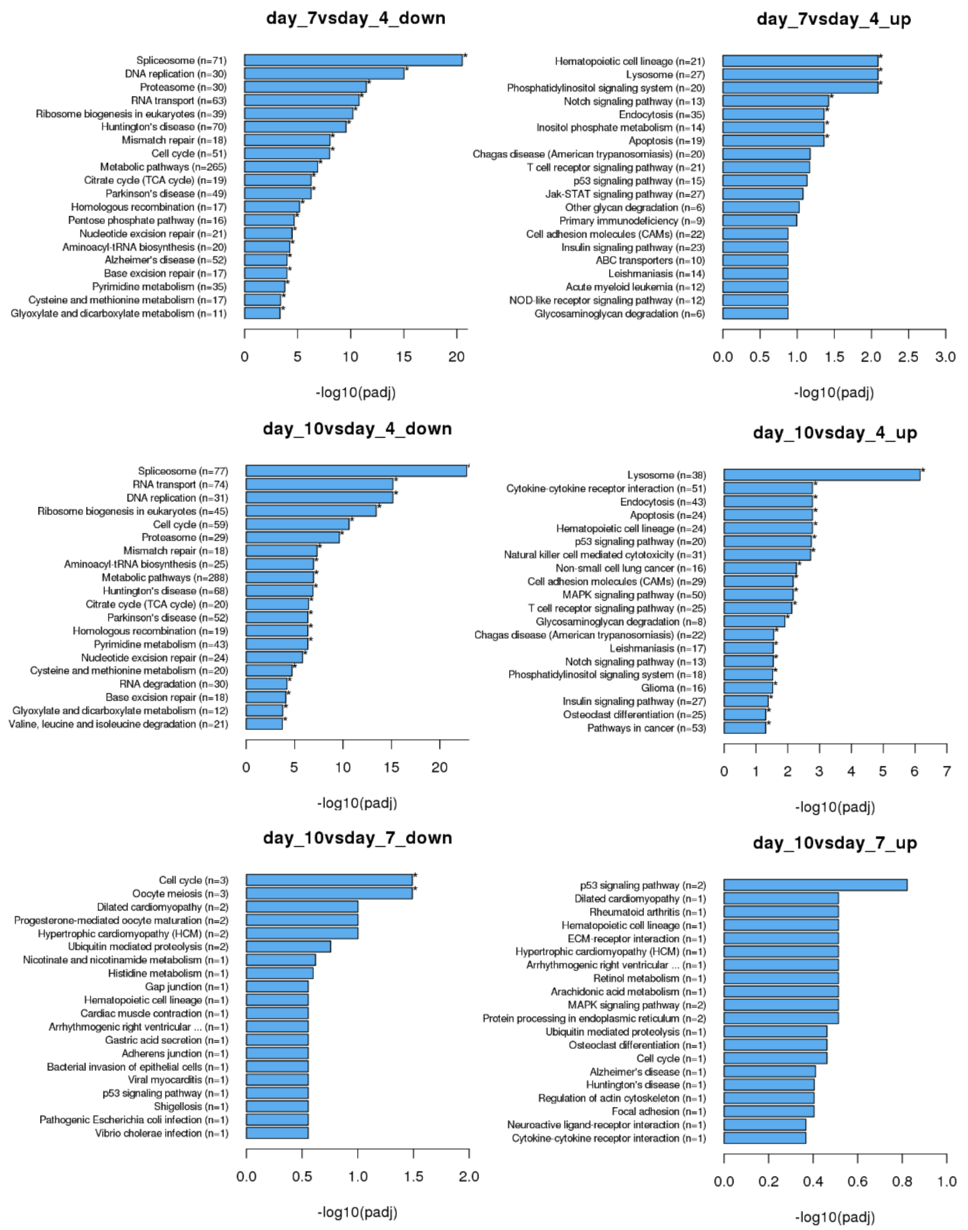

Figure 21: KEGG pathway analysis during T-cell manufacturing.

KEGG pathway analysis was performed as described in the methods section. The left graphs show the pathways that are upregulated between the samples. The right graphs show the pathways are that are downregulated between the samples. For each up or down regulation, the later time point is referenced (i.e. day_7vsday_4_down indicates pathways that were down regulated in the day 7 sample vs the day 4 sample). * indicates statistical significance , P>0.05.

Gene Short Term	Gene Full Name	Cellar Process	Day 10 / Day 4 (log_2 fold)		
			Donor 1	Donor 2	Donor 3
DAPK2	death-associated_protein_kinase_2	Pro-Apotosis	3.39	3.80	4.09
IL10RA	interleukin_10_receptor_alpha	Inhibitory Cytokine	2.21	2.36	1.94
MATK	megakaryocyte-associated_tyrosine_kinase	Proliferation Inhibition	1.79	2.13	1.87
LAG3	lymphocyte-activation_gene_3	Treg Susceptibility	1.54	1.58	1.68
PIK3IP1	phosphoinositide-3-kinase_interacting_protein_1	Potential PI3K Inhibitor	1.95	1.98	1.44
PCNA	proliferating_cell_nuclear_antigen	Positive Proliferation	-1.51	-1.85	-1.60
IL2RA	interleukin_2_receptor_alpha	Positive Cytokine	-2.39	-2.79	-1.87
CDK4	cyclin-dependent_kinase_4	Postive Proliferation	-1.67	-2.54	-2.48

Table 1: Genes of interest differentially expressed within apoptotic, cell cycle, or T-cell growth pathways.

From the list of differentially expressed genes (DEGs), a manual search was performed for genes which were highly differentially expressed (>2.5 fold) and significant ($p<0.05$) between the day 4 and day 10 manufactured samples. Ratio of gene expression is shown as the log2(fold expression) between day 10 and day 4 samples.

Chapter 3: Loss of CD28 with age and the bottleneck in CD3 + CD28 T-cell expansion

The heterogeneity in T-cell expression profiles observed suggested that necessary criteria for a selective pressure existed. This pressure, in theory, may potentially limit the replicative potential of specific T cell populations. From the analysis of costimulatory molecules, it was clear that there was a loss of CD28 expression in the starting CD8 cells and throughout the T-cell expansion protocol. Reasonably, this would create two types of CD8 T cells, those which would benefit from the CD28 costimulation given and those that would not benefit. Following this train of thought, an investigation into the significance of CD28 loss was performed. The following figures highlight an intrinsic CD28 importance and the correlations that exist between the starting CD28 phenotype and multiple manufacturing metrics.

The age correlated loss of CD28 in CD8 T cells.

For there to be a selective pressure between donors, there must be an intrinsic heterogeneity between donors. From the CD28 profiling, I noticed that the older the donor was, the lower the starting percentage of CD8 cells which expressed CD28, with an R^2 correlation of 0.7132 (figure 22). Of note, multiple other investigations have shown a similar loss of CD28 expression in the aging CD8 compartment (Weng, Akbar, and Goronzy 2009).

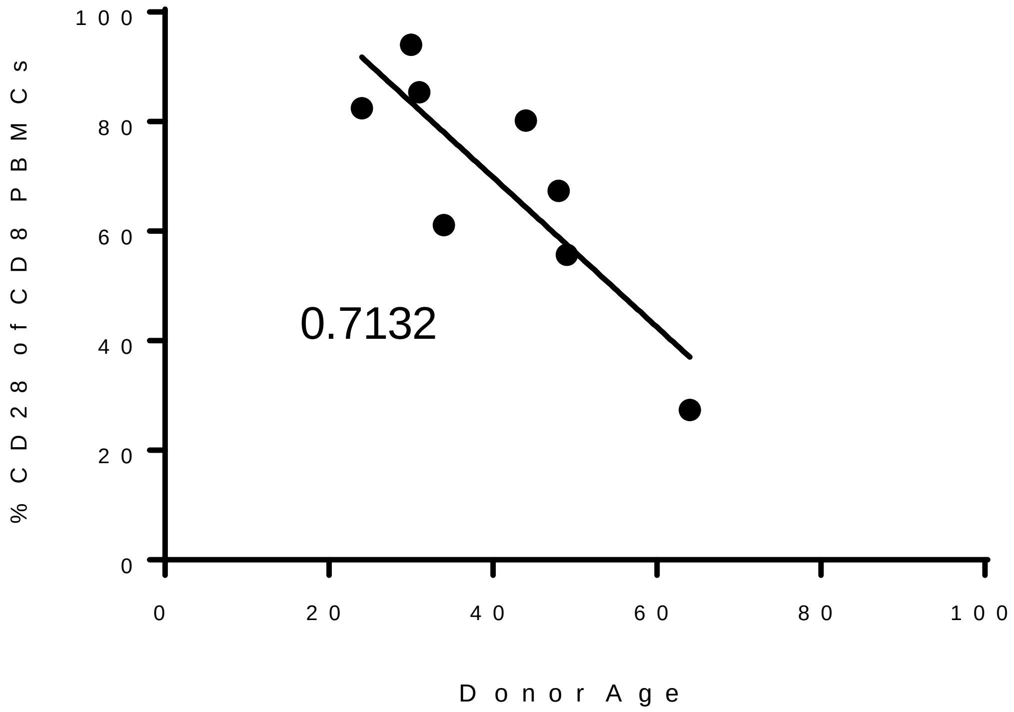

Figure 22: The age correlated loss of CD28 expression. Eight donors (21-64 years old) were analyzed by flow cytometry for CD28 expression. An R^2 = 0.7132 linear correlation was observed. CD28 expression data provided by CMC department at Immaics US Inc.

CD28 starting percentage correlates with final CD8 percentage during T-cell expansions.

Since CD28 expression in the CD8 compartment was correlated with age, I reasoned that other manufacturing metrics which would depend on CD28 expression may also be biased. At the end of T-cell expansion, the ratio of CD8 to CD4 cells is often measured as it is primarily the CD8 compartment which performs tumor cytolytic function, though cytolytic CD4 cells have been identified (Takeuchi and Saito 2017). There was a correlation between the starting CD28 expression in the CD8 cells and the final percentage of cells which were CD8 positive with an R^2 correlation of 0.6927 (figure 23). This was the first sign that CD28 expression may serves as the driving force for proposed Darwinian pressure.

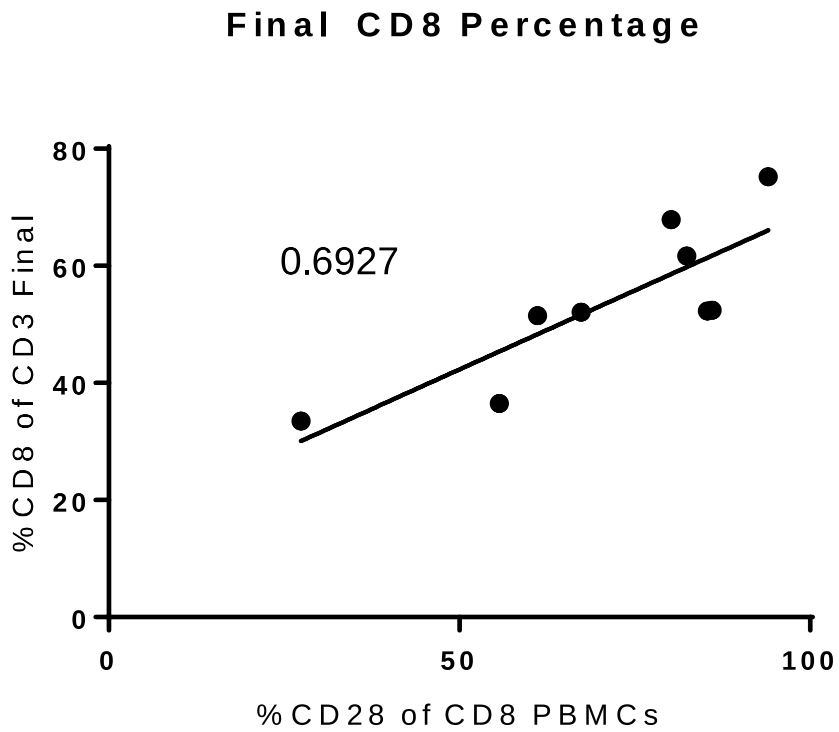

Figure 23: CD28 starting percentage correlates with final CD8 percentage. PBMCs were cultured as described in the methods section. Starting CD28 percentage and final CD8 percentage were calculated by flow cytometry. There is an R^2 correlation of 0.6927 between the starting percentage of CD28 and the final CD8%. CD28 expression data provided by CMC department at Immaics US Inc.

CD28 starting percentage correlates with fold expansion.

Clinical T-cell expansion protocols often measure the fold expansion of the final product as a metric to understand the number of population doublings that have taken place. By day 7 in the expansion protocol, there was a clear correlation between fold expansion and the starting CD28 expression level with an R^2 correlation of 0.6493 (figure 24). This was the second piece of evidence supporting that the starting CD28 level was indicative of T-cell expansion outcome.

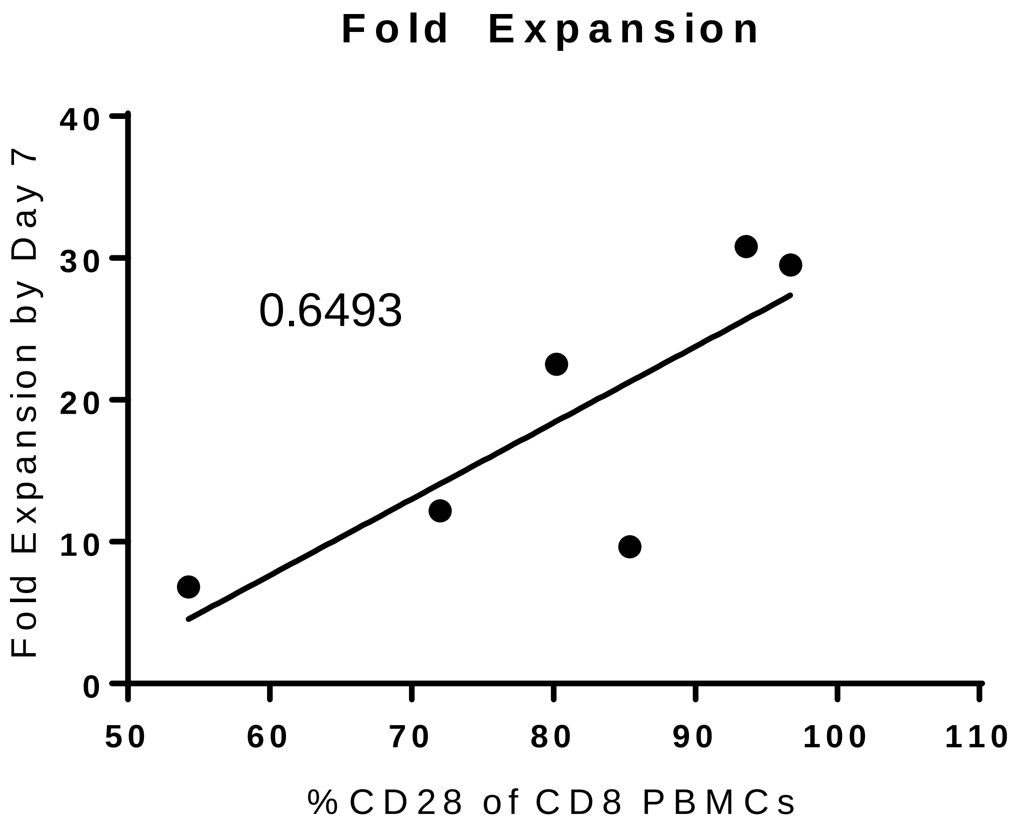

Figure 24: CD28 starting percentage correlates with fold expansion. PBMCs were cultured as described in the methods section. Starting CD28 percentage by flow cytometry. Total fold expansion was calculated from the day of transduction to the day 7 in the culturing period. There is an R^2 correlation of 0.6493 between the starting percentage of CD28 and the final fold expansion. CD28 expression data provided by CMC department at Immaics US Inc.

Chapter 4: Single molecule DNA sequencing supports *ex vivo* bottleneck in CD3 + CD28 T-cell expansions

The correlations of CD28 expression with multiple manufacturing metrics strongly suggested that the presence or absence of CD28 may dictate the result of the T-cell expansion. I reasoned that CD28 expression was the *ex vivo* Darwinian pressure (bottleneck), though it did not prove or disprove a model in which a bottleneck was selecting against CD28-expressing cells. To fully examine whether the bottleneck existed, I needed a method to track individual T-cell clones throughout the T-cell expansions and investigate whether there was a significant loss of T-cell clonal frequencies, analogous to tracking a specific animal's fossil records throughout history. I predicted that for older patients with less CD28 expression, there would be a significant loss in the T-cell clonal diversity because of the bottleneck. Additionally, for younger donors with a lot of CD28 expression, there would be relatively little loss in the T-cell diversity due to no significant advantage or disadvantage within the T-cell populations.

From a single active T-cell expansion culture, I sampled up to 10% of the cells at four different time points in the expansion: post activation, and day 4, 7, and 10 of the T-cell expansions and measured:

1) Percentage of clones which showed differential growth patterns (contraction vs expansion) during the T-cell expansion

2) Clonality of the sample as measure of the percentage of clones which were derived from a single clonal family

3) Median number of cell divisions per clone

4) Clonal richness as a normalized indicator of the number of unique clones within a samples

Contraction and expansion of clones correlates with starting CD28 percentage

From the single culture, individual T-cell clonal frequencies were tracked and compared to the post-activation (day 2) time-point. From this comparison, clones which significantly went up and down in frequency were assessed with the sum being the percentage that were differentially abundant. There was a strong correlation between the percent differentially abundant and the starting CD28 percentage ($R^2 = 0.9726$) (figure 25). The lower the amount of CD28 in the starting sample, the higher the percentage of clones which became differentially abundant. This suggests that the lack of CD28 in a certain population creates an ecological niche for other clones to grow into and the lack of CD28 creates populations which are likely to die during the T-cell expansion elongated protocol.

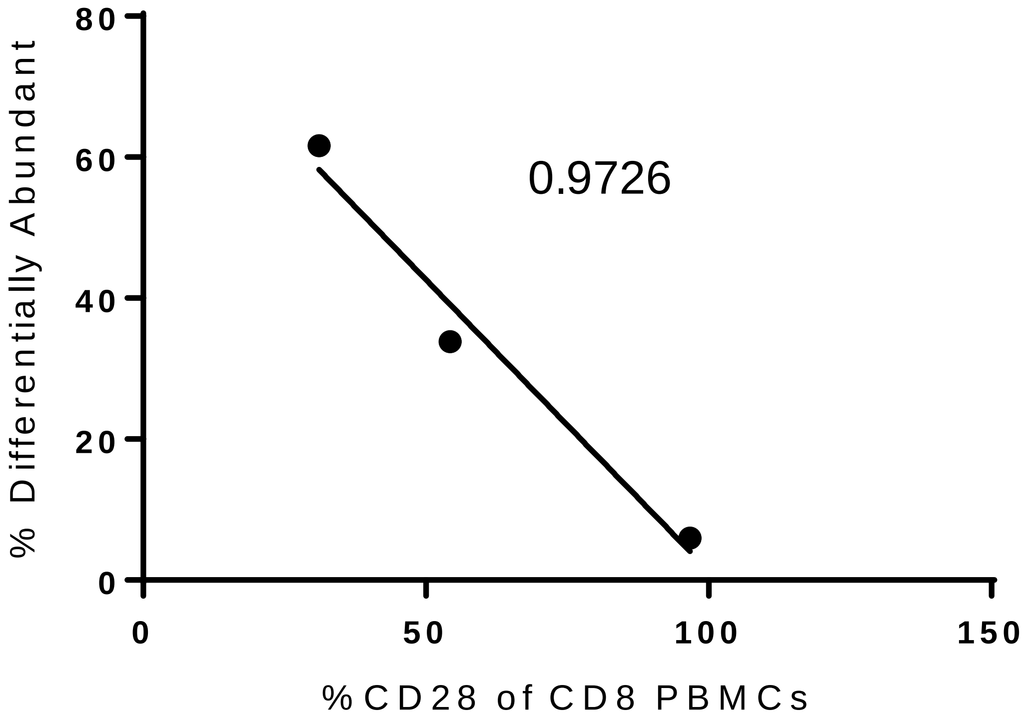

Figure 25: Contraction and expansion of clones correlates with starting CD28 percentage. From 3 healthy donors, single molecule DNA sequencing was performed, and individual T-cell clones were tracked over time as described above. The percent differentially abundant represents the fraction of all T-cell clones by day 10 in expansion that either expanded or contracted of the total number of evaluable T-cell clones relative to post-activation. Percentage of CD28 expressing cells was calculated by flow cytometry from the starting PBMCs. CD28 expression data provided by CMC department of Immatics US Inc.

Lower CD28 expressing donors show a delayed T-cell expansion with negative median clonal divisions.

If the CD28 bottleneck exists in the T-cell culture, there would be an expected delay in the T-cell population expansion based on the starting percentage of cells which expressed CD28. Likewise, if all the T-cell clones were able to expand right away, then we would expect a positive number of divisions per clone early in the expansion protocol. For the low and medium CD28 expressing cultures, there was a negative population growth between the post-activation (day 2) and day 4 into the expansion (figure 26), this suggests a contraction in the number of cells between these two time points and meets the definition of a Darwinian bottleneck event. Additionally, only for the high CD28 expressing cultures, did we see overall positive clonal divisions, indicating that in this culture a high percentage of the T-cell clones were able to immediately divide.

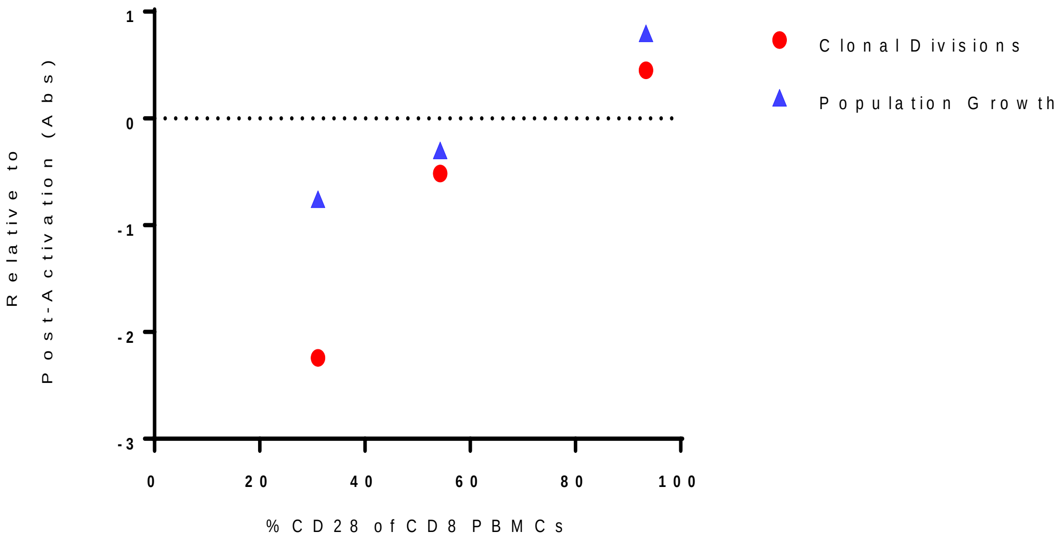

Figure 26: Low CD28 expressing donors show delayed T-cell expansion with negative clonal divisions. Population growth is calculated based on total viable cells and represents fold growth. Clonal divisions are calculated as the log2(clonal fold expansion) and represent the median value obtained, negative values are obtained when clonal frequency contract in a culture, positive values are obtained when clonal frequencies expand in a culture. All points are relative to the post-activation baseline and calculated to day 4 in the T-cell expansion process. CD28 expression data provided by CMC department of Immatics US Inc.

Reduction of unique T-cell clones during expansion in donors with lower expression of CD28 by DNA clonal sequencing.

If we track the number of unique T-cell clones throughout a culture to, then we would expect that if the bottleneck was present, there would be large swings in the number of unique T-cell clones post-bottleneck event. Clonal Richness is the measurement which calculates the number of unique T-cell clones normalized to the number of DNA molecule reads from sequencing. From the Clonal Richness calculations, there was a striking drop in the number of unique T-cell clones following day 4 in the expansion protocol for the two lower CD28 expressing starting populations (figure 27). On the other hand, for the highest CD28 expressing population, there was a strong maintenance in the number of unique T-cell clones relative to the post-activation time-point. For cultures starting with lower CD28 expression, there is a drop in the number of unique T-cell clones following the peak levels post-stimulation. This drop is presumably due to differential survival of T-cell clones based on their individual level of CD28 expression.

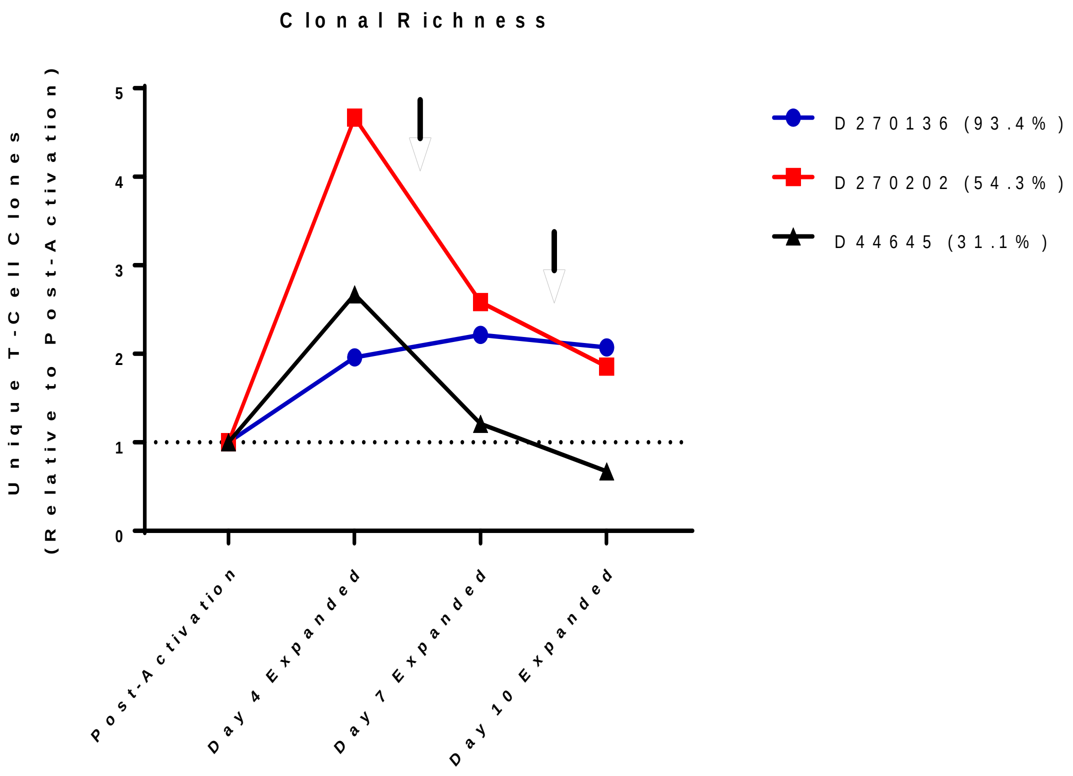

Figure 27: Reduction in unique T-cell clones in donors with lower CD28 expression. Following the burst in unique clones following stimulation, there is a continual reduction in unique clones in donors with lower CD28 (shown in parenthesis in the key). The proposed bottlenecks are marked by black arrows and occur as the expansion protocol is elongated past day 4. Unique T-cell clones are derived from the number of unique DNA molecule reads of the T-Cell receptor CDR3 region as described in the methods section. All values are normalized to the number of unique T-cell clones at post-activation. Dotted black line at value of 1 marks the point where there are fewer T-cell clones than existed post-activation.

Results: Increased CD28 expression in starting PBMCs confers advantageous growth dynamics during T-cell manufacturing

In effort to characterize the expansion of clonal populations during the T-cell expansion, I tracked the expansion kinetics of individual T-cell clones during the manufacturing process. When tracking individual clones, I measured the clonal divisions as well as the absolute numbers of T cells within a T-cell clonal population. An increase in CD28 expression in starting PBMCs conferred an early growth advantage, with nearly two-thirds of T-cell clones expanding between the activation step (day 2) and day 4 in manufacturing (figure 28A). In contrast lower CD28 expressing starting populations displayed a kinetics in which most T-cell clones contracted during this early stage of manufacturing, with the lower CD28 population containing on 1.19% of early expanding clones (figure 28A). As we tracked the divisions of the clonal populations, it was observed that the lower CD28 sample displayed a non-normally distributed division pattern, while the mid and high CD28 population showed a more normally distributed characterization. Additionally, the lower the starting CD28 expression, the more divisions it took to reach the same number of T-cells (figure 28B). Together this data indicates that high CD28 starting populations undergo a more advantageous T-cell expansion marked by reduced T-cell contraction and a lower number of necessary T-cell divisions.

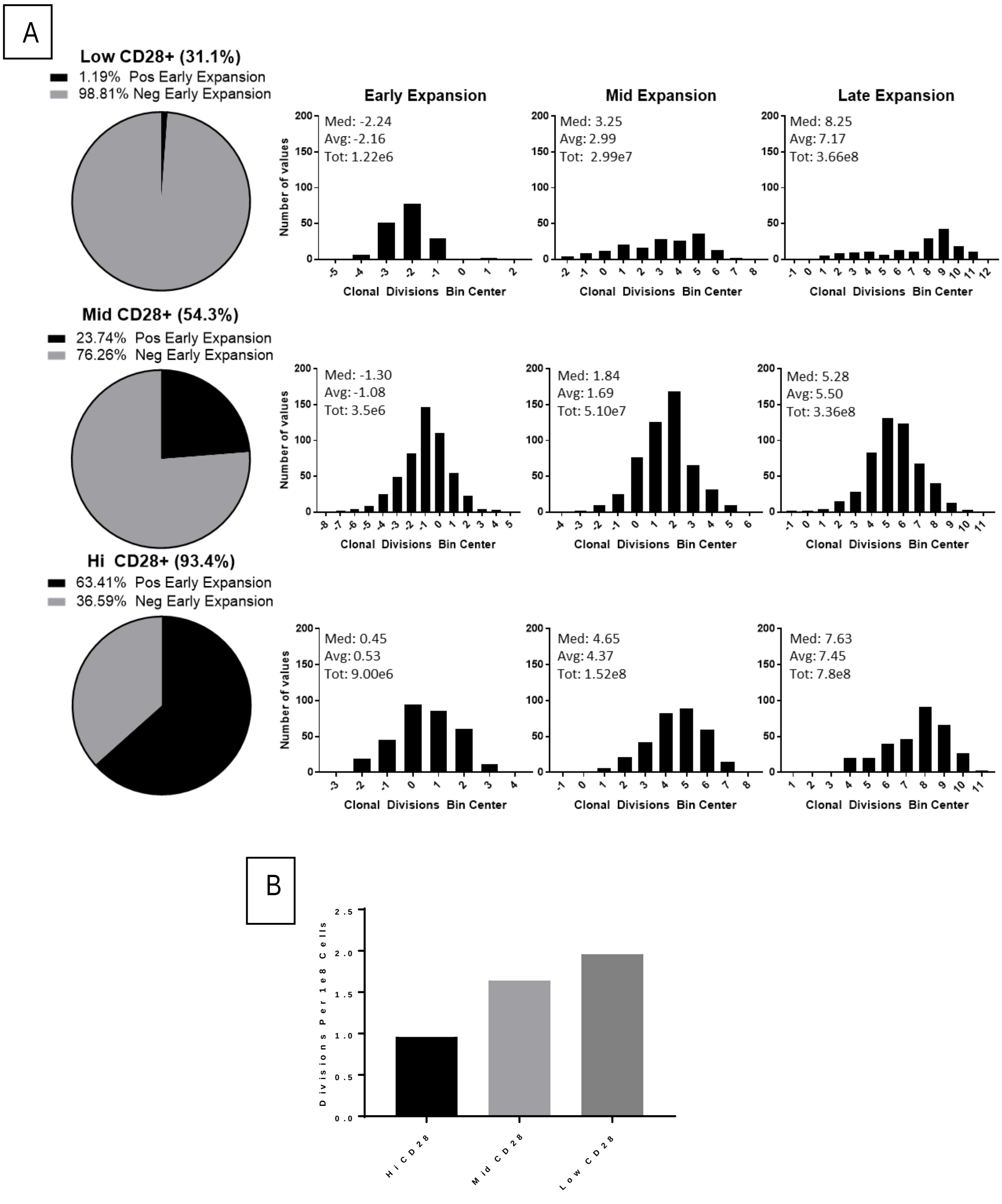

Figure 28: Characterization of T-cell expansion kinetics.

T-cell clones were tracked by clonal DNA sequencing and absolute numbers within each clonal population (A) was calculated during the early (day 4), mid (day 7), and late (day 10) of the expansion process. Median (Med), Average (Avg), and Total cell numbers (Tot) are inserts within each graph. (B) The number of divisions required to reach 1e8 total T cells was calculated. CD28 expression data provided by CMC department of Immatics US Inc.

Younger patients have an improved response to CD19 CAR therapy when manufactured with CD28 co-stimulation

To further explore any significance of the proposed *ex vivo* T-cell expansion bottleneck, I performed a clinical trial meta-analysis to investigate whether the loss of CD28 expression in elderly patients would create clinical trends. From the previous data, I reasoned that older patients would perform differently compared to younger patients based on the manufacturing (CD3 alone or in conjunction with CD28).

As T-cell therapy clinical trials are still in their infancy (40 published clinical trials available for analysis) and many of them are early stage trials with unconfirmed moieties (e.g. an untested new TCR or CAR molecule), the meta-analysis required filtering steps to create a uniform comparable data set (figure 29). After filtering and compilation, I was left with 7 clinical trials targeting CD19 malignancies for a total for 107 patient data points. From this analysis, I determined that patients younger than 45 had a better clinical prognosis when their cells were manufactured with the CD3 + CD28 method. Contrastingly, when patients were older than 45, there was a benefit to being manufactured with CD3 alone rather than the CD3 + CD28 method (Table 2).

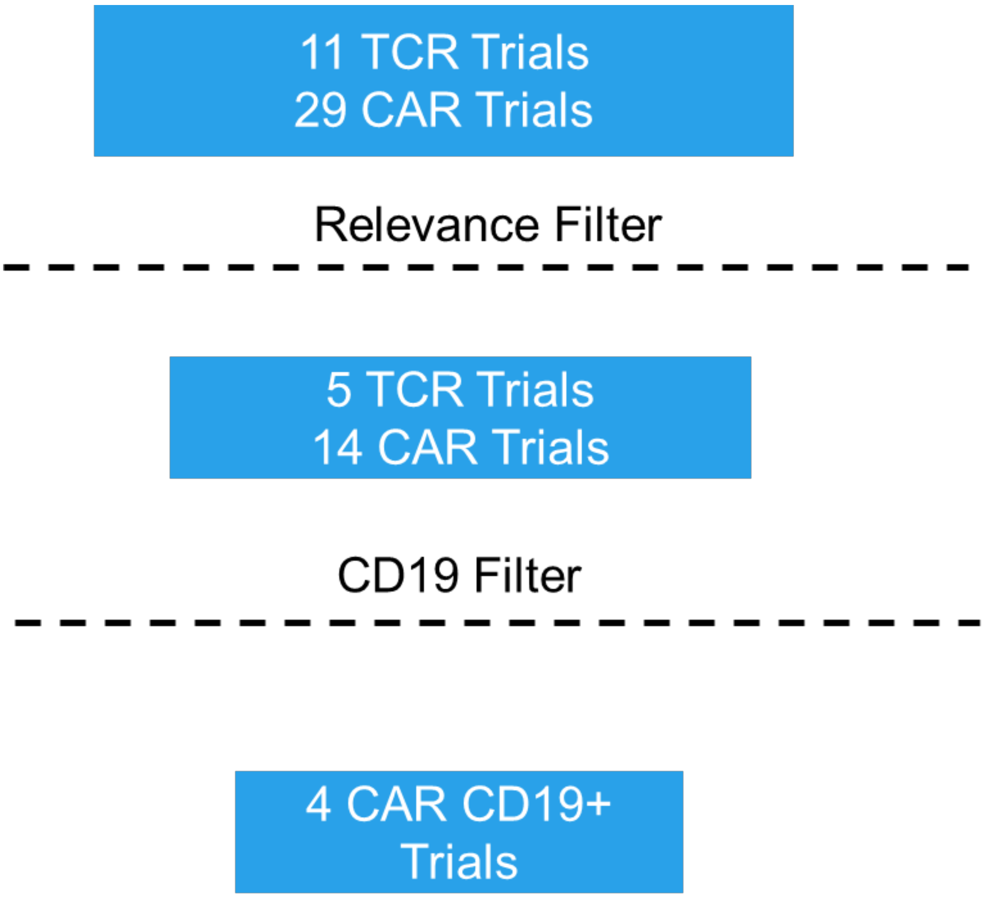

Figure 29: **Clinical Gene Therapy Transfer Trial Meta-Analysis.** 40 clinical trials were analyzed and filtered based on defined selection criteria: relevance filter and CD19 filter, resulting in a total of 4 comparable CAR clinical trials. The relevance filter excluded trials that were in combination or following stem cell transplants, virus specific T-cell products, extensive patient toxicities, CD4 specific trials, and complex T-cell manufacturing unseen in other trials. The CD19 filter was applied to compare only trials in which the target (CD19) had been clinically validated and with comparable manufacturing strategies (e.g. Gardner2017 trial eliminated because it used a split CD4 vs CD8 manufacturing)

		CR	PR	SD	NR/PD	NE	Total	ORR (PR + CR)	Clinical Trials
Patients >45 Years of Age									
	+ CD28	2	1	4	1	2	10	30.00%	Lee2014A,Brentjens2011
	- CD28	3	2		2		7	71.43%	Dai2015,Locke2017
Patients <45 Years of Age									
	+CD28	14		3	4		21	66.67%	Lee2014A,Brentjens2011
	-CD28	3	1		2	3	9	44.44%	Dai2015,Locke2017
						Total	47		

Table 2: **The differential effects of CD28 costimulation.** Data is from the meta-analysis of 4 CD19 CAR trials with 47 total data points. Patients younger than 45 performed better when given CD28 costimulation in the manufacturing as compared to patients older than 45, who performed better when not given CD28 costimulation. Statistical analysis was not performed. See methods section for list of clinical trials and detailed data handling. CR= complete response, PR=partial response, SD= stable disease, NR/PD= no response/progressive disease, NE= not evaluable. Each clinical response was defined based on the source clinical trial analysis.

Clinical response rates correlate with the fold growth *ex vivo* in clinical trial against multiple myeloma

Multiple clinical and preclinical investigations have suggested that phenotypically younger less differentiated T cells outperform in comparison to older more differentiated T cell products (see discussion for references). Based on the manufacturing data we have compiled (figures 23 - 28), high CD28 expressing (younger) starting PBMCs are able to achieve a higher fold expansion *ex vivo* and yield a phenotypically less differentiated final product. Based on these observations, it is likely that if you manufacture T cells for same period, then cultures which achieve a higher fold expansion were likely derived from more youthful less differentiated starting PBMCs, yielding a less differentiated product, and potentially a more potent clinical product.

As shown in table 3 from a αBCMA multiple myeloma CAR clinical trial, there was a 57% response rate when cell cultures achieved greater than 10-fold expansion *ex vivo*. In comparison, there was a 0% response rate when cultures failed to achieve 10-fold expansion. These observations further support the translational relevance of my findings and support a manufacturing centric model in predicting T cell potency (see discussion for details)

Disease	Target	Age	Dosage (10^9)	Response	Fold Expansion Day 9	Response Rate
MM	BCMA	NA	0.0003/kg	PR	28.96	57% Response Rate
MM	BCMA	NA	0.001/kg	SD	24.89	
MM	BCMA	NA	0.009/kg	CR	15.00	
MM	BCMA	NA	0.009/kg	SD	13.92	
MM	BCMA	NA	0.003/kg	PR	13.63	
MM	BCMA	NA	0.0003/kg	SD	11.99	
MM	BCMA	NA	0.009/kg	PR	10.96	
MM	BCMA	NA	0.0003/kg	SD	9.91	0% Response Rate
MM	BCMA	NA	0.003/kg	SD	9.35	
MM	BCMA	NA	0.001/kg	SD	5.62	
MM	BCMA	NA	0.003/kg	SD	3.85	
MM	BCMA	NA	0.001/kg	SD	2.72	

Table 3: ***Ex vivo* manufacturing metrics correlate with clinical response in multiple myeloma.** Data from clinical manufacturing (Ali et al. 2016) were combined with the clinical response rates and sorted by the fold expansion of CD3+ cells achieved during manufacturing. Response rates were calculated as the number of patients who achieved a PR or CR in relation to the total number of patients in the group. PR = partial response, SD = stable disease, CR = complete response.

Discussion

As gene-transfer cellular therapies emerge for solid and liquid malignancies, the *ex vivo* manufacturing process will be continually evolving as we gain insight into therapeutic correlatives. It should be noted that with multiple forms of cellular therapy emerging, it will be an active area of research to understand which factors can be universally applied and which are unique to a specific therapy. Nonetheless, as we still do not have such a thorough understanding, it is practical to test and design manufacturing from the information derived from multiple forms of cellular therapy (e.g. TIL, *ex vivo* endogenous stimulated, and gene therapy). While there is an extensive literature with respect to pre-clinical correlates, given the complexity of these modalities, clinical data should be prioritized above any pre-clinical guidance. Additionally, the assays used to characterize cellular therapies should be heavily designed with the knowledge of the clinical correlatives.

The work in this dissertation heavily focused on designing an *in vitro* assay to test the hypothesis that early manufactured TCR gene-transferred T cells would be superior to later expanded cultures in the clinically correlated criteria. The assay was designed to focus on the ability of T-cells to persist post-manufacturing, which has been correlated with TIL clinical response rates (Robbins et al. 2004) and the ability of T-cells to expand, clinically correlated in recent TCR GT trials (D'Angelo et al. 2018). The hypothesis was guided by work from the melanoma TIL field in which responding patients were shown to be significantly enriched when cultured for a shortened period (Besser et al. 2010) and pre-clinical mouse studies which emphasized the need to reduce the gain of effector function which accumulates as expansion proceeds (Gattinoni, Klebanoff, et al. 2005).

The resulting cytokine sensitivity assay (CSA) was designed to measure the ability of the post-manufactured human T cells to respond to a set of common gamma chain cytokines (IL2, IL7, and IL15). Importantly, these signals were selected as they are likely to be encountered post-infusion in the clinic. IL2 is very often administered as an adjuvant in GT T-cell therapy (Robbins et al. 2011) and IL7 and IL15 are known homeostatic cytokines present in lymphocyte rich compartments of the body and known to drive T-cell expansion in the periphery (De Bock et al. 2013).

The CSA results suggested that a shorter manufacturing time, in the context of CD3 + CD28 manufacturing, retains the potential of the T-cells to respond to the growth cytokines (figure 2). This effect correlated weakly with the level of cytokine receptor expression (figure 6-8), suggesting that the loss of distinct cytokine receptors may be a factor in the observed proliferative senescence. In addition to the reduced proliferation, there was an increased rate of active apoptosis and a lack of entry into early cell division (figure 4-5). The increased response to growth cytokines suggests that fewer T cells would be needed for infusion as there would be a more dramatic expansion *in vivo*. In line with this observation, other groups have reported similar findings in the context of CAR T cells in which a six fold lower infusion of early minimally expanded T cells was superior to a longer expansion protocol (Ghassemi et al. 2018).

In addition to the loss of functionality, there was a dramatic shift in the T-cell memory phenotype with day 4 cells retaining a Tnaive_scm and Tcm phenotype compared to the day 7 and day 10 expanded cells. Surprisingly, across the 21-day assay, in the context of IL15 and IL7 (key homeostatic cytokines), there was an improved retention of these same memory compartments (figure 9-11). This behavior was not evident when culturing with IL2, perhaps due to the faster downregulation of the IL2 CD25 receptor compared to the IL7 CD127 and the IL15 CD122 receptors.

The lack of T-cell persistence in the CSA suggested that as the T-cell expansion was elongated, they began acquiring a senescent phenotype in response to homeostatic cytokines. Clinically infused TIL products have been shown to persist *in vivo* in correlation to their final telomere length (Zhou et al. 2005) and thus I began investigating these changes as a potential correlate for the observed *in vitro* senescence.

There was a reduction in telomere length for all donors as the expansions were elongated (figure 12). Additionally, a statistically significant ($p<0.05$) difference was observed for telomerase activity between the day 4, 7, and 10 expanded T-cell products (figure 13), with the earlier expansions producing the highest rate of telomerase activity. Of interest was the observation that the final relative telomere length correlated with the starting percentage of CD28 expressing CD8 cells (figure 14). Additionally, there was a sharpened reduction in the final telomere length when cancer patient derived T-cells were manufactured compared to healthy donors, though this is less surprising given the more elderly age of the cancer derived cells. This fits with recent data showing that only a subset of the CD28 expressing CD8 T-cells can upregulate telomerase following CD3 + CD28 based stimulation (Huang et al. 2017) and recent genetic screens that have highlighted the reduced proliferation of T cells when CD28 is genetically deleted (Shifrut et al. 2018). Its noteworthy to mention that there have been recent attempts to overexpress telomerase to counteract the loss of telomere length and proliferative senescence (Bai et al. 2015), though to my knowledge, none of these approaches have entered the clinic, likely due to the ability of telomerase to transform cells.

In order to more completely investigate the changes occurring during the expansion, I turned to whole RNA sequencing analysis. Gene cluster analysis clearly outlined that the day 4 expanded cells displayed a differential gene expression pattern compared to the day 7 and day 10 expanded T cells (figure 17). Confirming this observation, differential gene expression analysis measured over 5,000 DEGs between day 4 to day 7 or day 10. Very surprisingly, there were fewer than 100 DEGs between day 7 and day 10 expanded T cells (figure 18). This bimodal breakdown strongly suggests that during *in vitro* T-cell expansion, a priming occurs early in the process, likely dependent on the initial T-cell stimulation and cytokine milieu, like events that take place *in vivo*.

Pathway analysis revealed a statistically significant upregulation of apoptosis related genes when comparing the day 4 to day 7 or day 10 samples. This was particularly interesting given the increased apoptotic behavior observed in the CSA. Within the apoptotic pathway, there was a significant increase in apoptotic effector molecules such as CASP8, BAX, RIPK1, and TRADD both of which are known be critical in the intrinsic apoptosis pathway involving mitochondrial disruption (Gu et al. 2005). Intriguingly, there was also an enrichment of apoptosis inhibiting proteins such CFLAR (cFLIP) and XIAP, which work independently to inhibit the CASP8 effector function and the formation of the apoptosome (He and He 2015). Given the heterogenous starting PBMC population, it is possible that within the expanding T-cell cultures, there exists subgroups of T-cell populations that exists in an anti-or-pro apoptotic state. Supporting this model, the functional results from CSA show that even within the later expanding cultures, there exists a population of T cells which remain proliferatively active (figure 2). In line with this finding, certain clonal populations expanded early in the manufacturing process while other clones contracted as measured by clonal DNA sequencing (figure 24A).

As expected from stimulated T-cell cultures, there was a significant enrichment in T-cell stimulatory pathways, such as phosphatidylinositol signaling and MAPK signaling as the manufacturing length increases (figure 19). This is not of much surprise given the known association between these pathways and T-cell expansion (Herrero-Sanchez et al. 2016). Of interest, is the contrasting reduction in cell cycle associated genes as the expansion length continues, with reduction in key cyclin dependent kinases CDK4/CDK6 along with proliferating cell nuclear antigen (PCNA) (table 1). This contrasting gene expression would suggest that there is an immediate upregulation of genes responsible for cellular division, followed by a later subsequent upregulation of growth pathway factors. Other groups have shown an improvement in T-cell clinically related functionality by the inhibition of the PI3K pathway with small molecular inhibitors, resulting in a more naive T cell product with increased T cell proliferative potential (Klebanoff et al. 2017). The results of the CSA are very much aligned with this finding given the increased T-cell proliferation observed in earlier cultures which have not yet upregulated the PI3K pathway signaling.

Cytokine signaling is necessary as the third signal for T-cell proliferation via cytokine receptor specific JAK/STAT signaling axis (Seif et al. 2017). Signaling through T-cell cytokine receptors can be inhibited by the activity of suppressor of cytokine signaling (SOCS) family of proteins which actively target cytokine receptors for proteasomal degradation (Yoshimura, Naka, and Kubo 2007). SOCS1 is known regulator for IL-2, IL-7, and IL-15 signaling and was recently identified a suppressor of T-cell proliferation via a genetic screening study (Shifrut et al. 2018). During the expansion, there was a significant upregulation of SOCS2. While SOCS2 is primarily thought to regulate signaling through the insulin growth factor receptor, it was recently reported that SOCS2 deficient NK cells are hypersensitive to IL-15 (Kim et al. 2017), suggesting that SOCS2 may have additional roles in regulating common gamma chain cytokine signaling during the CSA.

The growth arrest seen in the cultures expanded for longer periods suggests an upregulation of proliferation inhibition pathways. A critical step in cellular proliferation is the downregulation of cyclin dependent kinase inhibitors. The major p16/pRb pathway has been shown to correlate with the proliferative senescence in *in vitro* activated human lymphocytes following stimulation with T-cell mitogens (Migliaccio et al. 2005). In line with this observation, we note that from our RNAseq data there is a nearly 2.2 fold increase in the expression of the p16 encoding CDKN2A mRNA as cells are manufactured from 4 to 10 days. While it is only a moderate change, we also observed a nearly 50% increase in pRB mRNA expression in the early day 4 manufactured cells compared to day 10 manufactured.

From the phenotyping results, there was a decline in doubly expressing CD27+ CD28+ T-cells throughout the expansion process. This decline is rather problematic given recent observations that the expression of CD27 is a predictor of clinical response (Fraietta et al. 2018). In the RNAseq data set, there was a significant loss CD86 expression during the manufacturing, suggesting that there may be a beneficial costimulatory effect taking place between CD28/CD86 early in the manufacturing process. While CD86 is thought to be primarily expressed by APCs, there is evidence that it is upregulated on T cells following activation (Paine et al. 2012). Mechanistically, this depletion of costimulatory cells makes further expansions with CD3 + CD28 a compounding issue, though there is evidence that overexpression of CD28 may revert the phenotypic loss and act as a surrogate for additional expansions (Mondal et al. 2013). While an overexpression strategy may be more permanent, there is evidence that altering the stimulation procedure may preserve the expression of CD28. Researchers have shown that stimulation through the 4-1BB costimulatory pathway may preserve the expression of CD28 expressing T cells *in vitro* (Habib-Agahi, Jaberipour, and Searle 2009). It is interesting to speculate that an additional 4-1BB stimulation during the T-cell stimulation with CD3 + CD28 may yield a more ploycional cellular product as research has shown the preferential retention of a CD28 positive T-cell population (Kim, Brutkiewicz, and Broxmeyer 2002).

From this data, it appears that during the manufacturing with heterologous human PBMCs, there is a quick dramatic change in gene expression patterns which is maintained as the manufacturing continues. Additionally, there appears to exist multiple states of T cells, with both populations that maintained in a state of proliferation and those in a state of apoptosis and contraction. As the expansion continues, there is an evident loss of proliferative ability, likely due to the decrease in actively dividing T cells capable of increased proliferation (figure 25).

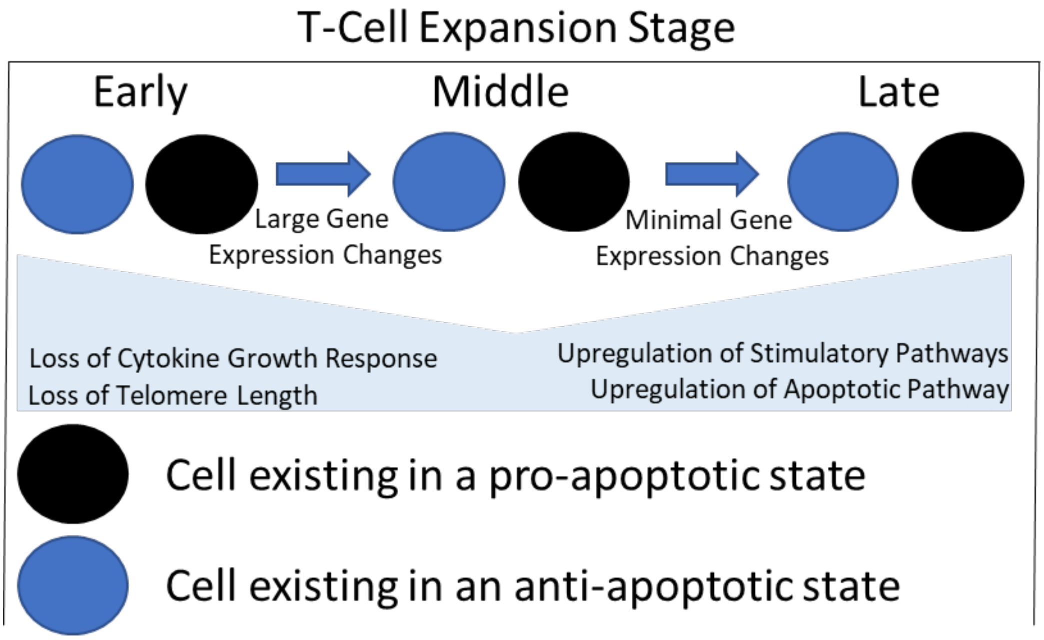

Figure 30: The changes occurring during T-cell manufacturing.

Early on in manufacturing cells seem to exist in two generalized states of either being pro-apoptotic or anti-apoptotic, with these two states being maintained throughout the manufacturing. As cells are manufactured, they lose their ability to respond to growth cytokines, lose telomere length, upregulate stimulatory and apoptotic gene pathways.

In addition to the loss throughout T-cell expansion, the starting expression of CD28 was shown to predict multiple manufacturing metrics, such as fold expansion and the final CD8 percentage. These correlations support a model in which CD28 expression, in the context of CD3 + CD28 manufacturing, serves as a master regulator for the T-cell manufacturing. I propose that this expression, or lack thereof, acts as an *ex vivo* bottleneck where the cells with CD28 expression will outperform the cells not expressing CD28. Given that minimum cell numbers must be reached for a therapeutic dosage, cell expansions are often elongated and, in this model, only a small percentage of the cells are actively expanding to reach this final dosage in older donors. This is a troubling scenario as the limited number of expanding cells endure shorter telomere lengths, increased differentiation, and loss of cytokine sensitivity as they carry the brunt of the expansion load.

To test this model out fully, I performed single molecule DNA sequencing to track T-cell clones throughout the expansion. There was a strong correlation between the number of T-cell clones that either expanded or contracted and the starting percentage of CD28 expression. In low CD28 expressing starting populations, there is clear early cell death, evident by the negative population expansion and negative clonal divisions by day 4 in the expansion process (figure 24). This behavior was also evident when tracking the percentages of clones which expanded or contracted early on, with a small ~1% of T-cell clones showing early expansion in the low CD28 population (figure 26). This cell death then potentially creates a homeostatic niche by which low frequency clones can begin dividing with less competition as suggested by the higher frequency of differentially abundant clones in lower CD28 versus higher CD28 expressing starting populations and the almost bimodal distribution pattern in clonal divisions in low CD28 PBMC cultures (figure 25 and 26). Finally, the decline in unique T-cell clones in donors with lower CD28 expression firmly supports an ‘extinction’ bottleneck event by which clones which cannot survive the manufacturing are removed from the sampling pool (figure 25). It is intriguing to speculate that this loss of clonal diversity may impact the ability of T cell products to persist *in vivo* as weak non-cognate TCR:HLA interactions have been shown provide a growth signal stimulatory effect (Ernst et al. 1999). This event is analogous to a specific T-cell ‘families’ being removed from the entire population of T cells. This model agrees with a recent discovery that CD28 induced 3BP2 drives late stage TCR independent activation and leads to prolonged T-cell proliferation *ex vivo* (Dimitriou et al. 2018). In a clinical setting, in which manufacturing is often ceased when cell number thresholds are met, this model would predict that lower CD28 starting cell populations will achieve an average of two times the number of cell divisions to achieve the same number of final cells (figure 26). With this data, I propose a model by which the starting percentage of CD28 within a PBMC sample can model the behavior of the T-cell culture and the final product characteristics and that the CD28+ T-cells eventually become exhausted as the T-cell expansion is extended (figure 29).

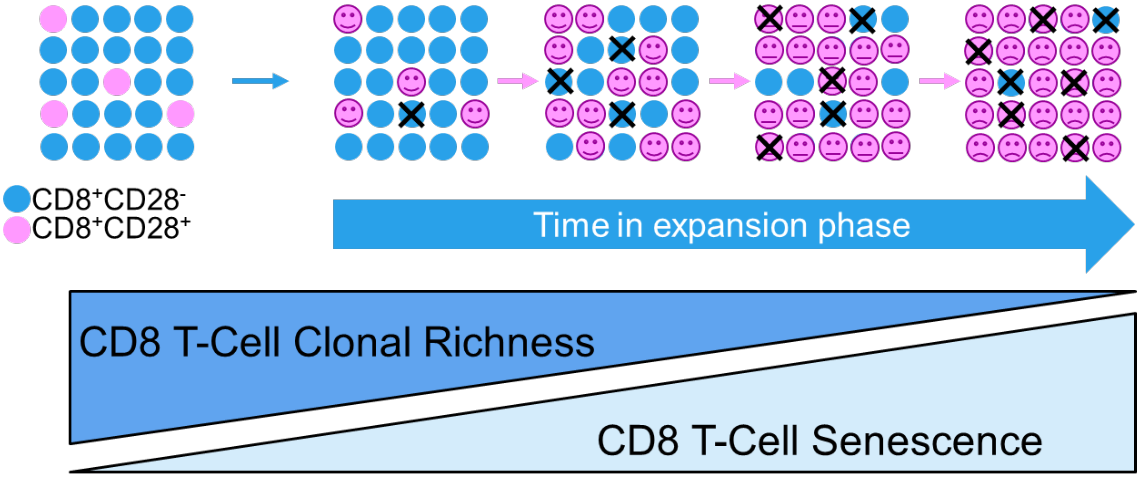

Figure 31: Bottleneck model of T-cell expansion with CD3 + CD28. Heterologous human PBMC T-cells (left panel circles) can be classified based on whether they express CD28 or not. Those that do express CD28 undergo a more rapid division (smiles) early on and during the expansion process, increasing in frequency during the expansion. As the expansion continues, these cells eventually become exhausted (frowns) and enter a T-cell senescence stage. As the T-cells move into this senescence stage, specific T-cell clones become lost from the population ('X' out circles).

If we accept that this CD28 dependent bottleneck exists, a reasonable assumption is that heterogeneous patient populations will vary in their T cells "fitness" for CD3 + CD28 based T-cell expansion protocols. From a total of 4 clinical CD19 trials, each patient's clinical response was codified and then the patients were divided based on age. Patients older than 45 performed approximately two times better in terms of objective response rates (partial response + complete response) when their cells were manufactured with CD3 stimulation without the costimulation of CD28. An inverse relationship was seen when patients were younger than 45, in this case, patients performed nearly one and half times better when their cells were manufactured with CD3 + CD28 stimulation expansion protocols. Perhaps the CD28 stimulation in older patients creates a competitive expansion environment in which older patient highly differentiated T cells cannot survive, this would be a biological explanation and is supported by observations of T-cell trans interactions taking placing during expansion protocols (Klebanoff et al. 2016) and the higher susceptibility of differentiated T cells to survive reactive oxygen rich environments. It is an objective of my post-doctoral work to investigate the exact mechanism behind this age bias in T-cell manufacturing as it appears that the T-cell manufacturing process can be enhanced by personalization to the patient population.

Conclusions

The specific aims of this dissertation and the relevant conclusions are shown below:

1) AIM: Develop an *in vitro* assay aimed at predicting long-term tumor control rather than short-term effector function

Conclusion: The cytokine sensitivity assay (CSA) was developed to measure the proliferative potential of T cells post T-cell expansion protocols

2) AIM: Compare the effect of *in-vitro* expansion durations on the quality of gene therapy transfer T-cells using the newly-developed assay and perform mechanism of action (MOA) studies

Conclusion: Using the CSA, I tested the effects of elongated expansion protocols and was able to show that elongated expansions correlated with signs of functional senescence in CSA.

Conclusion: MOA studies were performed, and it is my leading hypothesis that *ex vivo* bottlenecks exist in T-cell expansion protocols and these bottlenecks differentially effect manufacturing outcome based on the expression of CD28 in the presence of CD3 + CD28 manufacturing. Future work is needed to investigate whether similar bottlenecks exist in other manufacturing protocols.

3) Determine the clinical relevance of the MOA studies using correlative studies aimed at testing the pre-clinical determined mechanism

Conclusion: While I was not able to test the model using actual clinical manufactured T-cells, I was able to apply the bottleneck model to guide a clinical trial meta-analysis to show that patient age was a criterion for which type of expansion protocol yielded the best results in the clinic. Future work is needed to elucidate the complete clinical meaning of this model and how it can be used to tailor manufacturing for certain patient populations.

Future Directions

With respect to nature of current clinical cellular therapy manufacturing, it is evident that there is a strong depersonalization of the personalized drug product. While there is great deal of patient immune-heterogeneity and thus a wide variability in the starting material used in manufacturing, the field is confined to a 'one-size-fits-all' manufacturing mentality. This dogmatic principle confines the flexibility in manufacturing and the ability to customize to the patient's unique cellular phenotype. For example, from the clinical meta-analysis, we see that there is an indication that the more elderly may benefit from a manufacturing in which CD3 is the sole source of T-cell stimulation.

From my perspective, the restrictive nature of cellular manufacturing is impacted largely by the nature of Federal Drug Administration (FDA) regulation of cellular therapies in the same manner as drug compounds. While rigid processes, strict manufacturing lengths, and tight lot-to-lot variability may work in the manufacturing of an inert drug product, the nature of personalized cellular therapy likely entails the necessity for a more flexible manufacturing specification.

Moving forward, it is reasonable to imagine that a patient is first phenotype upon entering clinic and a customized manufacturing is tailor made to their unique specifications. For example, if you have a more exhausted cellular phenotype, perhaps a 4-1BBL stimulation is considered as there is evidence that it may restore a more naive CD28+ phenotype (Habib-Agahi, Jaberipour, and Searle 2009). Within the same thinking, sub-compartment isolation may be considered depending on the heterogeneity of the T-cell compartment.

Furthermore, the data from the CSA assay (figure 5) suggests that each patient may respond to certain cytokines better than others and thus an optimized cytokine cocktail may be in order.

If we are to go to such a flexible modular manufacturing, then there will undoubtably be an increased pressure on the manufacturer to demonstrate the feasibility and logic behind their decisions. With such restrictions, it is likely that an increased effort will be required in the pre-clinical stages of development as a more complex process development will be required. It will require a strong academic-industry-regulatory alliance if we are to shoulder the increased demands in pursuit of truly personalized cellular therapies.

There is a selective pressure perspective that takes place during T-cell culturing and the pressures must be understood. The work presented here aims to be a small piece in a launching-off pad for personalized cellular medicine. Its aim is to highlight our diverse heterogeneity and questions the current way we currently manufacture T cells.

Bibliography

Ackerman. 2003. 'Early phagosomes in in dendritic cells form a cellular compartment sufficient for cross presentation of exogenous antigens', *PNAS*, 100: 12889-94.

Akira, S. 2006. 'Pathogen recognition and innate immunity', *Cell*, 124: 783-801.

Ali, S. A., V. Shi, I. Maric, M. Wang, D. F. Stroncek, J. J. Rose, J. N. Brudno, M. Stetler-Stevenson, S. A. Feldman, B. G. Hansen, V. S. Fellowes, F. T. Hakim, R. E. Gress, and J. N. Kochenderfer. 2016. 'T cells expressing an anti-B-cell maturation antigen chimeric antigen receptor cause remissions of multiple myeloma', *Blood*, 128: 1688-700.

Andersen, R., M. Donia, E. Ellebaek, T. H. Borch, P. Kongsted, T. Z. Iversen, L. R. Holmich, H. W. Hendel, O. Met, M. H. Andersen, P. Thor Straten, and I. M. Svane. 2016. 'Long-Lasting Complete Responses in Patients with Metastatic Melanoma after Adoptive Cell Therapy with Tumor-Infiltrating Lymphocytes and an Attenuated IL2 Regimen', *Clin Cancer Res*, 22: 3734-45.

Asseman, Chrystelle, Smita Mauze, Michael W. Leach, Robert L. Coffman, and Fiona Powrie. 1999. 'An Essential Role for Interleukin 10 in the Function of Regulatory T Cells That Inhibit Intestinal Inflammation', *The Journal of Experimental Medicine*, 190: 995-1004.

Attaf, M., M. Legut, D. K. Cole, and A. K. Sewell. 2015. 'The T cell antigen receptor: the Swiss army knife of the immune system', *Clin Exp Immunol*, 181: 1-18.

Bai, Y., S. Kan, S. Zhou, Y. Wang, J. Xu, J. P. Cooke, J. Wen, and H. Deng. 2015. 'Enhancement of the in vivo persistence and antitumor efficacy of CD19 chimeric antigen receptor T cells through the delivery of modified TERT mRNA', *Cell Discov*, 1: 15040.

Banchereau, Jacques, and Ralph M. Steinman. 1998. 'Dendritic cells and the control of immunity', *Nature*, 392: 245-52.

Baybutt, T. R., J. C. Flickinger, Jr., E. M. Caparosa, and A. E. Snook. 2018. 'Advances in Chimeric Antigen Receptor (CAR)-T Cell Therapies for Solid Tumors', *Clin Pharmacol Ther*.

Beckman, Evan. 1994. 'Recognition of a lipid antigen by CD1-restricted alpha beta+ T cells', *Nature*, 372: 691-94.

Berger, C., M. C. Jensen, P. M. Lansdorp, M. Gough, C. Elliott, and S. R. Riddell. 2008. 'Adoptive transfer of effector CD8+ T cells derived from central memory cells establishes persistent T cell memory in primates', *J Clin Invest*, 118: 294-305.

Berglund, P., D. Finzi, J. R. Bennink, and J. W. Yewdell. 2007. 'Viral alteration of cellular translational machinery increases defective ribosomal products', *J Virol*, 81: 7220-9.

Besser, M. J., R. Shapira-Frommer, A. J. Treves, D. Zippel, O. Itzhaki, L. Hershkovitz, D. Levy, A. Kubi, E. Hovav, N. Chermoshniuk, B. Shalmon, I. Hardan, R. Catane, G. Markel, S. Apter, A. Ben-Nun, I. Kuchuk, A. Shimoni, A. Nagler, and J. Schachter. 2010. 'Clinical responses in a phase II study using adoptive transfer of short-term cultured tumor infiltration lymphocytes in metastatic melanoma patients', *Clin Cancer Res*, 16: 2646-55.

Blueston, Jerffrey A., and Abul K. Abbas. 2003. 'Natural versus adaptive regulatory T cells', *Nature Reviews Immunology*, 3: 253-57.

Carlson, C. S., R. O. Emerson, A. M. Sherwood, C. Desmarais, M. W. Chung, J. M. Parsons, M. S. Steen, M. A. LaMadrid-Herrmannsfeldt, D. W. Williamson, R. J. Livingston, D. Wu, B. L. Wood, M. J. Rieder, and H. Robins. 2013. 'Using synthetic templates to design an unbiased multiplex PCR assay', *Nat Commun*, 4: 2680.

Chamaillard. 2003. 'An essential role for NOD1 in host recognition of bacterial peptidoglycan containing diaminopimelic acid', *Nature Immunology*, 4: 702-07.

Chapuis, A. G., J. A. Thompson, K. A. Margolin, R. Rodmyre, I. P. Lai, K. Dowdy, E. A. Farrar, S. Bhatia, D. E. Sabath, J. Cao, Y. Li, and C. Yee. 2012. 'Transferred melanoma-specific CD8+ T cells persist, mediate tumor regression, and acquire central memory phenotype', *Proc Natl Acad Sci U S A*, 109: 4592-7.

Chatterjee, B., A. Smed-Sorensen, L. Cohn, C. Chalouni, R. Vandlen, B. C. Lee, J. Widger, T. Keler, L. Delamarre, and I. Mellman. 2012. 'Internalization and endosomal degradation of receptor-bound antigens regulate the efficiency of cross presentation by human dendritic cells', *Blood*, 120: 2011-20.

Chen, P. L., W. Roh, A. Reuben, Z. A. Cooper, C. N. Spencer, P. A. Prieto, J. P. Miller, R. L. Bassett, V. Gopalakrishnan, K. Wani, M. P. De Macedo, J. L. Austin-Breneman, H. Jiang, Q. Chang, S. M. Reddy, W. S. Chen, M. T. Tetzlaff, R. J. Broaddus, M. A. Davies, J. E. Gershenwald, L. Haydu, A. J. Lazar, S. P. Patel, P. Hwu, W. J. Hwu, A. Diab, I. C. Glitza, S. E. Woodman, L. M. Vence, Wistuba, II, R. N. Amaria, L. N. Kwong, V. Prieto, R. E. Davis, W. Ma, W. W. Overwijk, A. H. Sharpe, J. Hu, P. A. Futreal, J. Blando, P. Sharma, J. P. Allison, L. Chin, and J. A. Wargo. 2016. 'Analysis of Immune Signatures in Longitudinal Tumor Samples Yields Insight into Biomarkers of Response and Mechanisms of Resistance to Immune Checkpoint Blockade', *Cancer Discov*, 6: 827-37.

Chester, C., S. Ambulkar, and H. E. Kohrt. 2016. '4-1BB agonism: adding the accelerator to cancer immunotherapy', *Cancer Immunol Immunother*, 65: 1243-8.

Cieri, N., B. Camisa, F. Cocchiarella, M. Forcato, G. Oliveira, E. Provasi, A. Bondanza, C. Bordignon, J. Peccatori, F. Ciceri, M. T. Lupo-Stanghellini, F. Mavilio, A. Mondino, S. Bicciato, A. Recchia, and C. Bonini. 2013. 'IL-7 and IL-15 instruct the generation of human memory stem T cells from naive precursors', *Blood*, 121: 573-84.

Cohen, C. J., J. J. Gartner, M. Horovitz-Fried, K. Shamalov, K. Trebska-McGowan, V. V. Bliskovsky, M. R. Parkhurst, C. Ankri, T. D. Prickett, J. S. Crystal, Y. F. Li, M. El-Gamil, S. A. Rosenberg, and P. F. Robbins. 2015. 'Isolation of neoantigen-specific T cells from tumor and peripheral lymphocytes', *J Clin Invest*, 125: 3981-91.

Collison, L. W., C. J. Workman, T. T. Kuo, K. Boyd, Y. Wang, K. M. Vignali, R. Cross, D. Sehy, R. S. Blumberg, and D. A. Vignali. 2007. 'The inhibitory cytokine IL-35 contributes to regulatory T-cell function', *Nature*, 450: 566-9.

Coulie, P. G., B. J. Van den Eynde, P. van der Bruggen, and T. Boon. 2014. 'Tumour antigens recognized by T lymphocytes: at the core of cancer immunotherapy', *Nat Rev Cancer*, 14: 135-46.

Couzin-Frankel, Jennifer. 2013. 'Cancer Immunotherapy', *Science*, 342: 1432-33.

Cunningham, A. C. 1997. 'A comparison of the antigen-presenting capabilities of class II MHC-expressing human lung epithelial and endothelial cells', *Immunology*, 91: 458-63.

Curtin, John. 1974. 'Restriction of in vitro T cell-mediated cytotoxicity in lymphocytic choriomeningitis within a syngeneic or semiallogeneic system', *Nature*, 248: 701-02.

D'Angelo, S. P., L. Melchiori, M. S. Merchant, D. Bernstein, J. Glod, R. Kaplan, S. Grupp, W. D. Tap, K. Chagin, G. K. Binder, S. Basu, D. E. Lowther, R. Wang, N. Bath, A. Tipping, G. Betts, I. Ramachandran, J. M. Navenot, H. Zhang, D. K. Wells, E. Van Winkle, G. Kari, T. Trivedi, T. Holdich, L. Pandite, R. Amado, and C. L. Mackall. 2018. 'Antitumor Activity Associated with Prolonged Persistence of Adoptively Transferred NY-ESO-1 (c259)T Cells in Synovial Sarcoma', *Cancer Discov*, 8: 944-57.

Davis, Mark M., and Pamela J. Bjorkman. 1988. 'T-cell antigen receptor genes and T-cell recognition', *Nature*, 334: 395-402.

De Bock, M., M. Fillet, M. Hannon, L. Seidel, M. P. Merville, A. Gothot, Y. Beguin, and F. Baron. 2013. 'Kinetics of IL-7 and IL-15 levels after allogeneic peripheral blood stem cell transplantation following nonmyeloablative conditioning', *PLoS One*, 8: e55876.

de Martel, Catherine, Jacques Ferlay, Silvia Franceschi, Jérôme Vignat, Freddie Bray, David Forman, and Martyn Plummer. 2012. 'Global burden of cancers attributable to infections in 2008: a review and synthetic analysis', *The Lancet Oncology*, 13: 607-15.

Deford-Watts, L. M., T. C. Tassin, A. M. Becker, J. J. Medeiros, J. P. Albanesi, P. E. Love, C. Wulfing, and N. S. van Oers. 2009. 'The cytoplasmic tail of the T cell receptor CD3 epsilon subunit contains a phospholipid-binding motif that regulates T cell functions', *J Immunol*, 183: 1055-64.

Dimitriou, I. D., K. Lee, I. Akpan, E. F. Lind, V. A. Barr, P. S. Ohashi, L. E. Samelson, and R. Rottapel. 2018. 'Timed Regulation of 3BP2 Induction Is Critical for Sustaining CD8(+) T Cell Expansion and Differentiation', *Cell Rep*, 24: 1123-35.

Dolan, B. P., L. Li, C. A. Veltri, C. M. Ireland, J. R. Bennink, and J. W. Yewdell. 2011. 'Distinct pathways generate peptides from defective ribosomal products for CD8+ T cell immunosurveillance', *J Immunol*, 186: 2065-72.

Embgenbroich, M., and S. Burgdorf. 2018. 'Current Concepts of Antigen Cross-Presentation', *Front Immunol*, 9: 1643.

Ernst, Bettina, Dong-Sup Lee, Jennifer M. Chang, Jonathan Sprent, and Charles D. Surh. 1999. 'The peptide ligands mediating positive selection in the thymus control T cell survival and homeostatic proliferation in the periphery', *Immunity*, 11: 173-81.

Fraietta, J. A., S. F. Lacey, E. J. Orlando, I. Pruteanu-Malinici, M. Gohil, S. Lundh, A. C. Boesteanu, Y. Wang, R. S. O'Connor, W. T. Hwang, E. Pequignot, D. E. Ambrose, C. Zhang, N. Wilcox, F. Bedoya, C. Dorfmeier, F. Chen, L. Tian, H. Parakandi, M. Gupta, R. M. Young, F. B. Johnson, I. Kulikovskaya, L. Liu, J. Xu, S. H. Kassim, M. M. Davis, B. L. Levine, N. V. Frey, D. L. Siegel, A. C. Huang, E. J. Wherry, H. Bitter, J. L. Brogdon, D. L. Porter, C. H. June, and J. J. Melenhorst. 2018. 'Determinants of response and resistance to CD19 chimeric antigen receptor (CAR) T cell therapy of chronic lymphocytic leukemia', *Nat Med*, 24: 563-71.

Fry, T. J., and C. L. Mackall. 2005. 'The Many Faces of IL-7: From Lymphopoiesis to Peripheral T Cell Maintenance', *The Journal of Immunology*, 174: 6571-76.

Gao, George F., Jose Tormo, Ulrich C. Gerth, Jessica R. Wyer, Andrew J. McMichael, David I. Suart, John I. Bell, Yvonne Jones, and Bent K. Jakobsen. 1997. 'Crystal structure of the complex between human CD8αα and HLA-A2', *Nature*, 387: 630-34.

Garboczi, David N., Partho Ghosh, Ursula Utz, Qing Fan, William Biddison, and Don Wiley. 2000. 'Structure of the complex between human T-cell receptor viral peptide and HLA-A2', *Nature*, 38: 134-41.

Gattinoni, L., S. E. Finkelstein, C. A. Klebanoff, P. A. Antony, D. C. Palmer, P. J. Spiess, L. N. Hwang, Z. Yu, C. Wrzesinski, D. M. Heimann, C. D. Surh, S. A. Rosenberg, and N. P. Restifo. 2005. 'Removal of homeostatic cytokine sinks by lymphodepletion enhances the efficacy of adoptively transferred tumor-specific CD8+ T cells', *J Exp Med*, 202: 907-12.

Gattinoni, L., C. A. Klebanoff, D. C. Palmer, C. Wrzesinski, K. Kerstann, Z. Yu, S. E. Finkelstein, M. R. Theoret, S. A. Rosenberg, and N. P. Restifo. 2005. 'Acquisition of full effector function in vitro paradoxically impairs the in vivo antitumor efficacy of adoptively transferred CD8+ T cells', *J Clin Invest*, 115: 1616-26.

Gattinoni, L., C. A. Klebanoff, and N. P. Restifo. 2012. 'Paths to stemness: building the ultimate antitumour T cell', *Nat Rev Cancer*, 12: 671-84.

Gattinoni, L., E. Lugli, Y. Ji, Z. Pos, C. M. Paulos, M. F. Quigley, J. R. Almeida, E. Gostick, Z. Yu, C. Carpenito, E. Wang, D. C. Douek, D. A. Price, C. H. June, F. M. Marincola, M. Roederer, and N. P. Restifo. 2011. 'A human memory T cell subset with stem cell-like properties', *Nat Med*, 17: 1290-7.

Ghafouri-Fard, Soudeh. 2014. 'Cancer-testis genes as candidates for immunotherapy in breast cancer', *Immunotherapy*, 6: 165-79.

Ghassemi, S., S. Nunez-Cruz, R. S. O'Connor, J. A. Fraietta, P. R. Patel, J. Scholler, D. M. Barrett, S. M. Lundh, M. M. Davis, F. Bedoya, J. Leferovich, S. F. Lacey, B. L. Levine, S. A. Grupp, C. H. June, J. J. Melenhorst, and M. C. Milone. 2018. 'Reducing Ex Vivo Culture Improves the Anti-leukemic Activity of Chimeric Antigen Receptor (CAR)-T Cells', *Cancer Immunol Res*.

Gu, Q., J. D. Wang, H. H. Xia, M. C. Lin, H. He, B. Zou, S. P. Tu, Y. Yang, X. G. Liu, S. K. Lam, W. M. Wong, A. O. Chan, M. F. Yuen, H. F. Kung, and B. C. Wong. 2005. 'Activation of the caspase-8/Bid and Bax pathways in aspirin-induced apoptosis in gastric cancer', *Carcinogenesis*, 26: 541-6.

Habib-Agahi, M., M. Jaberipour, and P. F. Searle. 2009. '4-1BBL costimulation retrieves CD28 expression in activated T cells', *Cell Immunol*, 256: 39-46.

Harris, D. T., and D. M. Kranz. 2016. 'Adoptive T Cell Therapies: A Comparison of T Cell Receptors and Chimeric Antigen Receptors', *Trends Pharmacol Sci*, 37: 220-30.

He, M. X., and Y. W. He. 2015. 'c-FLIP protects T lymphocytes from apoptosis in the intrinsic pathway', *J Immunol*, 194: 3444-51.

Herrero-Sanchez, M. C., C. Rodriguez-Serrano, J. Almeida, L. San Segundo, S. Inoges, A. Santos-Briz, J. Garcia-Brinon, L. A. Corchete, J. F. San Miguel, C. Del Canizo, and B. Blanco. 2016. 'Targeting of PI3K/AKT/mTOR pathway to inhibit T cell activation and prevent graft-versus-host disease development', *J Hematol Oncol*, 9: 113.

Hsieh, Chyi-Song, Steven E. Macatonia, Catherine S. Tripp, Stanley F. Wolf, Anne O'Garra, and Kenneth M. Murphy. 1993. 'Development of TH1 CD4 T cells through IL-12 produced by Listeria induced macrophages', *Science*, 260: 547-49.

Huang, E. E., E. Tedone, R. O'Hara, C. Cornelius, T. P. Lai, A. Ludlow, W. E. Wright, and J. W. Shay. 2017. 'The Maintenance of Telomere Length in CD28+ T Cells During T Lymphocyte Stimulation', *Sci Rep*, 7: 6785.

Huang, J., K. W. Kerstann, M. Ahmadzadeh, Y. F. Li, M. El-Gamil, S. A. Rosenberg, and P. F. Robbins. 2006. 'Modulation by IL-2 of CD70 and CD27 Expression on CD8+ T Cells: Importance for the Therapeutic Effectiveness of Cell Transfer Immunotherapy', *The Journal of Immunology*, 176: 7726-35.

Johnson, D. B., M. V. Estrada, R. Salgado, V. Sanchez, D. B. Doxie, S. R. Opalenik, A. E. Vilgelm, E. Feld, A. S. Johnson, A. R. Greenplate, M. E. Sanders, C. M. Lovly, D. T. Frederick, M. C. Kelley, A. Richmond, J. M. Irish, Y. Shyr, R. J. Sullivan, I. Puzanov, J. A. Sosman, and J.

M. Balko. 2016. 'Melanoma-specific MHC-II expression represents a tumour-autonomous phenotype and predicts response to anti-PD-1/PD-L1 therapy', *Nat Commun*, 7: 10582.

Johnson, L. A., R. A. Morgan, M. E. Dudley, L. Cassard, J. C. Yang, M. S. Hughes, U. S. Kammula, R. E. Royal, R. M. Sherry, J. R. Wunderlich, C. C. Lee, N. P. Restifo, S. L. Schwarz, A. P. Cogdill, R. J. Bishop, H. Kim, C. C. Brewer, S. F. Rudy, C. VanWaes, J. L. Davis, A. Mathur, R. T. Ripley, D. A. Nathan, C. M. Laurencot, and S. A. Rosenberg. 2009. 'Gene therapy with human and mouse T-cell receptors mediates cancer regression and targets normal tissues expressing cognate antigen', *Blood*, 114: 535-46.

June, C. H., and M. Sadelain. 2018. 'Chimeric Antigen Receptor Therapy', *N Engl J Med*, 379: 64-73.

Kane, Lawrence P., Pietro G. Andres, Kimberly C. Howland, Abul K. Abbas, and Arthur Weiss. 2001. 'Akt provides the CD28 costimulatory signal for up-regulation of IL-2 and IFNg but not Th2 cytokines', *Nature Immunology*, 2: 37-44.

Kawai, T., and S. Akira. 2010. 'The role of pattern-recognition receptors in innate immunity: update on Toll-like receptors', *Nat Immunol*, 11: 373-84.

Kim, W. S., M. J. Kim, D. O. Kim, J. E. Byun, H. Huy, H. Y. Song, Y. J. Park, T. D. Kim, S. R. Yoon, E. J. Choi, H. Jung, and I. Choi. 2017. 'Suppressor of Cytokine Signaling 2 Negatively Regulates NK Cell Differentiation by Inhibiting JAK2 Activity', *Sci Rep*, 7: 46153.

Kim, Y. J., R. R. Brutkiewicz, and H. E. Broxmeyer. 2002. 'Role of 4-1BB (CD137) in the functional activation of cord blood CD28(-)CD8(+) T cells', *Blood*, 100: 3253-60.

Kirsch, I., M. Vignali, and H. Robins. 2015. 'T-cell receptor profiling in cancer', *Mol Oncol*, 9: 2063-70.

Klebanoff, C. A., J. G. Crompton, A. J. Leonardi, T. N. Yamamoto, S. S. Chandran, R. L. Eil, M. Sukumar, S. K. Vodnala, J. Hu, Y. Ji, D. Clever, M. A. Black, D. Gurusamy, M. J. Kruhlak, P. Jin, D. F. Stroncek, L. Gattinoni, S. A. Feldman, and N. P. Restifo. 2017. 'Inhibition of

AKT signaling uncouples T cell differentiation from expansion for receptor-engineered adoptive immunotherapy', *JCI Insight*, 2.

Klebanoff, C. A., C. D. Scott, A. J. Leonardi, T. N. Yamamoto, A. C. Cruz, C. Ouyang, M. Ramaswamy, R. Roychoudhuri, Y. Ji, R. L. Eil, M. Sukumar, J. G. Crompton, D. C. Palmer, Z. A. Borman, D. Clever, S. K. Thomas, S. Patel, Z. Yu, P. Muranski, H. Liu, E. Wang, F. M. Marincola, A. Gros, L. Gattinoni, S. A. Rosenberg, R. M. Siegel, and N. P. Restifo. 2016. 'Memory T cell-driven differentiation of naive cells impairs adoptive immunotherapy', *J Clin Invest*, 126: 318-34.

Kohl, U., S. Arsenieva, A. Holzinger, and H. Abken. 2018. 'CAR T Cells in Trials: Recent Achievements and Challenges that Remain in the Production of Modified T Cells for Clinical Applications', *Hum Gene Ther*, 29: 559-68.

Krummel, M. F. 1995. 'CD28 and CTLA-4 have opposing effects on the response of T cells to stimulation', *Journal of Experimental Medicine*, 182: 459-65.

Le Bourhis, L., E. Martin, I. Peguillet, A. Guihot, N. Froux, M. Core, E. Levy, M. Dusseaux, V. Meyssonnier, V. Premel, C. Ngo, B. Riteau, L. Duban, D. Robert, S. Huang, M. Rottman, C. Soudais, and O. Lantz. 2010. 'Antimicrobial activity of mucosal-associated invariant T cells', *Nat Immunol*, 11: 701-8.

Le Gros, G., Shlomo Z. Ben-Sasson, Robert Seder, Fred D. Finkelman, and William E. Paul. 1990. 'Generation of interleukin 4 (IL-4)-producing cells in vivo and in vitro: IL-2 and IL-4 are required for in vitro generation of IL-4- producing cells', *Journal of Experimental Medicine*, 172: 921-29.

Lennon-Duménil, Ana-Maria, Arnold H. Bakker, René Maehr, Edda Fiebiger, Herman S. Overkleeft, Mario Rosemblatt, Hidde L. Ploegh, and Cécile Lagaudrière-Gesbert. 2002. 'Analysis of Protease Activity in Live Antigen-presenting Cells Shows Regulation of the Phagosomal Proteolytic Contents During Dendritic Cell Activation', *The Journal of Experimental Medicine*, 196: 529-40.

Li, Y., M. Bleakley, and C. Yee. 2005. 'IL-21 Influences the Frequency, Phenotype, and Affinity of the Antigen-Specific CD8 T Cell Response', *The Journal of Immunology*, 175: 2261-69.

Lichtman, E. I., and G. Dotti. 2017. 'Chimeric antigen receptor T-cells for B-cell malignancies', *Transl Res*, 187: 59-82.

Linette, G. P., E. A. Stadtmauer, M. V. Maus, A. P. Rapoport, B. L. Levine, L. Emery, L. Litzky, A. Bagg, B. M. Carreno, P. J. Cimino, G. K. Binder-Scholl, D. P. Smethurst, A. B. Gerry, N. J. Pumphrey, A. D. Bennett, J. E. Brewer, J. Dukes, J. Harper, H. K. Tayton-Martin, B. K. Jakobsen, N. J. Hassan, M. Kalos, and C. H. June. 2013. 'Cardiovascular toxicity and titin cross-reactivity of affinity-enhanced T cells in myeloma and melanoma', *Blood*, 122: 863-71.

Lu, Y. C., X. Yao, J. S. Crystal, Y. F. Li, M. El-Gamil, C. Gross, L. Davis, M. E. Dudley, J. C. Yang, Y. Samuels, S. A. Rosenberg, and P. F. Robbins. 2014. 'Efficient identification of mutated cancer antigens recognized by T cells associated with durable tumor regressions', *Clin Cancer Res*, 20: 3401-10.

Mantegazza, A. R., A. Savina, M. Vermeulen, L. Perez, J. Geffner, O. Hermine, S. D. Rosenzweig, F. Faure, and S. Amigorena. 2008. 'NADPH oxidase controls phagosomal pH and antigen cross-presentation in human dendritic cells', *Blood*, 112: 4712-22.

Maus, M. V., and C. H. June. 2016. 'Making Better Chimeric Antigen Receptors for Adoptive T-cell Therapy', *Clin Cancer Res*, 22: 1875-84.

Migliaccio, M., K. Raj, O. Menzel, and N. Rufer. 2005. 'Mechanisms That Limit the In Vitro Proliferative Potential of Human CD8+ T Lymphocytes', *The Journal of Immunology*, 174: 3335-43.

Mondal, A. M., I. Horikawa, S. R. Pine, K. Fujita, K. M. Morgan, E. Vera, S. J. Mazur, E. Appella, B. Vojtesek, M. A. Blasco, D. P. Lane, and C. C. Harris. 2013. 'p53 isoforms regulate aging- and tumor-associated replicative senescence in T lymphocytes', *J Clin Invest*, 123: 5247-57.

Morgan, R. A., N. Chinnasamy, D. Abate-Daga, A. Gros, P. F. Robbins, Z. Zheng, M. E. Dudley, S. A. Feldman, J. C. Yang, R. M. Sherry, G. Q. Phan, M. S. Hughes, U. S. Kammula, A. D. Miller, C. J. Hessman, A. A. Stewart, N. P. Restifo, M. M. Quezado, M. Alimchandani, A. Z. Rosenberg, A. Nath, T. Wang, B. Bielekova, S. C. Wuest, N. Akula, F. J. McMahon, S. Wilde, B. Mosetter, D. J. Schendel, C. M. Laurencot, and S. A. Rosenberg. 2013. 'Cancer regression and neurological toxicity following anti-MAGE-A3 TCR gene therapy', *J Immunother*, 36: 133-51.

Morgan, Richard A., Mark E. Dudley, John. R. Wunderlich, Marybeth S. Hughes, James C. Yang, Richard M. Sherry, Richard E. Royal, Suzanne L. Topalian, Udai S. Kammula, Nicholas P. Restifo, Zhili Zheng, Azam Nahvi, Chrisiaan R. de Vries, Linda J. Rogers-Freezer, Sharon A. Mavroukakis, and Steven A. Rosenberg. 2006. 'Cancer Regression in Patients after transfer of genetically engineered lymphocytes', *Science*, 314: 126-29.

Nan-Ping Weng, Bruce L. Levine, Carl H. June, Richard J. Hodes. 1995. 'Human naive and memory T lymphocytes differ in telomeric length and replicative potential', *Proc. Natl. Acad. Sci.*, 92: 11091-94.

Neefjes, J., M. L. Jongsma, P. Paul, and O. Bakke. 2011. 'Towards a systems understanding of MHC class I and MHC class II antigen presentation', *Nat Rev Immunol*, 11: 823-36.

Newick, K., S. O'Brien, E. Moon, and S. M. Albelda. 2017. 'CAR T Cell Therapy for Solid Tumors', *Annu Rev Med*, 68: 139-52.

Niedobitek, G. 2000. 'Epstein-Barr virus infection in the the pathogenesis of nasopharyngeal carcinoma', *Journal of Clinical Pathology*, 53: 248-54.

Nikolich-Zugich, J., M. K. Slifka, and I. Messaoudi. 2004. 'The many important facets of T-cell repertoire diversity', *Nat Rev Immunol*, 4: 123-32.

Oderup, C., L. Cederbom, A. Makowska, C. M. Cilio, and F. Ivars. 2006. 'Cytotoxic T lymphocyte antigen-4-dependent down-modulation of costimulatory molecules on dendritic cells in CD4+ CD25+ regulatory T-cell-mediated suppression', *Immunology*, 118: 240-9.

Paine, A., H. Kirchner, S. Immenschuh, M. Oelke, R. Blasczyk, and B. Eiz-Vesper. 2012. 'IL-2 upregulates CD86 expression on human CD4(+) and CD8(+) T cells', *J Immunol*, 188: 1620-9.

Pfeifhofer-Obermair, C., N. Thuille, and G. Baier. 2012. 'Involvement of distinct PKC gene products in T cell functions', *Front Immunol*, 3: 220.

Powell, D. J., Jr., M. E. Dudley, P. F. Robbins, and S. A. Rosenberg. 2005. 'Transition of late-stage effector T cells to CD27+ CD28+ tumor-reactive effector memory T cells in humans after adoptive cell transfer therapy', *Blood*, 105: 241-50.

Prasad, V., and V. Kaestner. 2017. 'Nivolumab and pembrolizumab: Monoclonal antibodies against programmed cell death-1 (PD-1) that are interchangeable', *Semin Oncol*, 44: 132-35.

Qian, Y., L. Yang, and S. Cao. 2014. 'Telomeres and telomerase in T cells of tumor immunity', *Cell Immunol*, 289: 63-9.

Radvanyi, Laszlo G. 2015. 'Tumor-Infiltrating Lymphocyte Therapy: Addressing Prevailing Questions', *Cancer Journal*, 21: 450-64.

Ramos, H. J., A. M. Davis, A. G. Cole, J. D. Schatzle, J. Forman, and J. D. Farrar. 2009. 'Reciprocal responsiveness to interleukin-12 and interferon-alpha specifies human CD8+ effector versus central memory T-cell fates', *Blood*, 113: 5516-25.

Read, Simon, Vivianne Malmström, and Fiona Powrie. 2000. 'Cytotoxic T Lymphocyte–Associated Antigen 4 Plays an Essential Role in the Function of Cd25+Cd4+Regulatory Cells That Control Intestinal Inflammation', *The Journal of Experimental Medicine*, 192: 295-302.

Robbins, P. F., M. E. Dudley, J. Wunderlich, M. El-Gamil, Y. F. Li, J. Zhou, J. Huang, D. J. Powell, and S. A. Rosenberg. 2004. 'Cutting Edge: Persistence of Transferred Lymphocyte Clonotypes Correlates with Cancer Regression in Patients Receiving Cell Transfer Therapy', *The Journal of Immunology*, 173: 7125-30.

Robbins, P. F., R. A. Morgan, S. A. Feldman, J. C. Yang, R. M. Sherry, M. E. Dudley, J. R. Wunderlich, A. V. Nahvi, L. J. Helman, C. L. Mackall, U. S. Kammula, M. S. Hughes, N. P.

Restifo, M. Raffeld, C. C. Lee, C. L. Levy, Y. F. Li, M. El-Gamil, S. L. Schwarz, C. Laurencot, and S. A. Rosenberg. 2011. 'Tumor regression in patients with metastatic synovial cell sarcoma and melanoma using genetically engineered lymphocytes reactive with NY-ESO-1', *J Clin Oncol*, 29: 917-24.

Robbins, Paul F., Yong F. Li, Mona El-Gamil, Yangbing Zhao, Jennifer A. Wargo, Zhili Zheng, Hui Xu, Richard A. Morgan, Steven A. Feldman, Laura A. Johnson, Alan D. Bennett, Steven M. Dunn, Tara M. Mahon, Bent K. Jakobsen, and Steven A. Rosenberg. 2008. 'Single and Dual Amino Acid Substitutions in TCR CDRs Can Enhance Antigen-Specific T Cell Functions', *The Journal of Immunology*, 180: 6116-31.

Robins, H., C. Desmarais, J. Matthis, R. Livingston, J. Andriesen, H. Reijonen, C. Carlson, G. Nepom, C. Yee, and K. Cerosaletti. 2012. 'Ultra-sensitive detection of rare T cell clones', *J Immunol Methods*, 375: 14-9.

Robins, H. S., P. V. Campregher, S. K. Srivastava, A. Wacher, C. J. Turtle, O. Kahsai, S. R. Riddell, E. H. Warren, and C. S. Carlson. 2009. 'Comprehensive assessment of T-cell receptor beta-chain diversity in alphabeta T cells', *Blood*, 114: 4099-107.

Rock, K. L., J. J. Lai, and H. Kono. 2011. 'Innate and adaptive immune responses to cell death', *Immunol Rev*, 243: 191-205.

Romero, P., A. Zippelius, I. Kurth, M. J. Pittet, C. Touvrey, E. M. Iancu, P. Corthesy, E. Devevre, D. E. Speiser, and N. Rufer. 2007. 'Four Functionally Distinct Populations of Human Effector-Memory CD8+ T Lymphocytes', *The Journal of Immunology*, 178: 4112-19.

Romieu-Mourez, R et al. 2007. 'Regulation of MHC Class II Expression and Antigen Processing in Murine and Human Mesenchymal Stromal Cells by IFN- , TGF- , and Cell Density', *The Journal of Immunology*, 179: 1549-58.

Rosa, Stephen C. De, Leonard A. Herzenberg, Leonore A. Herzenberg, and Mario Roederer. 2001. '11-color, 13-parameter flow cytometry: Identification of human naive T cells by phenotype, function, and T-cell receptor diversity', *Nature Medicine*, 7: 245-48.

Russano, A. M., G. Bassotti, E. Agea, O. Bistoni, A. Mazzocchi, A. Morelli, S. A. Porcelli, and F. Spinozzi. 2007. 'CD1-Restricted Recognition of Exogenous and Self-Lipid Antigens by Duodenal + T Lymphocytes', *The Journal of Immunology*, 178: 3620-26.

Sabatino, M., J. Hu, M. Sommariva, S. Gautam, V. Fellowes, J. D. Hocker, S. Dougherty, H. Qin, C. A. Klebanoff, T. J. Fry, R. E. Gress, J. N. Kochenderfer, D. F. Stroncek, Y. Ji, and L. Gattinoni. 2016. 'Generation of clinical-grade CD19-specific CAR-modified CD8+ memory stem cells for the treatment of human B-cell malignancies', *Blood*, 128: 519-28.

Sadelain, M., R. Brentjens, and I. Riviere. 2009. 'The promise and potential pitfalls of chimeric antigen receptors', *Curr Opin Immunol*, 21: 215-23.

Sallusto, Federica. 1998. 'Rapid and coordinated switch in chemokine receptor expression during dendritic cell maturation', *European Journal of Immunology*, 28: 2760-69.

Sallusto, Federica, Danielle Lenig, Reinhold Forster, Martin Lipp, and Antonio Lanzavecchia. 1999. 'Two subsets of memory T lymphocytes with distinct homing potentials and effector functions', *Nature*, 401: 708-12.

Schadendorf, D., F. S. Hodi, C. Robert, J. S. Weber, K. Margolin, O. Hamid, D. Patt, T. T. Chen, D. M. Berman, and J. D. Wolchok. 2015. 'Pooled Analysis of Long-Term Survival Data From Phase II and Phase III Trials of Ipilimumab in Unresectable or Metastatic Melanoma', *J Clin Oncol*, 33: 1889-94.

Seif, F., M. Khoshmirsafa, H. Aazami, M. Mohsenzadegan, G. Sedighi, and M. Bahar. 2017. 'The role of JAK-STAT signaling pathway and its regulators in the fate of T helper cells', *Cell Commun Signal*, 15: 23.

Shaw, Jeng-Pyng, Paul J. Utz, David B. Durand, T. Jay Toole, Elizaeth Ann Emmel, and Gerald R. Grabtree. 1988. 'Identification of a putative regulator of early T cell activation genes', *Science*, 241: 202-05.

Shaw, T, J Quan, and M C Totoritis. 2003. 'B cell therapy for rheumatoid arthritis- the rituximab (anti-CD20) experience', *Annals of the Rheumatic Disease*, 62: ii55-ii59.

Shen, L., L. J. Sigal, M. Boes, and K. L. Rock. 2004. 'Important role of cathepsin S in generating peptides for TAP-independent MHC class I crosspresentation in vivo', *Immunity*, 21: 155-65.

Shi, Yan. 2000. 'Cell injury releases endogenous adjuvants that stimulate cytotoxic T cell responses', *PNAS*, 97: 14590-95.

Shifrut, E., J. Carnevale, V. Tobin, T. L. Roth, J. M. Woo, C. T. Bui, P. J. Li, M. E. Diolaiti, A. Ashworth, and A. Marson. 2018. 'Genome-wide CRISPR Screens in Primary Human T Cells Reveal Key Regulators of Immune Function', *Cell*.

Spiering, Martin J. 2015. 'Primer on the Immune System', *Alcohol Research*, 37: 171-75.

Straathof, K. C., C. M. Bollard, U. Popat, M. H. Huls, T. Lopez, M. C. Morriss, M. V. Gresik, A. P. Gee, H. V. Russell, M. K. Brenner, C. M. Rooney, and H. E. Heslop. 2005. 'Treatment of nasopharyngeal carcinoma with Epstein-Barr virus--specific T lymphocytes', *Blood*, 105: 1898-904.

Takeuchi, A., and T. Saito. 2017. 'CD4 CTL, a Cytotoxic Subset of CD4(+) T Cells, Their Differentiation and Function', *Front Immunol*, 8: 194.

Tran, E., P. F. Robbins, Y. C. Lu, T. D. Prickett, J. J. Gartner, L. Jia, A. Pasetto, Z. Zheng, S. Ray, E. M. Groh, I. R. Kriley, and S. A. Rosenberg. 2016. 'T-Cell Transfer Therapy Targeting Mutant KRAS in Cancer', *N Engl J Med*, 375: 2255-62.

Tumeh, P. C., R. C. Koya, T. Chodon, N. A. Graham, T. G. Graeber, B. Comin-Anduix, and A. Ribas. 2010. 'The impact of ex vivo clinical grade activation protocols on human T-cell phenotype and function for the generation of genetically modified cells for adoptive cell transfer therapy', *J Immunother*, 33: 759-68.

Van Rhijn, I., A. Kasmar, A. de Jong, S. Gras, M. Bhati, M. E. Doorenspleet, N. de Vries, D. I. Godfrey, J. D. Altman, W. de Jager, J. Rossjohn, and D. B. Moody. 2013. 'A conserved human T cell population targets mycobacterial antigens presented by CD1b', *Nat Immunol*, 14: 706-13.

Viallard, C., and B. Larrivee. 2017. 'Tumor angiogenesis and vascular normalization: alternative therapeutic targets', *Angiogenesis*, 20: 409-26.

Voehringer, D., M. Koschella, and H. Pircher. 2002. 'Lack of proliferative capacity of human effector and memory T cells expressing killer cell lectinlike receptor G1 (KLRG1)', *Blood*, 100: 3698-702.

Vyas, J. M., A. G. Van der Veen, and H. L. Ploegh. 2008. 'The known unknowns of antigen processing and presentation', *Nat Rev Immunol*, 8: 607-18.

Walter, S., L. Herrgen, O. Schoor, G. Jung, D. Wernet, H. J. Buhring, H. G. Rammensee, and S. Stevanovic. 2003. 'Cutting Edge: Predetermined Avidity of Human CD8 T Cells Expanded on Calibrated MHC/Anti-CD28-Coated Microspheres', *The Journal of Immunology*, 171: 4974-78.

Wang, J. H., and E. L. Reinherz. 2012. 'The structural basis of alphabeta T-lineage immune recognition: TCR docking topologies, mechanotransduction, and co-receptor function', *Immunol Rev*, 250: 102-19.

Wang, Jai-Huai, Rob Meijers, Yi Xiong, Jin-huan Liu, Toshiko Sakihama, Rongguang Zhang, Andrzej Joachimiak, and Ellis L. Reinherz. 2001. 'Crystal structure of the human CD4 N-terminal two domain fragment complexed to a class II MHC molecule', *PNAS*, 989: 10799-804.

Weng, N. P., A. N. Akbar, and J. Goronzy. 2009. 'CD28(-) T cells: their role in the age-associated decline of immune function', *Trends Immunol*, 30: 306-12.

Weninger, Wolfgang, Maura A. Crowley, N. Manjunath, and Ulrich H. von Andrian. 2001. 'Migratory Properties of Naive, Effector, and Memory Cd8+T Cells', *The Journal of Experimental Medicine*, 194: 953-66.

Wu, Z., X. Jia, L. de la Cruz, X. C. Su, B. Marzolf, P. Troisch, D. Zak, A. Hamilton, B. Whittle, D. Yu, D. Sheahan, E. Bertram, A. Aderem, G. Otting, C. C. Goodnow, and G. F. Hoyne. 2008.

'Memory T cell RNA rearrangement programmed by heterogeneous nuclear ribonucleoprotein hnRNPLL', *Immunity*, 29: 863-75.

Xing, Y., and K. A. Hogquist. 2012. 'T-cell tolerance: central and peripheral', *Cold Spring Harb Perspect Biol*, 4.

Xu, Y., M. Zhang, C. A. Ramos, A. Durett, E. Liu, O. Dakhova, H. Liu, C. J. Creighton, A. P. Gee, H. E. Heslop, C. M. Rooney, B. Savoldo, and G. Dotti. 2014. 'Closely related T-memory stem cells correlate with in vivo expansion of CAR.CD19-T cells and are preserved by IL-7 and IL-15', *Blood*, 123: 3750-9.

Yokosuka, T., M. Takamatsu, W. Kobayashi-Imanishi, A. Hashimoto-Tane, M. Azuma, and T. Saito. 2012. 'Programmed cell death 1 forms negative costimulatory microclusters that directly inhibit T cell receptor signaling by recruiting phosphatase SHP2', *J Exp Med*, 209: 1201-17.

Yoneyama, M., M. Kikuchi, T. Natsukawa, N. Shinobu, T. Imaizumi, M. Miyagishi, K. Taira, S. Akira, and T. Fujita. 2004. 'The RNA helicase RIG-I has an essential function in double-stranded RNA-induced innate antiviral responses', *Nat Immunol*, 5: 730-7.

Yoshimura, A., T. Naka, and M. Kubo. 2007. 'SOCS proteins, cytokine signalling and immune regulation', *Nat Rev Immunol*, 7: 454-65.

Yossef, R., E. Tran, D. C. Deniger, A. Gros, A. Pasetto, M. R. Parkhurst, J. J. Gartner, T. D. Prickett, G. Cafri, P. F. Robbins, and S. A. Rosenberg. 2018. 'Enhanced detection of neoantigen-reactive T cells targeting unique and shared oncogenes for personalized cancer immunotherapy', *JCI Insight*, 3.

Zelenay, S., and C. Reis e Sousa. 2013. 'Adaptive immunity after cell death', *Trends Immunol*, 34: 329-35.

Zhou, J., X. Shen, J. Huang, R. J. Hodes, S. A. Rosenberg, and P. F. Robbins. 2005. 'Telomere Length of Transferred Lymphocytes Correlates with In Vivo Persistence and Tumor Regression in Melanoma Patients Receiving Cell Transfer Therapy', *The Journal of Immunology*, 175: 7046-52.

Zhou, L., Ivanov, II, R. Spolski, R. Min, K. Shenderov, T. Egawa, D. E. Levy, W. J. Leonard, and D. R. Littman. 2007. 'IL-6 programs T(H)-17 cell differentiation by promoting sequential engagement of the IL-21 and IL-23 pathways', *Nat Immunol*, 8: 967-74.

Vita

Amir Isaac Alpert was born in Dallas, Texas, the son of Rachel Lazarovich and Isreal Alpert. After completing his work at North Dallas High School, Dallas, Texas in 2006, he entered The University of Texas at Austin. He received his Bachelor of Science with a major in cell and molecular biology from UT Austin in May, 2010. For the next two years, he worked as a research technician and completed early graduate school work at UT Austin Microbiology Department. In August of 2012, he entered The University of Texas MDAnderson Cancer Center UTHealth Graduate School of Biomedical Sciences.